

GEOSCIENCE WISCONSIN

*Editor: M.G. Mudrey, Jr.
Associate Editors: Richard A. Paull
Peter A. Nielsen
Kenneth R. Bradbury
Lee Clayton*

CARBONATE DIAGENESIS AND DOLOMITIZATION OF THE LOWER ORDOVICIAN PRAIRIE DU CHIEN GROUP

George L. Smith and J. Antonio Simo

COMPLEX BRECCIATION HISTORY ASSOCIATED WITH EVAPORITE AND CARBONATE DISSOLUTION IN THE LOWER ORDOVICIAN ONEOTA FORMATION (PRAIRIE DU CHIEN GROUP) NEAR SPRING GREEN, WISCONSIN

George L. Smith

AUTHIGENIC SILICA FABRICS ASSOCIATED WITH CAMBRO-ORDOVICIAN UNCONFORMITIES IN THE UPPER MIDWEST

George L. Smith, Robert H. Dott, Jr., and Charles W. Byers

PROPOSED REFERENCE SECTIONS AND CORRELATION OF UPPER SILURIAN AND DEVONIAN STRATA, EASTERN WISCONSIN

Charles W. Rovey II

GRAVITY SIGNATURE OF THE WAUKESHA FAULT, SOUTHEASTERN WISCONSIN

Keith A. Sverdrup, William F. Kean, Sharon Herb, Susan A. Brukardt, and Ronald J. Friedel

RADON EMANATION FROM SOIL OF KENOSHA, RACINE AND WAUKESHA COUNTIES, SOUTHEASTERN WISCONSIN

Nancy S. Kochis and Steven W. Leavitt



Published by and available from

Wisconsin Geological and Natural History Survey

3817 Mineral Point Road, Madison, Wisconsin 53705-5100

☎ 608/263.7389 FAX 608/262.8086 <http://www.uwex.edu/wgnhs/>

James M. Robertson, Director and State Geologist

ISSN: 0164-2049

This report is an interpretation of the data available at the time of preparation. Every reasonable effort has been made to ensure that this interpretation conforms to sound scientific principles; however, the report should *not* be used to guide site-specific decisions without verification. Proper use of this publication is the sole responsibility of the user.

Issued in furtherance of Cooperative Extension work, Acts of May 8 and June 30, 1914, in cooperation with the U.S. Department of Agriculture, University of Wisconsin-Extension, Cooperative Extension. University of Wisconsin-Extension provides equal opportunities in employment and programming, including Title IX and ADA requirements. If you need this information in an alternative format, contact the Office of Equal Opportunity and Diversity Programs or the Wisconsin Geological and Natural History Survey (☎ 608/262.1705).

Mission of the Wisconsin Geological and Natural History Survey

The Survey conducts earth-science surveys, field studies, and research. We provide objective scientific information about the geology, mineral resources, water resources, soil, climate, and biology of Wisconsin. We collect, interpret, disseminate, and archive natural resource information. We communicate the results of our activities through publications, technical talks, and responses to inquiries from the public. These activities support informed decision-making by government, industry, business, and individual citizens of Wisconsin.

PREFACE v

CARBONATE DIAGENESIS AND DOLOMITIZATION OF THE LOWER ORDOVICIAN PRAIRIE DU CHIEN GROUP 1

George L. Smith and J. Antonio Simo

COMPLEX BRECCIATION HISTORY ASSOCIATED WITH EVAPORITE AND CARBONATE DISSOLUTION IN THE LOWER ORDOVICIAN ONEOTA FORMATION (PRAIRIE DU CHIEN GROUP) NEAR SPRING GREEN, WISCONSIN 17

George L. Smith

AUTHIGENIC SILICA FABRICS ASSOCIATED WITH CAMBRO-ORDOVICIAN UNCONFORMITIES IN THE UPPER MIDWEST 25

George L. Smith, Robert H. Dott, Jr., and Charles W. Byers

PROPOSED REFERENCE SECTIONS AND CORRELATION OF UPPER SILURIAN AND DEVONIAN STRATA, EASTERN WISCONSIN 37

Charles W. Rovey II

GRAVITY SIGNATURE OF THE WAUKESHA FAULT, SOUTHEASTERN WISCONSIN 47

Keith A. Sverdrup, William F. Kean, Sharon Herb, Susan A. Brukardt, and Ronald J. Friedel

RADON EMANATION FROM SOIL OF KENOSHA, RACINE AND WAUKESHA COUNTIES, SOUTHEASTERN WISCONSIN 55

Nancy S. Kochis and Steven W. Leavitt

PREFACE

Geoscience Wisconsin is a serial that addresses itself to the geology of Wisconsin—geology in the broadest sense to include rock and rock as related to soil, water, climate, environment, and so forth. It is intended to present timely information from knowledgeable sources and make it accessible via scientific review and publication for the benefit of private citizens, government, scientists, and industry.

Manuscripts are invited from scientists in academic, government, and industrial fields. Once a manuscript has been reviewed and accepted, the authors will submit a revised copy of the paper, and the Wisconsin Geological and Natural History Survey will publish the paper as funds and time permit, distribute copies at nominal cost, and maintain the publication as a part of the Survey list of publications. This will help to insure that results of research are not lost in the archival system of large libraries or lost in the musty drawers of an open file.

This collection of papers from academic colleagues represents a cross section of Wisconsin geology.

Smith, with three papers that include colleagues Simo, Dott and Byers, presents analysis of various textures and mineralogy of the Prairie du Chien Formation in southwestern Wisconsin. His analysis constrains mechanisms for the formation of dolomite, associated breccia, and development of hard ground. Understanding these relations will help in deciphering mineralization history in the Upper Mississippi Valley Zinc-Lead District of southwestern Wisconsin and utility of the Prairie du Chien for construction material and aquifer understanding.

Rovey reexamined available drillcore and some newly acquired core to make revisions to the Devonian strata in Milwaukee and adjacent counties. Since the original description of Devonian units in the past century, urbanization has covered almost all exposures. His analysis refines our understanding and permits correlation to equivalent units in Michigan and Illinois.

Sverdrup, Kean, Herb, Brukardt, and Friedel analyzed gravity data in Waukesha County to document the position and amount of throw on the Waukesha Fault. Their controversial interpretation of the data suggest that the Waukesha Fault is not vertical at depth (as has been assumed for many years), but is rather a listric fault, dipping about 10° to 20° to the southeast, with a throw of 600 m.

Kochis and Leavitt undertook a radiometric analysis of soils and surficial material in southeastern Wisconsin. Their analysis suggests that physical parameters, such as porosity and permeability, are the significant factors in radon migration and entry into homes.

We encourage submission of manuscripts relating to Wisconsin geology. Special consideration will be given to papers which deal with timely topics, present new ideas, and have regional or statewide implications.

M.G. Mudrey, Jr.
Editor, *Geoscience Wisconsin*
Wisconsin Geological and Natural History Survey

WISCONSIN GEOLOGICAL AND NATURAL HISTORY SURVEY

James M. Robertson, *Director and State Geologist*

Ronald G. Hennings, *Assistant Director*

Lyle J. Anderson, *office manager*

John W. Attig, *geologist*

William G. Batten, *geotechnician*

Kenneth R. Bradbury, *hydrogeologist*

W.A. Broughton, *geologist*

Bruce A. Brown, *geologist*

Kim J. Cates, *soil scientist*

Lee Clayton, *geologist*

Brian L. Coulter, *information manager*

Michael L. Czechanski, *cartographer*

Kim M. Dawson, *Map Sales assistant*

Timothy T. Eaton, *hydrogeologist*

Thomas J. Evans, *geologist*

Rilla M. Hinkes, *office manager*

Susan L. Hunt, *graphic designer*

Mindy C. James, *publications manager*

Marcia J. Jespersen, *word processing operator*

Rochelle V. Juedes, *Map Sales manager*

Kathy A. Kane, *computer specialist*

Pamela Naber Knox, *State Climatologist*

Irene D. Lippelt, *water resources specialist*

Kristine L. Lund, *soil and water analyst*

Frederick W. Madison, *soil scientist*

Kathleen M. Massie-Ferch, *subsurface geologist*

Matthew Menne, *assistant State Climatologist*

M.G. Mudrey, Jr., *geologist*

Maureen A. Muldoon, *hydrogeologist*

Stanley A. Nichols, *biologist*

Deborah L. Patterson, *cartographer*

Roger M. Peters, *subsurface geologist*

Kathy Campbell Roushar, *cartographer*

Alexander Zaporozec, *hydrogeologist*

Kathie M. Zwettler, *administrative manager*

plus approximately 10 graduate and undergraduate student workers.



RESEARCH ASSOCIATES

Gregory J. Allord, *USGS*

Mary P. Anderson, *UW-Madison*

Larry K. Binning, *UW-Madison*

Michael F. Bohn, *Wis. Dept. of Nat. Res.*

Stephen M. Born, *UW-Madison*

Phillip E. Brown, *UW-Madison*

Charles W. Byers, *UW-Madison*

William F. Cannon, *USGS*

Kevin Connors, *Dane Co. Land Conserv. Dept.*

C. Patrick Ervin, *Northern Ill. Univ.*

Robert F. Gurda, *Wis. State Cartographer's Office*

Nelson R. Ham, *St. Norbert Coll.*

Mark T. Harris, *UW-Milwaukee*

Karen G. Havholm, *UW-Eau Claire*

Randy J. Hunt, *USGS*

Mark D. Johnson, *Gustavus Adolphus Coll.*

John Klasner, *Western Ill. Univ.*

James C. Knox, *UW-Madison*

George J. Kraft, *Central Wis. Groundwater Center*

James T. Krohelski, *USGS*

Gene L. LaBerge, *UW-Oshkosh*

Eiliv Larsen, *Geological Survey of Norway*

Brian J. Mahoney, *UW-Eau Claire*

Kevin McSweeney, *UW-Madison*

Christine Mechenich, *Central Wis. Groundwater Center*

David M. Mickelson, *UW-Madison*

Donald G. Mikulic, III, *Geol. Survey*

William N. Mode, *UW-Oshkosh*

James O. Peterson, *UW-Madison*

Jeffrey K. Postle, *Wis. Dept. Ag., Trade & Consumer Protection*

Kenneth W. Potter, *UW-Madison*

Todd W. Rayne, *Hamilton Coll.*

Allan F. Schneider, *UW-Parkside*

Byron H. Shaw, *UW-Stevens Point*

J. Antonio Simo, *UW-Madison*

Kent M. Syverson, *UW-Eau Claire*

Jeffrey A. Wyman, *UW-Madison*

The Wisconsin Geological and Natural History Survey also maintains collaborative relationships with a number of local, state, regional, and federal agencies and organizations regarding educational outreach and a broad range of natural resource issues.

CARBONATE DIAGENESIS AND DOLOMITIZATION OF THE LOWER ORDOVICIAN PRAIRIE DU CHIEN GROUP

George L. Smith¹ and J. Antonio Simo²

ABSTRACT

The carbonate diagenetic history of the Lower Ordovician Prairie du Chien Group includes syndepositional diagenesis, shallow-burial diagenesis, hydrothermal diagenesis, and near-surface weathering. Syndepositional diagenesis included calcium carbonate and dolomite cementation, micritic fabric-retentive replacement dolomitization, and anhydrite precipitation. Shallow-burial diagenesis was associated with the development of at least two regional unconformities. Shallow-burial diagenesis included carbonate dissolution and karst development, patchy silicification, and possibly the early phases of coarse, fabric-destructive replacement dolomitization and dolomite cementation. Hydrothermal diagenesis included pervasive dolomite cementation and fabric-destructive replacement dolomitization, minor dedolomitization and calcite cementation, and patchy Mississippi Valley-type sulfide mineralization. Near surface weathering has included karst development and the precipitation of aragonitic and calcitic speleothems.

This study illustrates some of the difficulties of interpreting the mechanisms responsible for the dolomitization of ancient dolostone, many of which have complicated diagenetic histories that include multiple episodes of dolomitization. In the case of the Prairie du Chien Group, hydrothermal dolomitization has petrographically overprinted many of the earlier diagenetic events but has not markedly shifted bulk-rock $\delta^{18}\text{O}$ and $\delta^{13}\text{C}$ values from Early Ordovician marine carbonate values. Thus, the history of carbonate diagenesis and dolomitization in the Prairie du Chien Group is based primarily on detailed petrography and cathodoluminescence petrography, but is not strongly supported by trace element or stable isotope geochemistry.

INTRODUCTION

Lower-Middle Ordovician dolostone of the upper Mississippi Valley region has been studied intermittently since the early 1900s (for example, Steidtmann, 1911; Van Tuyl, 1914) as part of a continuing, broader effort to develop a general model for regional fabric-destructive dolomitization. To date, regional dolomitization in the study area has been variously attributed to seawater or evaporative brines (Calvin and Bain, 1900; Leonard, 1905; Asquith, 1967), meteoric water and/or hydrothermal fluids (Deininger, 1964), and mixed meteoric-marine water (Badiozamani, 1973). Other than Deininger (1964), studies of hydrothermal minerals in the Upper Mississippi Lead-Zinc District (for example, Bain, 1906; Agnew and others, 1956; Heyl and others, 1959) have generally ignored the problem of dolomitization outside of ore deposits.

Our study examines the dolomitization and other carbonate diagenesis of the Lower Ordovician Prairie du Chien Group throughout the upper Mississippi Val-

ley-southern Wisconsin outcrop area (fig. 1).

Throughout this area the Prairie du Chien Group exhibits a complex diagenetic history, and multiple episodes of dolomite cementation and fabric-destructive replacement dolomitization are a major feature of this diagenetic history. In the Prairie du Chien Group, regional hydrothermal dolomitization has overprinted many of the earlier diagenetic events (Smith, 1990; Smith and Simo, 1991), resulting in somewhat ambiguous stable-isotope and trace-element signatures. Detailed petrography and cathodoluminescence petrography have been essential to placing Prairie du Chien Group dolomite fabrics in sequence. This study illustrates some of the difficulties of interpreting the mechanisms responsible for the dolomitization of ancient dolostone.

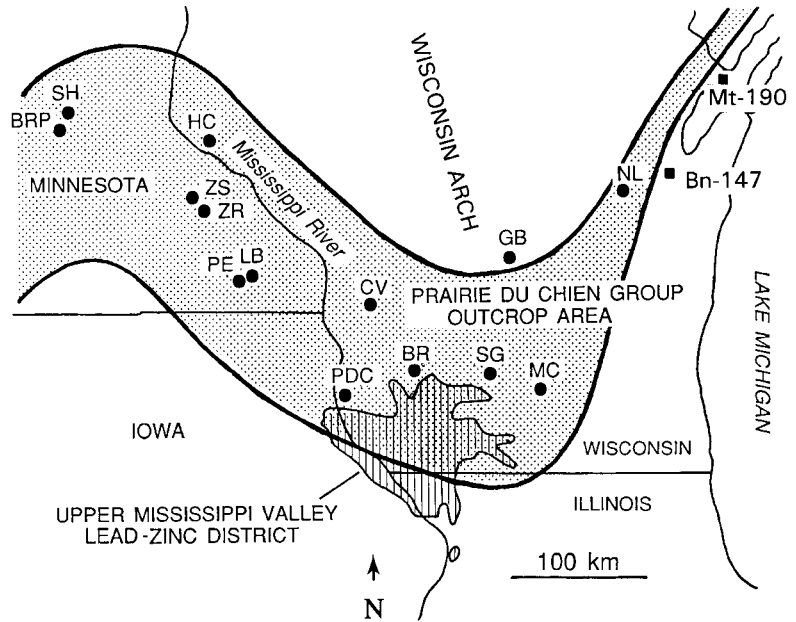
SEDIMENTOLOGY AND STRATIGRAPHY

The Lower Ordovician Prairie du Chien Group crops out from Minnesota to Michigan (fig. 1). The carbon-

¹Department of Geology, Lawrence University, Appleton, Wisconsin 54912-0599; currently at Department of Earth Sciences, SUNY College at Brockport, Brockport, New York 14420-2936

²Department of Geology and Geophysics, University of Wisconsin-Madison, Madison, Wisconsin 53706

Figure 1. Map showing location of study area, Prairie du Chien outcrop area, Wisconsin arch, and Upper Mississippi Valley Lead-Zinc district. Alphabetical abbreviations identify locations of measured sections (all Wisconsin, unless otherwise noted): BR-Blue River; BRP-Bryant Rock Products, Shakopee, Minnesota; CV-Coon Valley; GB-Glovers Bluff (Plainfield); HC-Hager City; LB-Lanesboro, Minnesota; MC-Millers Curve (Cross Plains); NL-New London; PDC-Prairie du Chien; PE-Preston, Minnesota; SG-Spring Green; SH-Shakopee, Minnesota; ZR-Zumbro River (Zumbrota, Minnesota); ZS-Zumbrota, Minnesota. Water wells are identified by Wisconsin Geological and Natural History Survey number: Bn-147 (Brown County), Mt-190 (Marinette County).



ate-dominated, mixed carbonate-siliciclastic sediment of the Prairie du Chien Group correspond mainly to the “restricted platform” carbonate facies belts of Wilson (1974; for example, Adams, 1978; Austin, 1971; Davis, 1966, 1970, 1971; Ostrom, 1970; Raasch, 1952; Shea, 1960; Smith, 1991; Smith and others, 1993, 1996). Abundant oolites, mudcracks, and moldic nodular anhydrite, and a moderately diverse macrofauna (Smith and others, 1993, 1996) and conodont microfauna (Smith and Clark, in press) indicate deposition in a variety of shallow-subtidal to supratidal, marine to hypersaline settings.

The Prairie du Chien Group consists of the Onota and Shakopee Formations (fig. 2), deposited during two major relative highstands of sea level that flooded the central North American craton during the Early Ordovician (Smith and others, 1993, 1996). The Prairie du Chien Group and correlative units mark the end of regional siliciclastic deposition and the inception of widespread Ordovician carbonate deposition. The Prairie du Chien Group is underlain by the Upper Cambrian Jordan Formation and overlain by the Middle Ordovician St. Peter Formation (fig. 2).

METHODS

Field data and samples were obtained from 14 measured outcrop sections and 2 water-wells (fig. 1). Dolomite associated with Mississippi Valley-type ores from the Upper Mississippi Lead-Zinc District (fig. 1) was sampled from a collection at the University of Wisconsin-Madison. Approximately 350 thin sections

were examined petrographically, including approximately 50 examined using cathodoluminescence. Dolomite phases with distinctive and correlatable cathodoluminescence colors were analyzed by electron microprobe in order to determine Ca:Mg ratios and weight-percentages of Fe, Mn, Sr, and Na. Electron beam width was 0.015 mm; beam voltage was 15 Kv; count times were 20-30 s.

Forty-three dolomite samples were analyzed for oxygen and carbon stable-isotopic ratios at the Stable Isotope Laboratory of the University of Wisconsin-Madison. Whole-rock samples (5-50 mg) were drilled and chipped from parts of thin section chips containing representative mixtures of dolomite types based on cathodoluminescence petrography of matching thin sections. Powdered samples were reacted for approximately 12 hours with phosphoric acid at 50°C in an evacuated reaction vessel. Carbon dioxide was drawn off, cryogenically purified, and analyzed in a Finnigan/MAT 251 mass spectrometer.

SYNDEPOSITIONAL DIAGENESIS

Overview

Evidence of syndepositional diagenesis is partially overprinted by later diagenetic events. Evidence of syndepositional diagenesis includes moldic and silicified nodular anhydrite, moldic halite, platy cm-thick intraclasts, intraclasts consisting of decimeter-thick grainstone slabs, grapestone clasts, ooids, stromatolites, and micritic envelopes and cement. Nodular anhydrite and minor halite precipitated within peloidal

packstone and wackestone deposited in supratidal settings. Platy cm-thick intraclasts composed of peloidal packstone probably formed as supratidal crusts and were later reworked into both supratidal and shallow-subtidal deposits. Syndepositional cement within supratidal crusts may have included halite, gypsum, anhydrite, calcite, aragonite, and dolomite. Decimeter-thick slabs of oolitic grainstone are weakly imbricated within an oolitic grainstone matrix, and are interpreted as reworked beachrock. Ooids and stromatolites indicate a range of shallow-subtidal to intertidal, marine to hypersaline settings.

Internal fabrics of ooids are commonly well preserved (for example, figs. 3 and 4), suggesting that many non-skeletal grains were originally calcite instead of aragonite (for example, Sandberg, 1983). In contrast, the aragonitic skeletal fragments of molluscs are preserved as molds. Grapestone clasts and micritic envelopes and cement (fig. 3) probably formed in shallow-subtidal settings.

Syndepositional dolomite and dolomitization

Based on petrography on stained thin sections and petrography using cathodoluminescence, the earliest dolomite within the Prairie du Chien Group is finely-crystalline (<0.02-0.1 mm) dolomite crystals with unzoned red-orange cathodoluminescence. These small dolomite crystals are ubiquitous, and are overgrown and partially replaced by later dolomite phases. Syndepositional dolomite crystals are best preserved within mud-rich rocks, such as peloidal micrites, peloidal wackestone, and boundstone. Perhaps partially-dolomitized micritic carbonates were protected from extensive later replacement dolomitization by their relatively low initial porosity and permeability.

Tidal pumping and evaporation are known to produce supratidal dolomitic crusts in some modern, tropical, supratidal settings (Carballo and others, 1987; Mazzullo and others, 1987; Lasemi and others, 1989). Syndepositional dolomite also precipitates in association with microbial, mat-forming communities on supratidal sabkhas (Patterson and Kinsman, 1977; McKenzie and others, 1980; Muller and others, 1990; Illing and Taylor, 1993). Abundant platy intraclasts are the best candidates for supratidal dolomitic crusts in the Prairie du Chien Group. In addition, muddy-peloidal sabkha sediment containing laminae and moldic anhydrite and gypsum are also likely to have been partially dolomitized syndepositionally.

Petrographic evidence suggests that reducing microenvironments within grains and micritic sediment may have facilitated syndepositional dolomitization of Prairie du Chien Group sediment. Syndepositional

dolomite crystals are commonly similar in size to the peloids that contain them (fig. 5), like the "one-per-peloid" pattern observed in Holocene sediment (Gunatilaka and others, 1984). In contrast, larger grains such as ooids typically contain remnants of multiple 0.02-0.1 mm-size syndepositional dolomite crystals overgrown by late-stage dolomite (fig. 6). In some cases, Prairie du Chien Group peloids are entirely replaced by dolomicrite (fig. 6, righthand part of figure), much of which may be of syndepositional origin.

Dolomite is likely to have also precipitated within subtidally-deposited Prairie du Chien Group sediment without the replacement of aragonite or calcite. Dolo-

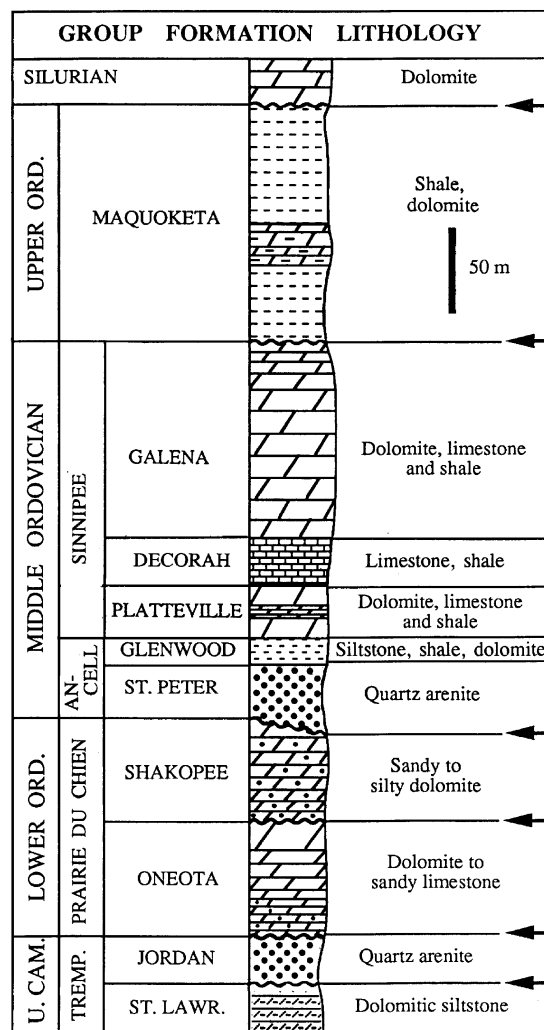


Figure 2. Generalized stratigraphic column for Prairie du Chien Group and associated Upper Cambrian to Upper Ordovician strata. Arrows indicate the positions of major subaerial unconformities.

Figure 3. *Dolomitized grapestone from lower Oneota Formation at Glovers Bluff (GB), Wisconsin. Grapestone and ooids indicate pervasive early cementation. Note dolomitized micritic envelopes. Scale bar = 1 mm.*

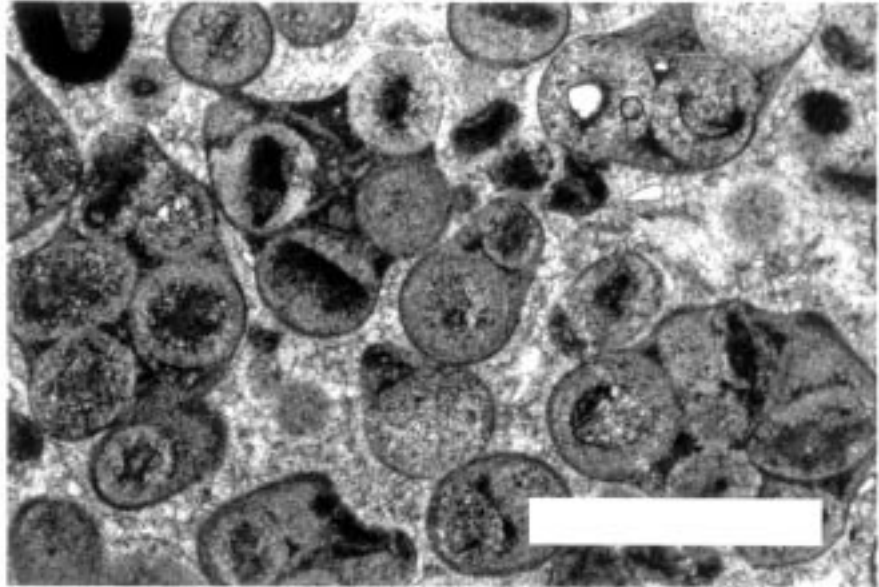
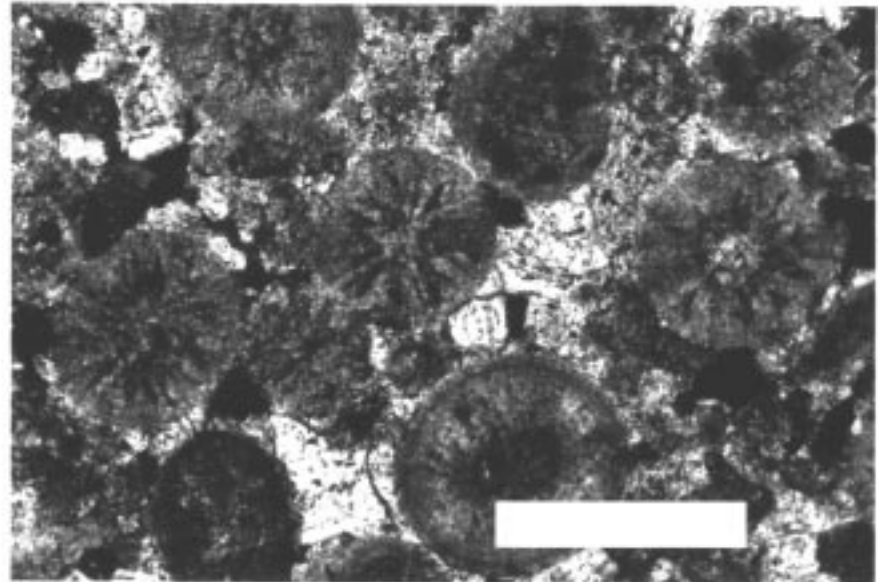
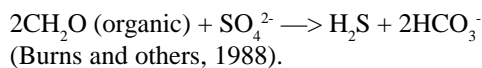


Figure 4. *Dolomitized ooid from lower Oneota Formation at Prairie du Chien, Wisconsin, showing preserved primary fabric. Lack of petrographic evidence for neomorphic recrystallization into coarse calcite suggests primary mineralogy was calcite instead of aragonite. Scale bar = 0.5 mm.*



omite precipitation in marine sediment appears to be in part thermodynamically driven by bacterially-mediated organic carbon oxidation and sulfate reduction according to the general reaction:



Assuming a diffusion-limited seawater source of Mg^{2+} and SO_4^{2-} , marine dolomitization should occur preferentially at shallow burial depths beneath the sediment-water interface (Baker and Burns, 1985; Compton and Siever, 1986; Burns and Baker, 1987). This model for

syndepositional dolomitization is supported by evidence from a variety of modern and ancient carbonate marine sediment (Behrens and Land, 1972; Bone and others, 1991, 1992; Gebelein and others, 1980; Gunatilaka and others, 1984; James and others, 1991; Sass and Katz, 1982; Bein and Land, 1983). Bone and others (1992) suggest that dolomite crystals of marine origin may nucleate later dolomite, although the marine origin of these nuclei could easily be obscured by recrystallization, replacement, and overgrowth. By inference, much of the finely-crystalline (<0.02-0.1 mm), red-orange luminescent dolomite

dispersed within subtidal Prairie du Chien Group sediment is interpreted as marine in origin.

SHALLOW-BURIAL DIAGENESIS

Overview

Shallow-burial diagenesis included carbonate dissolution and karst development, patchy silicification, and possibly the early phases of coarse, fabric-destructive replacement dolomitization and dolomite cementation. Aside from possible dolomitization, these diagenetic events occurred during prolonged subaerial exposure associated with unconformity development

(Smith 1989, 1992; Smith and others, 1993, 1996).

The large-scale paleokarst features formed during the development of the Oneota-Shakopee and Shakopee-St. Peter unconformities have been mapped regionally (summarized in Smith and others, 1996). In contrast, the microscale carbonate fabrics associated with shallow burial and unconformity development are the least well-documented aspect of Prairie du Chien Group diagenesis, in part because later diagenetic overprinting such as regional hydrothermal dolomitization preferentially altered carbonate fabrics associated with high-permeability.

Examples of calcium-carbonate cement fabrics

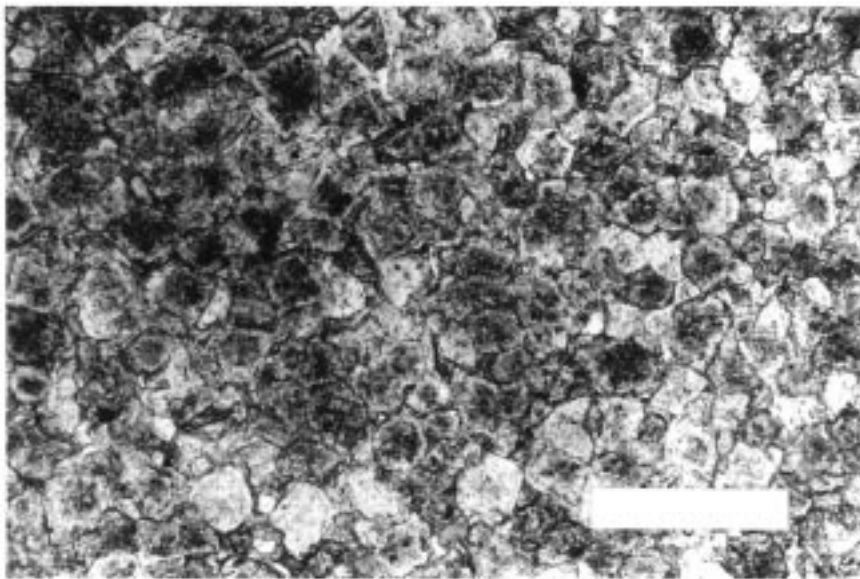


Figure 5. Dolomitized peloidal packstone-wackestone from basal Shakopee Formation at Preston (PE), Minnesota. Dolomite crystal size and peloid size are similar. Scale bar = 0.5 mm.



Figure 6. Dolomitized ooid within dolomitized peloidal packstone-wackestone matrix, from lower Oneota Formation at Madison, Wisconsin. Note relatively coarse dolomite crystals within ooid (left) and finer dolomite crystals within micritic-textured peloidal packstone-wackestone (right). Ooid core is a grain of quartz silt. Scale bar = 0.2 mm.

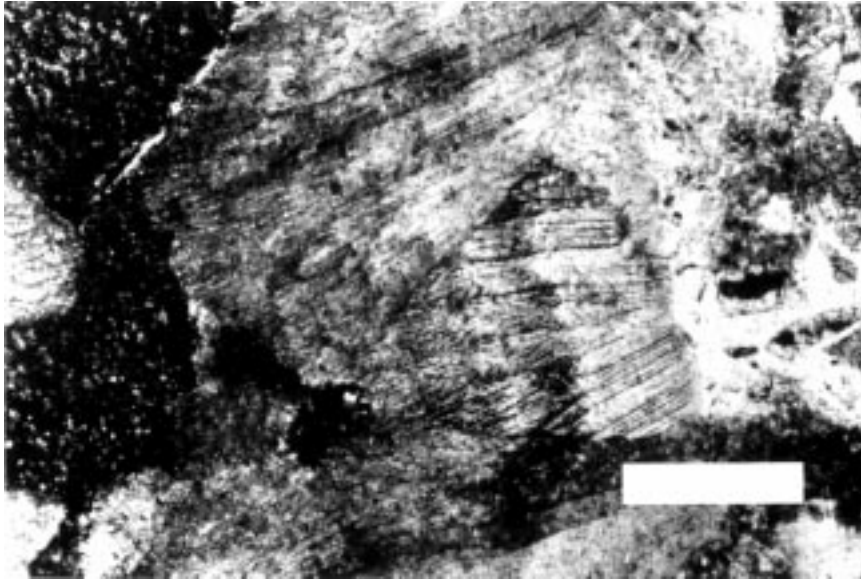


Figure 7. *Dolomitized fibrous (formerly aragonite?) fracture-filling cement, from lower Oneota Formation at Spring Green (SG), Wisconsin. Scale bar = 0.5 mm.*

formed during shallow-burial diagenesis are exceedingly rare within the Prairie du Chien Group. One example contains the ghosts of fibrous cement within later dolomite (fig. 7). The fibrous cement is interpreted as aragonitic fracture-filling cement precipitated within centimeter-wide fractures during paleokarst development. Alternatively, the fibrous cement may have been fibrous high-magnesium calcite precipitated during marine transgression across a karsted land surface.

Shallow-burial dolomite and dolomitization

The Prairie du Chien Group contains a somewhat heterogeneous assortment of dolomite cement and replacement phases unified by the fact that they post-date syndepositional diagenetic features and some paleokarst development, and precede the main events of regional hydrothermal mineralization. Shallow-burial dolomite, as they are termed here, forms cement and fabric-destructive replacement fabrics composed of idiomorphic, subhedral-to-euhedral crystals. Shallow-burial dolomite crystals (0.1-0.5 mm) are larger than the syndepositional dolomite crystals (<0.02-0.1 mm) upon which they nucleated. Under cathodoluminescence, shallow-burial dolomite typically exhibits a distinctive microzoning composed of red-orange and orange microzones, quite unlike the relatively uniform red-orange color of early dolomite, and unlike the blocky microzoning of later hydrothermal dolomite (fig. 8). The distinctively microzoned dolomite is best developed in vuggy pores of the Oneota Formation. Smaller dolomite crystals without dis-

tinct microzones but with similar petrographic relationships and cathodoluminescence colors are present in the overlying Shakopee Formation.

The earliest work on the regional dolomitization of Ordovician carbonates in the study area attributed dolomitization to seawater or evaporative brine (for example, Calvin and Bain, 1900; Leonard, 1905). This work was later corroborated by Asquith (1967) and Deininger (1964), both of whom also primarily examined Middle Ordovician dolostone of the Sinnipee Group. Alternative dolomitization mechanisms that have been proposed include mixing-zone dolomitization (Badiozamani, 1973) and dolomitization by hydrothermal fluids (Deininger, 1964; Sheppard, 1982).

Finely microzoned shallow-burial dolomite from the Prairie du Chien Group is similar in cathodoluminescence pattern to detrital dolomite obtained from the continental shelf of South Australia by Bone and others (1991, 1992). Trace element composition and stable isotopic data suggest that the microzoned Australian dolomite precipitated from seawater below the sediment-water interface (Bone and others, 1992). In contrast, geochemical analyses of Prairie du Chien Group dolomite are inconclusive regarding physiochemical conditions, and Prairie du Chien Group petrography suggests dolomitization of well-lithified strata, not unconsolidated sediment. In addition, the extensive fabric-destructive replacement of precursor carbonate material by shallow-burial dolomite in the Prairie du Chien Group suggest dolomitization by a fluid more corrosive than seawater.

Alternatively, shallow-burial dolomite may have

precipitated within a coastal mixing zone. Mixing zones would have been widespread across our study area during the marine transgressions that followed the regional development of formation-bounding disconformities. The concept of mixing-zone dolomitization (Hanshaw and others, 1971) was first applied to Ordovician carbonates of the study area by Badiozamani (1973), who used it to explain partial dolomitization of the Middle Ordovician Platteville Formation. The chemical underpinning of the mixing-zone model have since been severely questioned (for example, Hardie, 1987). Recent work suggests that modern mixing zones are typically dominated by carbonate dissolution instead of pervasive dolomitization (for example, Back and others, 1986; Sanford and Konikow, 1989), although some dolomite has been shown to precipitate within the seawater-dominated parts of mixing zones (for example, Ward and Halley, 1985).

Regional, fabric-destructive dolomitization of well-lithified limestone by seawater and/or seawater-derived fluids has also been hypothesized (for example, Saller, 1984; Pleydell and others, 1990; Goldstein and others, 1991; James and others, 1991). In all of these cases the dolomitizing fluid appears to have been seawater or seawater-derived evaporative brines, although the actual conditions of dolomitization are not well constrained in all cases.

The Prairie du Chien Group would have been thoroughly flushed by seawater, brackish water, and fresh water during the sea level changes that accompanied development of formation-bounding disconformities. Some mixing-zone dolomitization, and dolomitization by seawater and evaporatively-derived brines probably accompanied marine regressions and transgressions. However it is also possible that the dolomite represents an initial phase (that is, warm, not hot) of hydrothermal dolomitization, and do not represent dolomitization by these other mechanisms. Once again, relevant geochemical evidence is lacking in the Prairie du Chien Group because of extensive replacement by later dolomite phases. All that is certain is that shallow-burial dolomitization followed syndepositional diagenesis and lithification, and preceded further dolomitization by hydrothermal brines.

HYDROTHERMAL DIAGENESIS

Overview

Non-economic occurrences of hydrothermal minerals indicate that regional hydrothermal mineralization affected a 100,000 km² area surrounding the Upper Mississippi Lead-Zinc District, including the study

area (Jenkins, 1968; Heyl and West, 1982). Petrographic and geochemical similarities between the ores and disseminated sulfides from outlying locations support the hypothesis of regional hydrothermal mineralization by the same fluids (Garvin and others, 1987).

Rubidium-strontium dating indicates that hydrothermal mineralization of the Upper Mississippi District occurred during the Early Permian (269 +/- 4 Ma, Rowan and others, 1995). Maximum burial of the district during hydrothermal mineralization is estimated at approximately 1 km, based on apatite fission-track analysis (Zimmerman, 1986).

The following paragenetic sequence has been documented for Mississippi Valley-type ores of the Upper Mississippi Valley: dolomitization, cherty silicification, marcasite and pyrite precipitation, sphalerite and galena precipitation, and calcite precipitation (Tupas, 1950; Heyl and others, 1959). Although the homogenization and final-melting temperatures of fluid inclusions in sphalerite and late-stage calcite have been studied, the earliest hydrothermal mineral phase (dolomite) lacks comparable documentation.

Homogenization temperatures of two-phase fluid inclusions in sphalerite indicate ore precipitation at 75-220°C in the main Upper Mississippi Valley mining district (Newhouse, 1933; Bailey and Cameron, 1951; McLimans, 1977), and precipitation of outlying ores at lower temperatures: 57-116°C (Jenkins, 1968; Coveney and Goebel, 1983; Coveney and others, 1987; Kutz and Spry, 1989). Final melting temperatures of two-phase fluid inclusions in sphalerite indicate precipitation from brines containing 16-24 equiv wt percent NaCl (McLimans, 1977; Kutz and Spry, 1989).

Homogenization temperatures of 38-78°C from late-stage calcite indicate that temperatures decreased toward the end of hydrothermal mineralization (Bailey and Cameron, 1951; Erickson, 1965; Kutz and Spry, 1989). Late-stage calcite precipitated from brine containing 5-23 equiv wt percent NaCl (Hall and Friedman, 1963; Erickson, 1965; Kutz and Spry, 1989), also suggesting local dilution of mineralizing brine by meteoric water (Hall and Friedman, 1963).

Hydrothermal dolomite and dolomitization

Hydrothermal dolomite is a relatively late diagenetic feature and is the youngest dolomite within the Prairie du Chien Group. Hydrothermal dolomite crystals are mainly subhedral to euhedral, idiomorphic (mainly) to xenotopic, and up to 2 mm in size (figs. 8 and 9). In general, xenotopic dolomite crystal textures indicate

Figure 8.
Cathodoluminescence photomicrograph of finely-microzoned dolomite within lower Oneota Formation at Cazenovia (CZ), Wisconsin. Finely microzoned dolomite (B) overgrow poorly-defined earlier dolomite (A), which are overgrown by hydrothermal dolomite (C). Solid black color indicates open porosity. Scale bar = 0.2 mm.

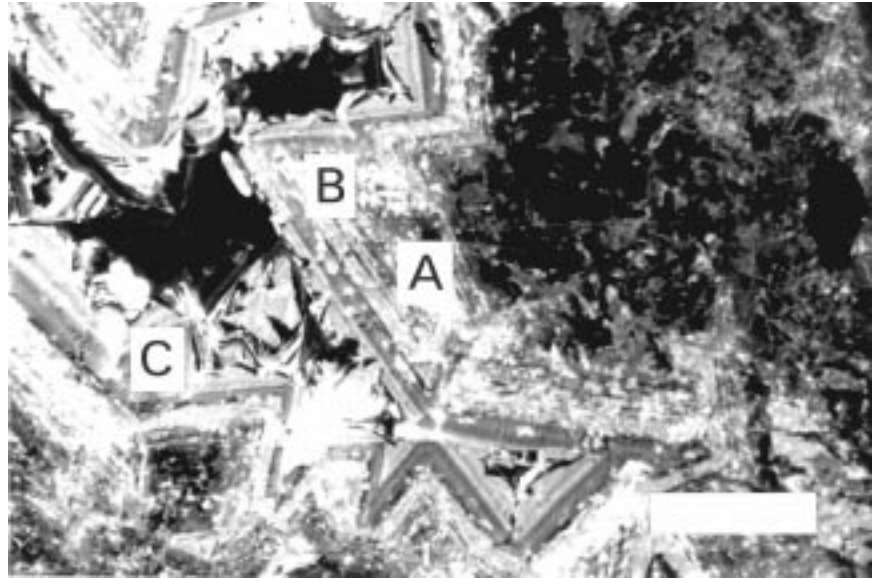
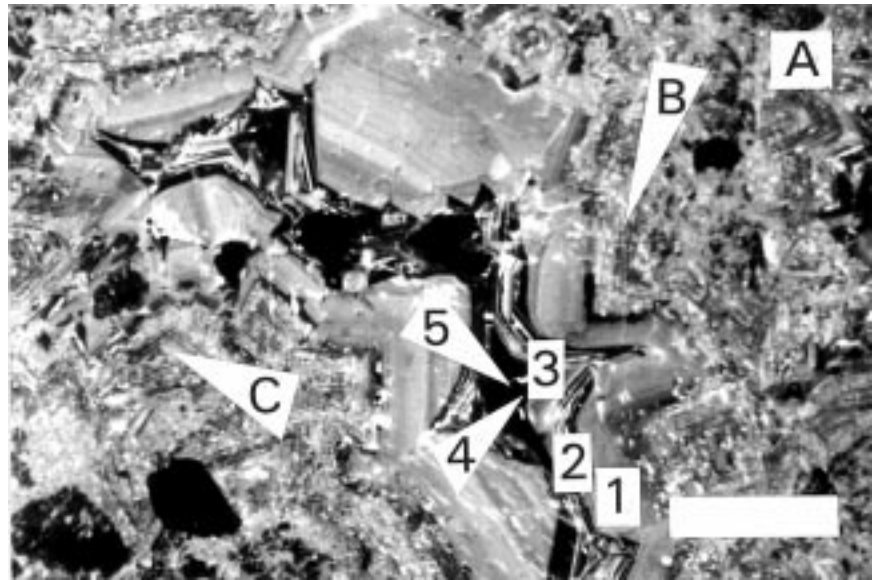


Figure 9.
Cathodoluminescence photomicrograph of hydrothermal dolomite 1-5 filling vuggy pore within lower Oneota Formation at Cazenovia, Wisconsin. Earlier dolomite (A), parts of which contain fine microzones (B), are overgrown and patchily replaced by hydrothermal dolomite 1-5. Note dolomite 3 replacing earlier dolomite at C. Scale bar = 0.2 mm.



crystallization at temperatures $>50\text{-}60^{\circ}\text{C}$ (Gregg, 1982; Gregg and Sibley, 1983, 1984; Radke and Mathis, 1980), however, the dominance of the idiotopic dolomite crystal growth form in the Prairie du Chien Group suggests $50\text{-}60^{\circ}\text{C}$ as the upper limit of fluid temperatures during Prairie du Chien Group dolomitization. These modest temperatures are consistent with petrographic evidence that dolomitization was an early phase of hydrothermal mineralization.

Hydrothermal dolomite replaces and overgrows part of all precursor carbonate material (figs. 8 and 9). This observed replacement of parts of lower-temperature dolomite by higher-temperature dolomite is gen-

erally expected because of the relative thermodynamic instability of calcium-rich, relatively disordered lower-temperature dolomite (for example, Land, 1980, 1985). Hydrothermal dolomite is itself locally replaced and/or overgrown by hydrothermal calcite (fig. 10), the last phase of regional hydrothermal mineralization in the Upper Mississippi Valley (Tupas, 1950).

Hydrothermal dolomite from Prairie du Chien Group outcrops displays a consistent sequence of cathodoluminescence colors (fig. 9): dull orange (dolomite 1), microzoned red and black (dolomite 2), red (dolomite 3), dark red (dolomite 4), and black

(dolomite 5). Dolomite 1, 2 (where present), and 3 are generally separated by microdissolution surfaces. Dolomite 1 is the most abundant hydrothermal dolomite phase (for example, fig. 9). The trend toward darker (“quenched”) cathodoluminescence is accompanied by an increase in Fe/Mn ratios from 1.3 to 12.8 (table 1). Dolomite 4 and 5 are particularly ferroan and average 5600 to 12,800 ppm Fe (table 1).

Dolomite 1 (dull orange) and 3 (red) can be visually correlated between ore bodies and dolomitized parts of the Prairie du Chien Group and Sinnipee Groups. Dolomite from Upper Mississippi Valley lead-zinc ore typically consists of dolomite 1 and a thin, discontinuous rim of dolomite 3. Within ore deposits, dolomite 3 precipitated just prior to sulfide precipitation and is commonly overgrown by marcasite or sphalerite (Heyl and others, 1959).

Dolomite 4 (dark red) and 5 (black) was only identified in Prairie du Chien Group samples from outside of ore deposits, although these ferroan dolomite phases also occur as isolated vein- and mold-filling cement in relatively unaltered limestone of the Platteville Formation (Sheppard, 1982). Precipitation of the ferroan dolomite throughout the outcrop area probably overlapped with precipitation of marcasite and pyrite in the ore bodies (for example, Tupas, 1950; Heyl and others, 1959), and with precipitation of disseminated epigenetic iron sulfide identified by Heyl and West (1982) and Garvin and others (1987).

Late-stage hydrothermal calcite

Four phases of progressively less-ferroan calcite precipitated after the peak of sulfide precipitation (fig. 10, table 1; Calcites I-IV of Tupas, 1950). Although each calcite phase partially replaces precursor carbonate phases, the hydrothermal calcite primarily form cement and are best developed within centimeter-scale

vuggy pores containing marcasite and pyrite.

Calcites I and II typically occur as isolated millimeter-scale cement crystals (fig. 10A). Calcite III forms larger, centimeter-scale scalenohedral cement crystals that are typically overgrown but not replaced by calcite IV (fig. 10B). Where these late-stage calcites are abundant, calcite IV commonly occludes remaining pore space. Calcites I-IV are locally abundant within the Prairie du Chien Group and have also been documented within the Platteville Formation (Sheppard, 1982).

NEAR-SURFACE WEATHERING

Based on the absence of Mesozoic and Tertiary sediment, the study area has experienced nondeposition and/or erosion throughout most of the Mesozoic and Cenozoic. Karst development continues to the present. Other, relatively recent paleokarst is buried beneath Pleistocene glacial sediment. Post-hydrothermal carbonate diagenesis has been dominated by near-surface weathering and karst development, accompanied by the precipitation of aragonitic and calcitic speleothems.

STABLE ISOTOPE GEOCHEMISTRY

The results of 43 whole-rock analyses of Prairie du Chien Group dolomite, dolomite from Upper Mississippi Valley District ores, and other Upper Cambrian and Middle Ordovician dolomite are shown in figure 11 and table 2. Oxygen isotope values of Prairie du Chien Group dolomite ranges from $\delta^{18}\text{O} = -6.39$ to -3.49 , whereas carbon isotopic values range from $\delta^{13}\text{C} = -5.91$ to -1.50 . Isotopic values for oxygen and carbon do not display consistent geographic or stratigraphic trends, and do not vary consistently based on rock type. The oxygen and carbon stable isotopic values of Upper Cambrian and Middle Ordovician dolo-

Table 1. Dolomite trace element data obtained by electron microprobe analysis. Values in parentheses indicate 95% confidence intervals.

Color*	Fe/Mn	Ca/Mg (moles)	Fe (ppm, wt)	Mn (ppm, wt)	Sr (ppm, wt)	Na (ppm, wt)
A. Pre-hydrothermal dolomite (bulk composition)						
orange and red	1.6	1.05 (1.04, 1.06)	450 (340, 570)	290 (230, 340)	120 (60, 180)	210 (72, 350)
B. Hydrothermal dolomites 1-5						
1- orange	3	1.03 (1.02, 1.04)	450 (370, 530)	350 (290, 410)	80 (40, 120)	40 (0, 170)
2- red/blk	0.9	1.05 (1.04, 1.06)	120 (50, 180)	130 (70, 190)	90 (40, 140)	150 (20, 290)
3- red	2.8	1.04 (1.03, 1.05)	2310 (1880, 2750)	820 (480, 1160)	90 (40, 150)	40 (0, 70)
4- dark red	7.5	1.04 (1.02, 1.05)	5630 (4860, 6410)	750 (550, 950)	30 (-30, 90)	30 (-20, 90)
5- black	12.8	1.00 (1.00, 1.02)	12780 (10560, 15010)	1000 (570, 1420)	110 (20, 200)	30 (-10, 70)

*Color = cathodoluminescence color

mite sampled from outcrops are generally similar to Prairie du Chien Group values.

Oxygen and carbon isotopes from Upper Mississippi Valley district ore samples are generally greater than values from outcrop samples. Oxygen isotopic values from Upper Mississippi samples range from $\delta^{18}\text{O} = -3.74$ to -2.42 , and carbon isotopic values vary from $\delta^{13}\text{C} = -0.29$ to -0.18 (table 2). These numbers fall within the range of previously published isotopic values of Upper Mississippi Valley ores (for example, fig. 11; Hall and Friedman, 1969; Garvin and others, 1987; $\delta^{18}\text{O} = -4$ to -2 , $\delta^{13}\text{C} = -0.5$ to $+0.5$) and are consistent with precipitation from hypersaline, evaporite-derived brines (for example, Kutz and Spry, 1989).

Because of their history of partial replacement and overgrowth, dolomite from Prairie du Chien Group outcrops is heterogeneous in composition (for example, fig. 9). Therefore, the $\delta^{18}\text{O}$ and $\delta^{13}\text{C}$ values of Prairie du Chien Group dolomite represent compositional averages of syndepositional, shallow-burial, and hydrothermal dolomite. The $\delta^{18}\text{O}$ values of Prairie du Chien Group dolomite are consistent with mainly seawater-derived, Early Ordovician calcium carbonate (for example, fig. 11; Lohmann, 1988, p. 67). The $\delta^{13}\text{C}$ values of Prairie du Chien Group dolomite is somewhat lower than Early Ordovician seawater-derived carbonate (for example, Lohmann, 1988, p. 67), but biogenic grains commonly display ^{12}C enrichment (for example, Tucker and Wright, 1990, p. 325). In spite of petro-

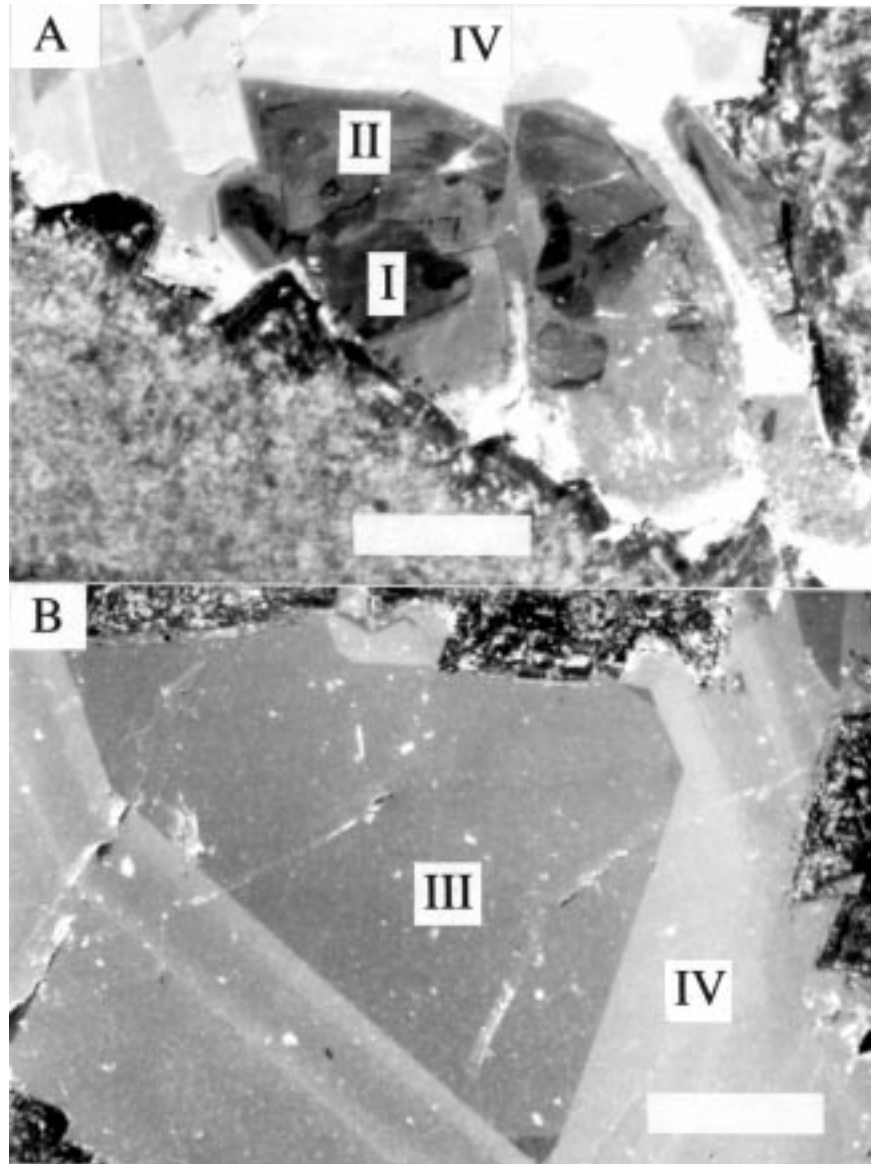


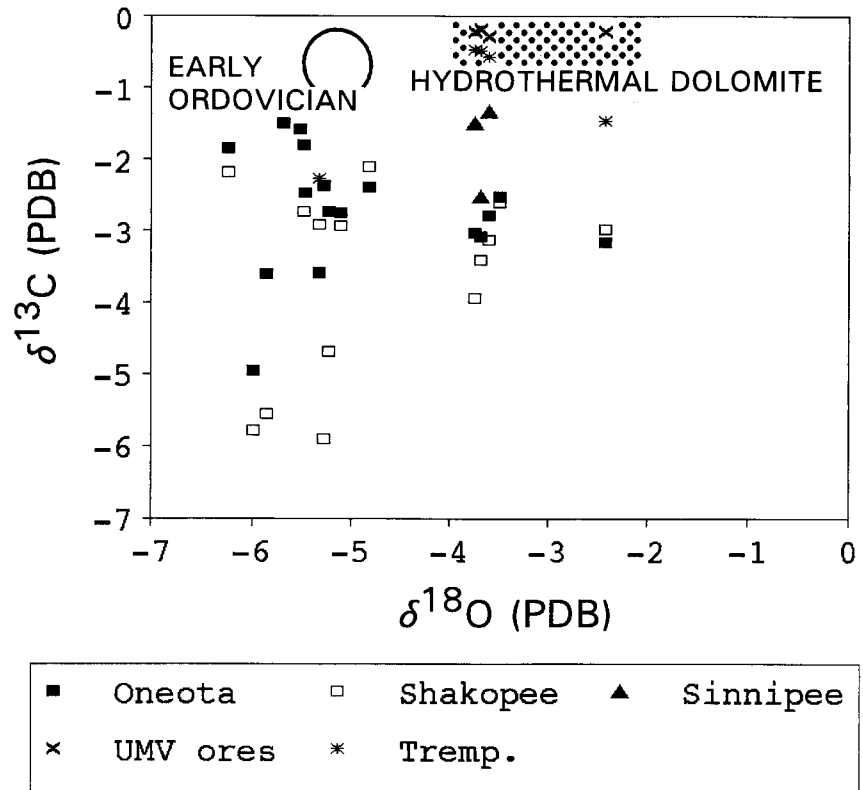
Figure 10. Examples of hydrothermal calcites I-IV, lower Oneota Formation, Preston (PE), Minnesota. Roman numerals I-IV from Tupas (1950). A. Scale bar = 0.2 mm. B. Scale bar = 0.5 mm.

graphic evidence for pervasive hydrothermal dolomitization, Prairie du Chien Group dolomite does not appear to have acquired the heavier $\delta^{18}\text{O}$ and $\delta^{13}\text{C}$ values characteristic of Upper Mississippi Valley dolomite. This combination of hydrothermally-overprinted microfabrics and non-Upper Mississippi Valley $\delta^{18}\text{O}$ and $\delta^{13}\text{C}$ values suggests that much of the replacive dolomitization in the Prairie du Chien Group has involved local dissolution and reprecipitation of precursor carbonate material.

Table 2. Values of $\delta^{13}\text{C}$ and $\delta^{18}\text{O}$ from Upper Cambrian to Middle Ordovician dolomite analyzed in this study. Values shown relative to the PDB standard. Samples are archived at the University of Wisconsin-Madison under “U.W.1866/number.”

Sample	$\delta^{13}\text{C}$ (PDB)	$\delta^{18}\text{O}$ (PDB)	Comments
A. Galena and Decorah Formations			
MVT-2A, U.W.1866/30	-0.22	-3.74	sulfide ore, zoned dolomite
MVT-2B-1, U.W.1866/31	-0.18	-3.68	sulfide ore, saddle dolomite
MVT-2A-2, U.W.1866/32	-0.29	-3.61	sulfide ore, zoned dolomite
MVT-15B, U.W.1866/33	-0.22	-2.42	sulfide ore, zoned dolomite
BV-GAL, U.W.1866/29	-1.49	-5.32	outcrop, peloidal-bioclastic packstone
B. Platteville Formation			
PE-PL, U.W.1866/36	-2.50	-6.24	outcrop, peloidal-bioclastic packstone
PDC-PL-D, U.W.1866/35	-1.34	-5.48	outcrop, peloidal-bioclastic packstone
C. Shakopee Formation (west to east, arranged stratigraphically for each location)			
PE-58, U.W.1866/47	-3.94	-4.82	outcrop, peloidal dolomicrite
PE-50-OO, U.W.1866/45	-3.41	-3.49	outcrop, oolitic grainstone
PE-50-ST, U.W.1866/46	-3.11	-5.10	outcrop, stromatolite
PDC-120, U.W.1866/44	-2.97	-5.22	outcrop, oolitic grainstone
PDC-74, U.W.1866/43	-2.90	-5.28	outcrop, peloidal dolomicrite
CZ-1, U.W.1866/37	-2.17	-5.98	outcrop, oolitic grainstone
CZ-33, U.W.1866/40	-2.73	-5.84	outcrop, oolitic grainstone
CZ-30, U.W.1866/39	-2.09	-5.51	outcrop, peloidal dolomicrite
CZ-2, U.W.1866/38	-2.59	-5.68	outcrop, oolitic packstone
HR-21, U.W.1866/41	-2.92	-5.46	outcrop, peloidal wackestone
HR-NR, U.W.1866/42	-4.68	-5.07	outcrop, peloidal wackestone
BN-2-1, U.W.1866/64	-5.91	-5.20	cuttings, oo-peloidal packstone
BN-2-2, U.W.1866/65	-5.79	-5.00	cuttings, oo-peloidal packstone
BN-3, U.W.1866/66	-5.55	-5.10	cuttings, oo-peloidal packstone
D. Oneota Formation (west to east, arranged stratigraphically for each location)			
PE-16-1, U.W.1866/57	-3.02	-4.86	outcrop, peloidal wackestone
PE-16-2, U.W.1866/58	-3.07	-4.87	outcrop, peloidal wackestone
PE-11, U.W.1866/56	-2.77	-5.15	outcrop, oolitic grainstone
PDC-7, U.W.1866/55	-3.16	-4.86	outcrop, peloidal dolomicrite
PDC-5, U.W.1866/54	-3.58	-4.90	outcrop, oolitic grainstone
CZ-3-1, U.W.1866/48	-1.84	-6.23	outcrop, oo-peloidal packstone
CZ-3-2, U.W.1866/49	-1.78	-6.39	outcrop, oo-peloidal packstone
CZ-9, U.W.1866/53	-2.37	-5.84	outcrop, oo-peloidal packstone
CZ-6, U.W.1866/52	-2.51	-5.79	outcrop, peloidal packstone
CZ-4-1, U.W.1866/50	-2.74	-5.55	outcrop, oolitic packstone
CZ-4-2, U.W.1866/51	-2.73	-5.61	outcrop, oolitic packstone
SW-7, U.W.1866/59	-2.36	-5.63	outcrop, stromatolite
BN-4, U.W.1866/67	-4.95	-5.39	cuttings, oolitic packstone
BN-5, U.W.1866/68	-3.61	-5.56	cuttings, oo-peloidal packstone
BN-6-1, U.W.1866/69	-1.57	-5.74	cuttings, oolitic grainstone
BN-6-2, U.W.1866/70	-1.50	-5.84	cuttings, oolitic grainstone
BN-7, U.W.1866/71	-2.47	-5.76	cuttings, oolitic grainstone
E. Trempealeau Group (St. Lawrence Formation, west to east)			
RW-STL-1, U.W.1866/62	-0.47	-5.48	outcrop, dolomitic siltstone
RW-STL-2, U.W.1866/63	-0.48	-5.46	outcrop, dolomitic siltstone
BE-STL, U.W.1866/60	-0.56	-5.48	outcrop, stromatolite
M-STL, U.W.1866/61	-1.45	-4.91	outcrop, stromatolite
BN-8, U.W.1866/72	-2.27	-6.11	cuttings, dolomitic siltstone

Figure 11. Scatter plot of $\delta^{18}\text{O}$ and $\delta^{13}\text{C}$ values from Upper Cambrian-Middle Ordovician dolomite analyzed in this study. Circle labeled "Early Ordovician" indicates estimate of seawater composition based on primary calcite compositions (Lohmann, 1988). Rectangular field labeled "hydrothermal dolomite" indicates range of values obtained by Hall and Friedman (1969) and Garvin and others (1987) from dolomite associated with Upper Mississippi Valley district ores.



CONCLUSIONS

Carbonate diagenesis of the Prairie du Chien Group included syndepositional diagenesis, shallow-burial diagenesis, hydrothermal diagenesis, and near-surface weathering. Dolomitization has been a prominent aspect of carbonate diagenesis, and occurred during syndepositional, shallow-burial, and hydrothermal diagenesis, although shallow-burial dolomitization may actually be an early, relatively low-temperature phase of hydrothermal diagenesis.

The sequence of diagenetic events within the Prairie du Chien Group is well-constrained by petrography and cathodoluminescence petrography. Iron and magnesium trace-element data corroborate previous work on Upper Mississippi Valley ore paragenesis, and support a more detailed interpretation of the timing of hydrothermal dolomitization and late-stage hydrothermal calcite precipitation relative to the main phases of Upper Mississippi Valley ore precipitation. Values of $\delta^{18}\text{O}$ and $\delta^{13}\text{C}$ are consistent with precipitation of most Prairie du Chien Group carbonate from Early Ordovician seawater. Although petrography and cathodoluminescence petrography indicate pervasive hydrothermal dolomite cementation and replacement of precursor carbonate, differences between the values

of $\delta^{18}\text{O}$ and $\delta^{13}\text{C}$ for Prairie du Chien Group dolomite and dolomite from Upper Mississippi Valley ore deposits suggest that most hydrothermal dolomitization within the Prairie du Chien Group involved the dissolution and local reprecipitation of precursor carbonate material. In summary, because of sequential, partial, patchy replacement of preexisting carbonate phases by later phases, the diagenetic history of the Prairie du Chien Group is supported primarily by petrography and cathodoluminescence petrography, not by geochemical data.

ACKNOWLEDGMENTS

This research was partially supported by grants from the American Association of Petroleum Geologists, ARCO Oil and Gas Company, the Gas Research Institute, Sigma Xi—The Scientific Research Society, and the University of Wisconsin Graduate School. Stable isotope analyses were conducted at the Stable Isotope Laboratory of the University of Wisconsin-Madison; we thank J.W. Valley for the use of the laboratory and K. Baker and P. Drzewieki for conducting stable isotope analyses. Our project benefitted from multiple discussions with D.F. Sibley of Michigan State University and P.E. Brown, C.W. Byers, R.H. Dott, Jr.,

and J.W. Valley of the University of Wisconsin-Madison. We thank B.H. Purser, D.F. Sibley, M.E. Tucker, and D.H. Zenger for their reviews of an earlier version of this manuscript, and B.A. Brown, M.T. Harris, M.G. Mudrey, Jr., and R.M. Peters for their reviews of this manuscript.

Note: The use of brand names in this paper does not imply support for this research or endorsement by the Wisconsin Geological and Natural History Survey or Lawrence University.

REFERENCES

- Adams, R.L., 1978, Stratigraphy and petrology of the lower Oneota Dolomite (Ordovician), south-central Wisconsin, in *Lithostratigraphy, petrology, and sedimentology of Late Cambrian-Early Ordovician rocks near Madison, Wisconsin*: Wisconsin Geological and Natural History Survey Field Trip Guide Book 3, p. 82-90.
- Agnew, A.F., Heyl, A.V., Behre, C.H., and Lyons, E.J., 1956, Stratigraphy of the Middle Ordovician rocks in the zinc-lead district of Wisconsin, Illinois, and Iowa: United States Geological Survey Professional Paper 274-K, p. 251-312.
- Asquith, G.B., 1967, The marine dolomitization of the Mifflin Member Platteville Limestone in southwest Wisconsin: *Journal of Sedimentary Petrology*, v. 37, p. 311-326.
- Austin, G.S., 1971, The stratigraphy and petrology of the Shakopee Formation, Minnesota: unpublished Ph.D. dissertation, University of Iowa, Iowa City, 216 p.
- Back, W., Hanshaw, B.B., Herman, J.S., and van Driel, J.N., 1986, Differential dissolution of a Pleistocene reef in the ground-water mixing zone of coastal Yucatan, Mexico: *Geology*, v. 14, p. 137-140.
- Badiozamani, K., 1973, The Dorag dolomitization model—application to the Middle Ordovician of Wisconsin: *Journal of Sedimentary Petrology*, v. 43, p. 965-984.
- Bailey, S.W., and Cameron, E.N., 1951, Temperatures of mineral formation in bottom-run lead-zinc deposits of the Upper Mississippi Valley, as indicated by liquid inclusions: *Economic Geology*, v. 46, p. 626-651.
- Bain, H.F., 1906, Zinc and lead deposits of the Upper Mississippi Valley: United States Geological Survey Bulletin 294, p. 17-52.
- Baker, P.A., and Burns, S.J., 1985, The occurrence and formation of dolomite in organic-rich continental margin sediments: *American Association of Petroleum Geologists Bulletin*, v. 69, p. 1917-1930.
- Behrens, E.W., and Land, L.S., 1972, Subtidal Holocene dolomite, Baffin Bay, Texas: *Journal of Sedimentary Petrology*, v. 42, p. 155-161.
- Bein, A., and Land, L.S., 1983, Carbonate sedimentation and diagenesis associated with Mg-Ca-Chloride brines—the Permian San Andres Formation in the Texas Panhandle: *Journal of Sedimentary Petrology*, v. 53, p. 243-260.
- Bone, Y., James, N.P., and Kyser, T.K., 1991, Multi-cycle Holocene dolomite in cool-water carbonate sediments, Lacepede Shelf, South Australia: *American Association of Petroleum Geologists Bulletin*, v. 75, p. 545.
- Bone, Y., James, N.P., and Kyser, T.K., 1992, Synsedimentary detrital dolomite in Quaternary cool-water carbonate sediments, Lacepede Shelf, South Australia: *Geology*, v. 20, p. 109-112.
- Burns, S.J., and Baker, P.A., 1987, A geochemical study of dolomite in the Monterey Formation, California: *Journal of Sedimentary Petrology*, v. 57, p. 128-139.
- Burns, S.J., Baker, P.A., and Showers, W.J., 1988, The factors controlling the formation and chemistry of dolomite in organic-rich sediments: Miocene Drakes Bay Formation, California, in Shukla, V., and Baker, P.A., eds., *Sedimentology and Geochemistry of Dolostones*: SEPM Special Publication 43, p. 41-52.
- Calvin, S., and Bain, H.F., 1900, Geology of Dubuque County: Iowa Geological Survey, v. 10, p. 379-622.
- Carballo, J.D., Land, L.S., and Miser, D.E., 1987, Holocene dolomitization of supratidal sediments by active tidal pumping, Sugarloaf Key, Florida: *Journal of Sedimentary Petrology*, v. 57, p. 153-165.
- Compton, J.S., and Siever, R., 1986, Diffusion and mass balance of Mg during early dolomite formation, Monterey Formation: *Geochimica et Cosmochimica Acta*, v. 50, p. 125-136.
- Coveney, R.M., and Goebel, E.D., 1983, New fluid inclusion homogenization temperatures for sphalerite from minor occurrences in the mid-continent area, in

- Kisvarsanyi, G., Grant, S.K., Pratt, W.P., and Koenig, J.W., eds., International conference on Mississippi Valley-type lead-zinc deposits, Proceedings Volume: University of Missouri-Rolla Press, p. 234-242.
- Coveney, R.M., Jr., Goebel, E.D., and Ragan, V.M., 1987, Pressures and temperatures from aqueous fluid inclusions in sphalerite from midcontinent country rocks: *Economic Geology*, v. 82, p. 740-751.
- Davis, R.A., Jr., 1966, Willow River Dolomite — Ordovician analogue of modern algal stromatolite environments: *Journal of Geology*, v. 74, p. 908-923.
- Davis, R.A., Jr., 1970, Prairie du Chien Group in the upper Mississippi Valley, in Field trip guidebook for Cambrian-Ordovician geology of western Wisconsin: Wisconsin Geological and Natural History Survey Information Circular 11, p. 35-44.
- Davis, R.A., Jr., 1972, Prairie du Chien Group (L. Ord.) in the upper Mississippi Valley: Wisconsin Geological and Natural History Survey Open-File Report 71-2, 71 p.
- Deininger, R.W., 1964, Limestone-dolomite transition in the Ordovician Platteville Formation in Wisconsin: *Journal of Sedimentary Petrology*, v. 34, p. 281-288.
- Erickson, A.J., Jr., 1965, Temperatures of calcite deposition in the Upper Mississippi Valley lead-zinc deposits: *Economic Geology*, v. 60, p. 506-528.
- Garvin, P.L., Ludvigson, G.A., and Ripley, E.M., 1987, Sulfur isotope reconnaissance of minor metal sulfide deposits fringing the Upper Mississippi Valley Zinc-Lead District: *Economic Geology*, v. 82, p. 1386-1394.
- Gebelein, C.D., Steinen, R.P., Garrett, P., Hoffman, E.J., Queen, J.M., and Plummer, L.N., 1980, Subsurface dolomitization beneath the tidal flats of central west Andros Island, Bahamas, in Zenger, D.H., Dunham, J.B., and Ethington, R.L., eds., Concepts and models of dolomitization: SEPM Special Publication 28, p. 31-49.
- Goldstein, R.H., Stephens, B.P., and Lehrmann, D.J., 1991, Fluid inclusions elucidate conditions of dolomitization in Eocene of Enewetak Atoll and mid-Cretaceous Valles Platform of Mexico: International Association of Sedimentologists Abstracts of Papers for Dolomieu Conference on Carbonate Platforms and Dolomitization, p. 92-93.
- Gregg, J.M., 1982, The origin of xenotopic dolomite texture: unpublished Ph.D. dissertation, Michigan State University, East Lansing, Michigan, 151 p.
- Gregg, J.M., and Sibley, D.F., 1983, Xenotopic dolomite texture—implications for dolomite neomorphism and late diagenetic dolomitization in the Galena Group (Ordovician), Wisconsin and Iowa, in Delgado, D.J., ed., Ordovician Galena Group of the Upper Mississippi Valley: Guidebook for the 13th Annual Field Conference, Great Lakes-SEPM, p. G1-G15.
- Gregg, J.M., and Sibley, D.F., 1984, Epigenetic dolomitization and the origin of xenotopic dolomite texture: *Journal of Sedimentary Petrology*, v. 54, p. 908-931.
- Gunatilaka, A., Sahleh, A., Al-Temeemi, A., and Nassar, N., 1984, Occurrence of subtidal dolomite in a hypersaline lagoon, Kuwait: *Nature*, v. 311, p. 450-452.
- Hall, W.E., and Friedman, I., 1963, Composition of fluid inclusions, Cave-in-Rock fluorite district, Illinois, and Upper Mississippi Valley zinc-lead district: *Economic Geology*, v. 38, p. 886-911.
- Hall, W.E., and Friedman, I., 1969, Oxygen and carbon stable isotopic composition of ore and host rock of selected Mississippi Valley deposits: United States Geological Survey Professional Paper 650-C, p. C140-C148.
- Hanshaw, B.B., Back, W., and Deike, R.G., 1971, A geochemical hypothesis for dolomitization by groundwater: *Economic Geology*, v. 66, p. 710-724.
- Hardie, L.A., 1987, Dolomitization: a critical view of some current views: *Journal of Sedimentary Petrology*, v. 57, p. 166-183.
- Heyl, A.V., Jr., Agnew, A.F., Lyons, E.J., and Behre, C.H., Jr., 1959, The geology of the Upper Mississippi Valley zinc-lead district: United States Geological Survey Professional Paper 309, 310 p.
- Heyl, A.V., and West, W.S., 1982, Outlying mineral occurrences related to Upper Mississippi Valley mineral district, Wisconsin, Iowa, Illinois and Minnesota: *Economic Geology*, v. 77, p. 1803-1817.

- Illing, L.V., and Taylor, J.C.M., 1993, Penecontemporaneous dolomitization in Sabkha Faishakh, Qatar: evidence from changes in the chemistry of the interstitial brines: *Journal of Sedimentary Petrology*, v. 63, p. 1042-1048.
- James, N.P., Bone, Y., and Kyser, T.K., 1991, Shallow burial dolomitization of mid-Cenozoic, cool-water, calcitic, deep-shelf limestones, South Australia: *American Association of Petroleum Geologists Bulletin*, v. 75, p. 602.
- Jenkins, R.A., 1968, Epigenetic sulfide mineralization in the Paleozoic rocks of eastern and southern Wisconsin: unpublished M.S. thesis, University of Wisconsin-Madison, Wisconsin, 46 p.
- Kutz, K.B., and Spry, P.G., 1989, The genetic relationship between Upper Mississippi Valley district lead-zinc mineralization and minor base metal mineralization in Iowa, Wisconsin, and Illinois: *Economic Geology*, v. 84, p. 2139-2154.
- Land, L.S., 1980, The isotopic and trace element geochemistry of dolomite—the state of the art, in Zenger, D.H., Dunham, J.B., and Ethington, R.L., eds., *Concepts and models of dolomitization: SEPM Special Publication 28*, p. 87-110.
- Land, L.S., 1985, The origin of massive dolomite: *Journal of Geological Education*, v. 33, p. 112-125.
- Lasemi, Z., Boardman, M.R., and Sandberg, P.A., 1989, Cement origin of supratidal dolomite, Andros Island, Bahamas: *Journal of Sedimentary Petrology*, v. 59, p. 249-257.
- Leonard, A.C., 1905, Geology of Clayton County: Iowa Geological Survey, v. 16, p. 213-318.
- Lohmann, K.C., 1988, Geochemical patterns of meteoric diagenetic systems and their application to studies of paleokarst, in James, N.P., and Choquette, P.W., eds., *Paleokarst*: Springer-Verlag, New York, p. 58-80.
- Mazzullo, S.J., Reid, A.M., and Gregg, J.M., 1987, Dolomitization of Holocene Mg-calcite supratidal deposits, Ambergris Cay, Belize: *Geological Society of America Bulletin*, v. 98, p. 224-231.
- McLimans, R.K., 1977, Geological fluid inclusion, and stable isotope studies of the Upper Mississippi Valley zinc-lead district, southwest Wisconsin: unpublished Ph.D. dissertation, Pennsylvania State University, State College, Pennsylvania, 175 p.
- McKenzie, J.A., Hsu, K.J., and Schneider, J.F., 1980, Movement of subsurface waters under the sabkha, Abu Dhabi, U.A.E., and its relation to evaporative dolomite genesis, in Zenger, D.H., Dunham, J.B., and Ethington, R.L., eds., *Concepts and Models of Dolomitization: SEPM Special Publication 28*, p. 175-189.
- Muller, D.W., McKenzie, J.A., and Mueller, P.A., 1990, Abu Dhabi sabkha, Persian Gulf, revisited—application of strontium isotopes to test an early dolomitization model: *Geology*, v. 18, p. 618-621.
- Newhouse, W.H., 1933, The temperature of formation of the Mississippi Valley lead-zinc deposits: *Economic Geology*, v. 28, p. 744-750.
- Ostrom, M.E., 1970, Sedimentation cycles in the lower Paleozoic rocks of western Wisconsin, in Field trip guidebook for Cambrian-Ordovician geology of western Wisconsin: Wisconsin Geological and Natural History Survey Information Circular 11, p. 10-34.
- Patterson, R.J., and Kinsman, D.J.J., 1977, Marine and continental groundwater sources in a Persian Gulf coastal sabkha: *American Association of Petroleum Geologists Studies in Geology*, v. 4, p. 381-397.
- Pleydell, S.M., Jones, B., Longstaffe, F.J., and Baadsgard, H., 1990, Dolomitization of the Oligocene-Miocene Bluff Formation on Grand Cayman, British West Indies: *Canadian Journal of Earth Science*, v. 27, p. 1098-1110.
- Raasch, G.O., 1952, Oneota Formation, Stoddard Quadrangle, Wisconsin: *Illinois Academy of Science Transactions*, v. 45, p. 85-95.
- Radke, B.M., and Mathis, R.L., 1980, On the formation and occurrence of saddle dolomite: *Journal of Sedimentary Petrology*, v. 50, p. 1149-1168.
- Rowan, E.L., Goldhaber, M.B., and Hatch, J.R., 1995, Duration of mineralization in the upper Mississippi Valley lead-zinc district: implications for the thermal-hydrologic history of the Illinois basin (abs.): *Geological Society of America Abstracts with Programs*, v. 27, p. A-328.

- Saller, A.H., 1984, Petrologic and geochemical constraints on the origin of subsurface dolomite, Enewetok Atoll: an example of dolomitization by normal seawater: *Geology*, v. 12, p. 221-225.
- Sandberg, P.A., 1983, An oscillating trend in Phanerozoic non-skeletal carbonate mineralogy: *Nature*, v. 305, p. 19-22.
- Sanford, W.E., and Konikow, L.F., 1989, Porosity development in coastal carbonate aquifers: *Geology*, v. 17, p. 249-252.
- Sass, E., and Katz, A., 1982, The origin of platform dolomites: *American Journal of Science*, v. 282, p. 1184-1213.
- Shea, J.H., Stratigraphy of the Lower Ordovician New Richmond Sandstone in the upper Mississippi Valley: unpublished M.S. thesis, University of Wisconsin-Madison, Wisconsin, 90 p.
- Sheppard, C.E., III, 1982, Stratigraphic, petrographic, and geochemical analysis of the diagenetic phases and processes in the Platteville Formation: unpublished M.S. thesis, State University of New York at Stony Brook, New York, 225 p.
- Smith, G.L., 1989, Karsting and eolian deposition during a pre-New Richmond (Early Ordovician) sea level drawdown, Prairie du Chien Group, Upper Mississippi Valley: *Geological Society of America Abstracts with Programs*, v. 21, p. A80.
- Smith, G.L., 1990, Dolomitization of the Lower Ordovician Prairie du Chien Group in southern Wisconsin and southeastern Minnesota—a case for confined and unconfined aquifer systems: *American Association of Petroleum Geologists Bulletin*, v. 74, p. 766.
- Smith, G.L., 1991, Sequence stratigraphy and diagenesis of the Lower Ordovician Prairie du Chien Group on the Wisconsin Arch and in the Michigan Basin: unpublished Ph.D. dissertation, University of Wisconsin-Madison, Wisconsin, 265 p.
- Smith, G.L., 1992, Silicification associated with the Sauk-Tippecanoe and older unconformities, Prairie du Chien Group (L. Ord.), Wisconsin: *Geological Society of America Abstracts with Programs*, v. 24, p. A287.
- Smith, G.L., Byers, C.W., and Dott, R.H., Jr., 1993, Sequence stratigraphy of the Lower Ordovician Prairie du Chien Group on the Wisconsin Arch and in the Michigan Basin: *American Association of Petroleum Geologists*, v. 77, p. 49-67.
- Smith, G.L., Byers, C.W., and Dott, R.H., Jr., 1996, Sequence stratigraphy of the Prairie du Chien Group, Lower Ordovician, Midcontinent, U.S.A., in Witzke, B.J., Ludvigson, G.A., and Day, J., eds., *Paleozoic Sequence Stratigraphy: Views from the North American Craton*: Geological Society of America Special Paper 306, p. 23-33.
- Smith, G.L., and Clark, D.L., in press, Conodonts of the Lower Ordovician Prairie du Chien Group of Wisconsin and Minnesota, *Journal of Micropaleontology*.
- Smith, G.L., and Simo, J.A., 1991, Warm-blooded dolomitization — an alternative explanation for type-Dorag dolomitization: International Association of Sedimentologists Abstracts of Papers for Dolomieu Conference on Carbonate Platforms and Dolomitization, p. 250.
- Steidtmann, E., 1911, The evolution of limestone and dolomite, I: *Journal of Geology*, v. 19, p. 323-345, 392-428.
- Tucker, M.E., and Wright, V.P., 1990, *Carbonate Sedimentology*: Blackwell Scientific, Oxford, p. 365-400.
- Tupas, M.H., 1950, The significance of mineral relationships in the Upper Mississippi Valley lead-zinc ores: unpublished Ph.D. dissertation, University of Wisconsin-Madison, Wisconsin.
- Van Tuyl, F.M., 1914, The origin of dolomite: Iowa Geological Survey, v. 25, p. 253-421.
- Ward, W.C., and Halley, R.B., 1985, Dolomitization in a mixing zone of near-seawater composition, Late Pleistocene, northeastern Yucatan Peninsula: *Journal of Sedimentary Petrology*, v. 55, p. 407-420.
- Wilson, J.L., 1974, Characteristics of carbonate platform margins: *American Association of Petroleum Geologists Bulletin*, v. 58, p. 810-824.
- Zimmerman, R.A., 1986, Fission-track dating of samples of the Illinois drill-hole: U.S. Geological Survey Bulletin 1622, p. 99-108.

COMPLEX BRECCIATION HISTORY ASSOCIATED WITH EVAPORITE AND CARBONATE DISSOLUTION IN THE LOWER ORDOVICIAN ONEOTA FORMATION (PRAIRIE DU CHIEN GROUP) NEAR SPRING GREEN, WISCONSIN

*George L. Smith*¹

ABSTRACT

Evaporite-dissolution brecciation focused subsequent porosity development and brecciation within carbonates of the Lower Ordovician Oneota Formation (Prairie du Chien Group) near Spring Green, Wisconsin. Stratiform breccia was formed first by the dissolution of bedded anhydrite. Younger, discordant carbonate breccia and existing caverns are superimposed on stratiform evaporite-dissolution breccia. The breccia and caverns continue to be zones of relatively high permeability and porosity.

INTRODUCTION

Studies of Lower Ordovician carbonate in North America generally emphasize the extensive paleokarst developed beneath the Lower-Middle Ordovician Sauk-Tippecanoe unconformity (for example, Kyle, 1976; Mussman and Read, 1986; Kerans, 1988; Mazzullo, 1989; Knight and others, 1991). The extent of buried paleokarst beneath this unconformity in Wisconsin is well documented (summarized by Mai and Dott, 1985). Paleokarst developed beneath the less well-known mid-Lower Ordovician unconformity is also recognized (Smith, 1989; Smith and others, 1993, 1996).

Breccia formed during evaporite dissolution is known to be an important source of porosity (for example, Middleton, 1961; Warren and Kendall, 1985), and is also known to promote the later dissolution and brecciation of interbedded carbonate strata (for example, Beales and Oldershaw, 1969; Park and Jones, 1985). This paper examines the role of evaporite dissolution in localizing subsequent karstification of shallow-marine carbonate of the Lower Ordovician Prairie du Chien Group in Wisconsin. Improved understanding of the relationship between former bedded evaporite and subsequent patterns of brecciation may result in improved prediction of zones of high permeability and porosity in carbonates of economic importance, such as hydrocarbon reservoirs and freshwater aquifers.

GEOLOGIC SETTING

Quarrying operations south of Spring Green, Wisconsin (fig. 1; SE1/4 sec. 3, T. 7 N., R. 3 E.), have exposed a 21 m-thick section of the Lower Ordovician Oneota Formation, which is unconformably overlain by a 1m-thick section of silicified oolitic grainstone and quartz arenite. Regional stratigraphic relationships determined from outcrops and water-well logs and a late-Early Ordovician-age conodont fauna (Smith, 1991) suggest that the grainstone and quartz arenite are part of the basal Shakopee Formation (figs. 2 and 3).

The Oneota Formation at this quarry displays an unusual degree of brecciation and cavern development (fig. 3), but is otherwise representative of the Oneota Formation in the outcrop area (Smith and others, 1993, 1996). The Oneota Formation is dominated by 10- to 30-cm thick laterally continuous beds of stromatolites, wavy-laminated peloidal boundstone, oolitic-peloidal grainstone and packstone, and other peritidal carbonate (fig. 2; Smith, 1991). Quartz sand and silt are abundant within the basal Oneota Formation and decrease in abundance up-section (fig. 2). Evidence for syndepositional subaerial exposure consists of desiccation cracks, and silicified and moldic anhydrite (Smith, 1991; Smith and others, 1993, 1996). Sediment of the Oneota Formation is interpreted as having been deposited in a shallow, tropical, epeiric sea, in shallow-subtidal to peritidal settings (Adams, 1978; Davis, 1970, 1971).

¹Department of Geology, Lawrence University, Appleton, Wisconsin 54912-0599; currently at Department of Earth Sciences, SUNY College at Brockport, Brockport, New York 14420-2936

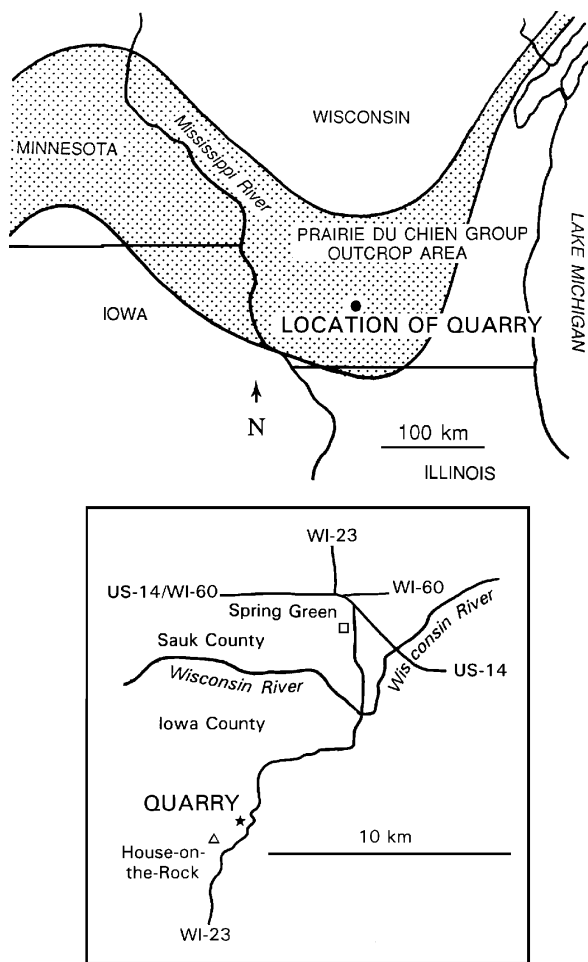


Figure 1. Location of quarry within Prairie du Chien outcrop area (stippled). Inset map at bottom shows location of quarry relative to nearby cultural features (after U.S. Geological Survey, 1960; S.E. 1/4, S. 3, T. 7 N., R. 3 E.).

RESULTS AND DISCUSSION

Stratiform breccia

Quarrying operations have exposed caverns and both stratiform and discordant breccia. Stratiform breccia is cross-cut by all other breccia and thus is the oldest breccia fabric in the quarry. Stratiform breccia is 10 to 25 cm thick, laterally-continuous over 200 m of quarry wall, and follow gentle undulations in bedding. The lower one- to two-thirds (5 to 20 cm) of most stratiform breccia have been silicified and consist of chalky-appearing chert (fig. 4). In thin section, the chalky chert contains abundant anhydrite crystal ghosts (fig. 5), suggesting that silicification accompanied anhydrite dissolution, a common phenomenon in

shallow-burial diagenetic settings (Milliken, 1979).

Carbonate strata underlying stratiform breccia are relatively undisturbed, whereas the 3 to 5 m of overlying strata typically display gentle folding and minor fracturing (fig. 6), indicating lithification prior to deformation. Brecciation and fracturing occurred as overlying carbonate strata collapsed into stratiform voids produced by the gradual dissolution of anhydrite beds. The lateral continuity of stratiform breccia suggests that dissolution and collapse took place gradually over a broad area, as suggested for analogous settings by Middleton (1961) and Warren and others (1990). Cross-cutting relationships indicate that stratiform breccia formed during subaerial exposure associated with development of the Oneota-Shakopee unconformity.

Discordant breccia

Discordant breccia is superimposed upon stratiform breccia (fig. 7). The timing of development of the discordant breccia is bracketed by the end of Oneota deposition and the inception of marine conditions during Shakopee deposition (approximately 495-490 Ma based on time scales summarized in Smith and others, 1993, 1996). Discordant breccia formed as Oneota carbonate beds collapsed into underlying caverns (fig. 7). Breccia consists of carbonate and/or chert clasts with carbonate and/or quartz-arenite matrix (fig. 8). Tilted beds were truncated prior to the deposition of the overlying Shakopee Formation (fig. 7).

Existing caverns

Existing caverns are largely localized within older discordant breccia and cavern fill, all of which are centered on and partially localized within stratiform breccia. As a consequence, caves line the walls of this quarry at levels corresponding to the positions of stratiform breccia (figs. 4 and 7). Caverns contain aragonitic and calcitic speleothems, aragonite-cemented breccia, and unlithified reddish-brown clay-rich sediment interstratified with fragments of speleothems (fig. 9).

SUMMARY

Stratiform breccia was formed by the dissolution of bedded anhydrite. Discordant breccia produced by later carbonate dissolution cross-cut stratiform breccias. Existing caverns cross-cut both stratiform and discordant breccia, but are localized along stratigraphic horizons containing stratiform breccia. In general, evaporite-dissolution brecciation has focused all major subsequent porosity development, empha-

Figure 2. Generalized stratigraphic column for southwestern Wisconsin. Dark vertical bar indicates stratigraphic interval examined in this study. After Smith and others (1993).

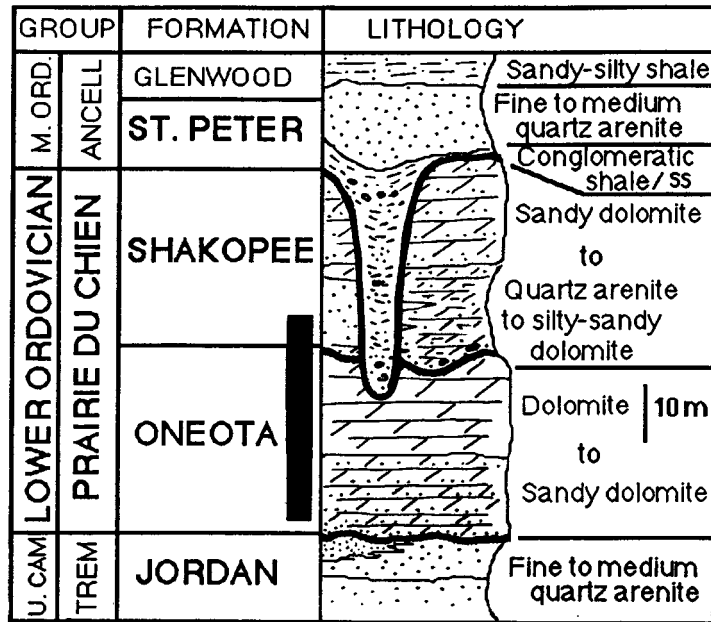


Figure 3. Composite measured section in quarry showing positions of stratiform breccia, discordant breccia, and caves.

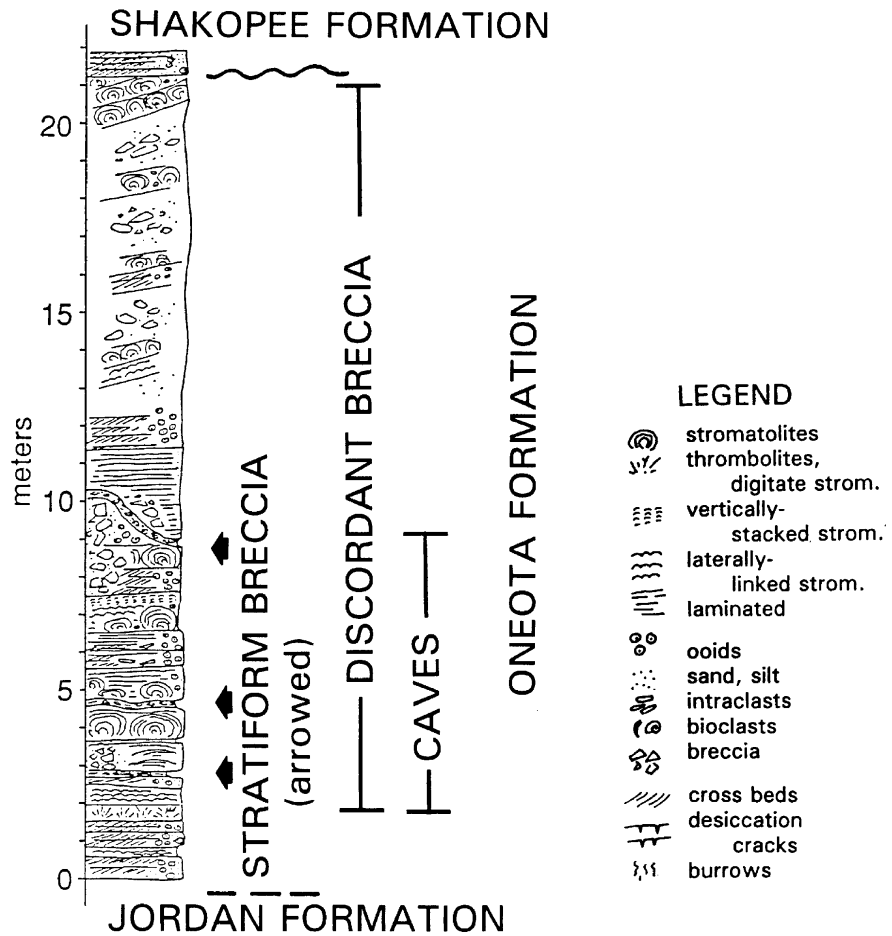


Figure 4. Photograph of east quarry face showing positions of stratiform breccia (arrows). Note preferential position caverns within the zone containing the three stratiform breccia. Scale bar is 10 m tall.



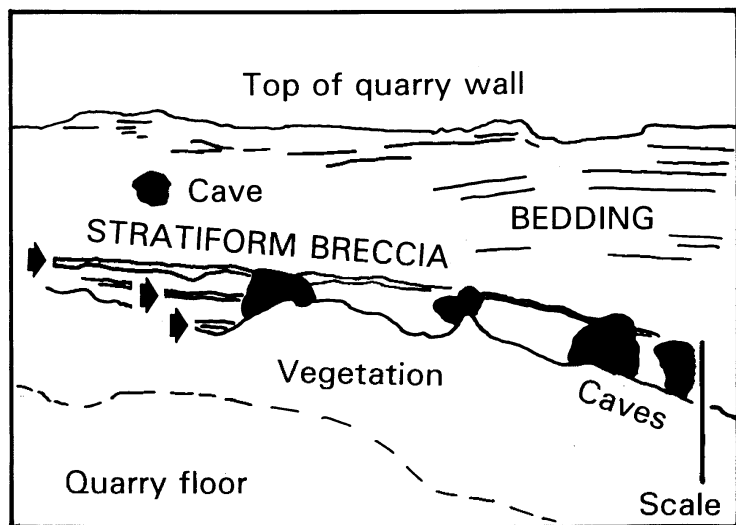
sizing the influence of bedded anhydrite on the pattern of porosity evolution.

ACKNOWLEDGMENTS

This research was partially supported by grants from the American Association of Petroleum Geologists, ARCO Oil and Gas Company, the Gas Research Institute, Sigma Xi—The Scientific Research Society, and the University of Wisconsin Graduate School. C.W. Byers and R.H. Dott, Jr., provided invaluable insights and assistance. This manuscript benefitted from thorough reviews by B.A. Brown, M.T. Harris, R.M. Peters, and M.G. Mudrey, Jr.

REFERENCES

- Adams, R.L., 1978, Stratigraphy and petrology of the lower Oneota dolomite (Ordovician), south-central Wisconsin, in *Lithostratigraphy, petrology, and sedimentology of Late Cambrian-Early Ordovician rocks near Madison, Wisconsin*: Wisconsin Geological and Natural History Survey Field Trip Guide Book 3, p. 82-90.
- Beales, F.W., and Oldershaw, A.E., 1969, Evaporite solution brecciation and Devonian carbonate reservoir porosity in western Canada: *American Association of Petroleum Geologists Bulletin*, v. 53, p. 503-512.
- Davis, R.A., Jr., 1970, Prairie du Chien Group in the upper Mississippi Valley, in *Field trip guidebook for Cambrian-Ordovician geology of western Wisconsin*: Wisconsin Geological and Natural History Survey Information Circular, p. 35-44.
- Davis, R.A., Jr., 1971, Prairie du Chien Group (L. Ord.) in the upper Mississippi Valley: Wisconsin Geological and Natural History Survey Open-File Report 71-2, 71 p.
- Kerans, C., 1988, Karst-controlled reservoir heterogeneity in Ellenburger Group carbonates of west Texas: *American Association of Petroleum Geologists Bulletin*, v. 72, p. 1160-1183.
- Knight, I., James, N.P., and Lane, T.E., 1991, The Ordovician St. George unconformity, northern Appalachians: the relationship of plate convergence at the St. Lawrence promontory to the Sauk/Tippecanoe sequence boundary: *Geological Society of America Bulletin*, v. 103, p. 1200-1225.
- Kyle, J.R., 1976, Brecciation, alteration, and mineralization in the central Tennessee zinc district: *Economic Geology*, v. 71, p. 892-903.
- Mai, H., and Dott, R.H., Jr., 1985, A subsurface study of the St. Peter sandstone in southern and eastern



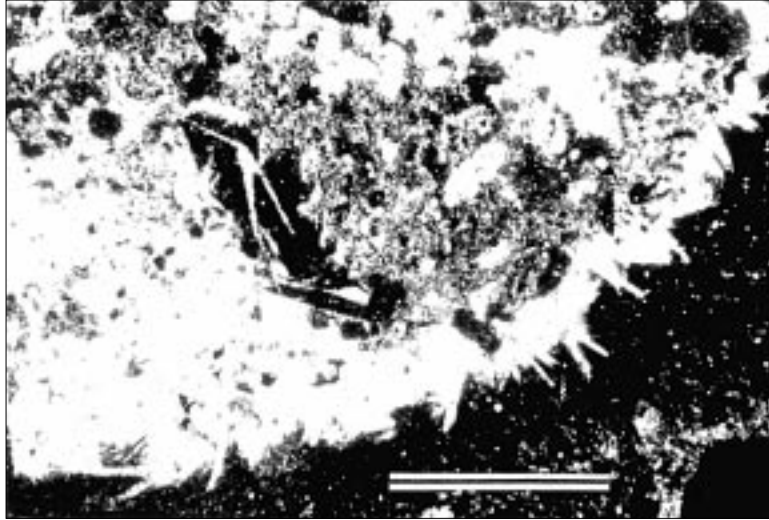


Figure 5. Thin section photomicrograph of anhydrite crystal ghosts. Sample is from silicified base of uppermost of three stratiform breccias identified in figures 3 and 4. Partial dissolution of anhydrite and some compaction preceded silicification. Crossed nicols. Scale bar is 2 mm long.

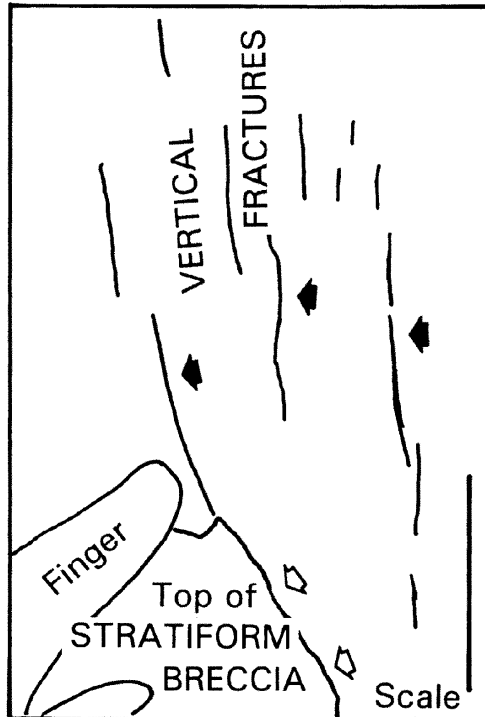
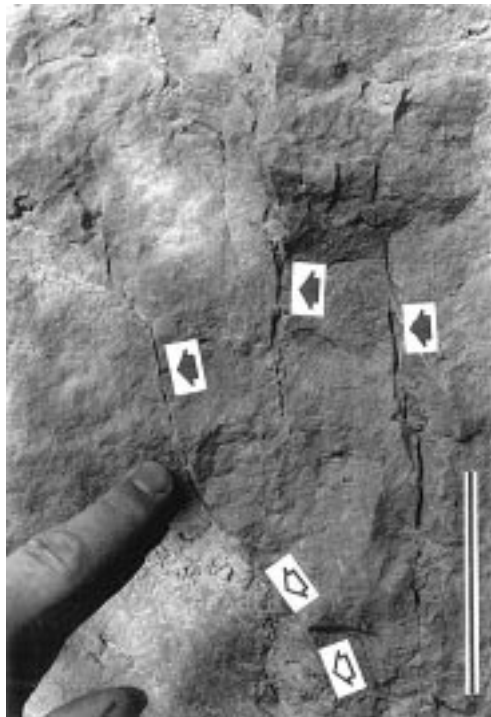


Figure 6. Field photograph of top of uppermost stratiform breccia shown in figures 3 and 4. Open arrows indicate contact between dolomitized carbonate breccia and overlying fractured dolostone. Black arrows indicate fractures extending upward from top of breccia through fractured dolostone. Scale bar is 10 cm tall.

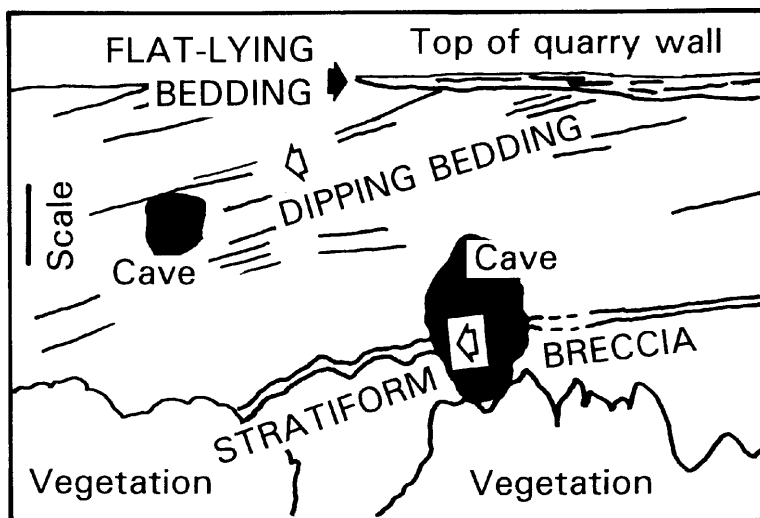
Wisconsin: Wisconsin Geological and Natural History Survey Information Circular 47, 26 p.

Mazzullo, S.J., 1989, Formational and zonal subdivisions of the Ellenburger Group (Lower Ordovician),

southern Midland basin, Texas, in Cunningham, B.K., and Romwell, D.W., eds., *The Lower Paleozoic of West Texas and Southern New Mexico—Modern Exploration Concepts: Permian Basin Section-SEPM Publication 89-31*, p. 113-122.



Figure 7. Photograph of west quarry face showing collapse feature within Oneota Formation. Part of quarry wall shown corresponds to zone of discordant breccia in figure 3. Black arrow indicates 1 m-thick section of flat-lying silicified oolitic grainstones and quartz arenites of the basal Shakopee Formation overlying truncated beds of the Oneota Formation. Upper open arrow indicates truncated, left-dipping Oneota strata. Lower open arrow indicates position of uppermost stratiform breccia. The large (2.8 m-tall) cavern opening, developed within discordant breccia, is centered on the highest stratiform breccia. Cavern opening in quarry wall connects to extensive (> 500 m-long) cavern system within hilltop. Scale bar is 2 m tall.



Middleton, G.V., 1961, Evaporite solution breccias from the Mississippian of southwest Montana: *Journal of Sedimentary Petrology*, v. 31, p. 189-195.

Milliken, K.L., 1979, The silicified evaporite syndrome — two aspects of silicification history of former evaporite nodules from southern Kentucky and northern Tennessee: *Journal of Sedimentary Petrology*, v. 49, p. 245-256.

Mussman, W.J., and Read, J.F., 1986, Sedimentology and development of a passive-to-convergent margin unconformity—Middle Ordovician Knox unconformity, Virginia Appalachians: *Geological Society of America Bulletin*, v. 97, p. 282-295.

Park, D.G., and B. Jones, 1985, Nature and genesis of breccia bodies in Devonian strata, Peace Point area, Wood Buffalo Park, northeast Alberta: *Bulletin of Canadian Petroleum Geology*, v. 33, p. 275-294.

Smith, G.L., 1989, Karsting and eolian deposition during a pre-New Richmond (Early Ordovician) sea level drawdown, Prairie du Chien Group, upper Mississippi Valley: *Geological Society of America Abstracts with Programs*, v. 21, p. A80.

Smith, G.L., 1991, Sequence stratigraphy and diagenesis of the Lower Ordovician Prairie du Chien Group on the Wisconsin arch and in the Michigan basin: unpublished Ph.D. dissertation,

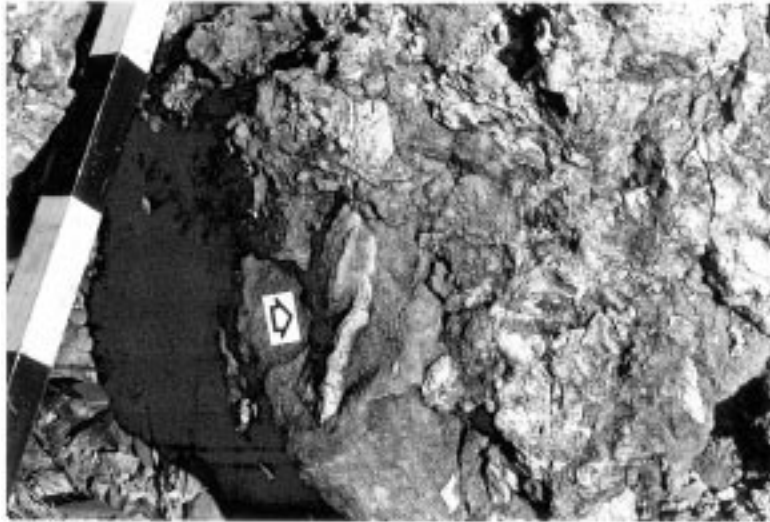


Figure 8. A quarried block of discordant breccia with quartz-arenite matrix containing chert (arrow) and dolomite fragments. Stripes on scale bar are 10 cm in length.

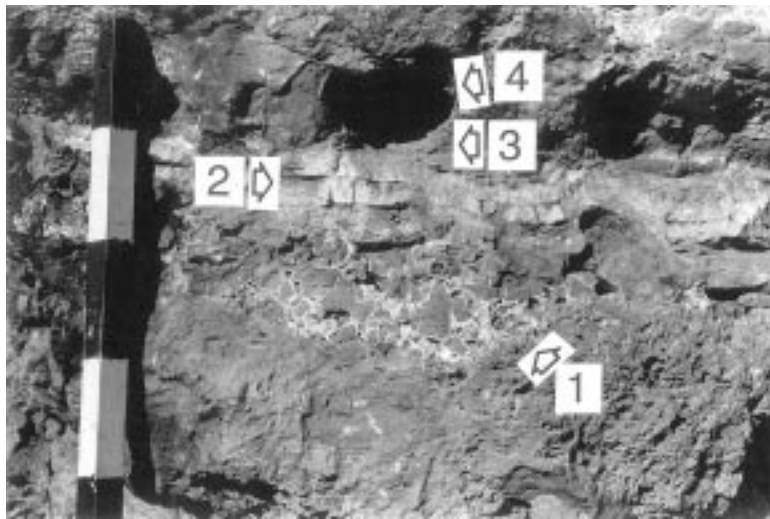


Figure 9. Field photograph of cavern exposed on north face of quarry: 1. aragonite-cemented dolomite breccia, 2. two generations of aragonitic flowstone, 3. unlithified reddish-brown clay, and 4. remaining cavernous porosity. Stripes on scale bar are 10 cm in length.

University of Wisconsin-Madison, Madison, Wisconsin, 265 p.

Smith, G.L., Byers, C.W., and Dott, R.H., Jr., 1993, Sequence stratigraphy of the Lower Ordovician Prairie du Chien Group on the Wisconsin arch and in the Michigan basin: *American Association of Petroleum Geologists Bulletin*, v. 77, p. 49-67.

Smith, G.L., Byers, C.W., and Dott, R.H., Jr., 1996, Sequence stratigraphy of the Prairie du Chien Group, Lower Ordovician, Midcontinent, U.S.A., in Witzke, B.J., Ludvigson, G.A., and Day, J., eds., *Paleozoic Sequence Stratigraphy: Views from the North American Craton*: Geological Society of America Special Paper 306, p. 23-33.

U.S. Geological Survey, 1960, Spring Green Quadrangle, Wisconsin, 15 Minute Series (topographic).

Warren, J.K., and Kendall, G.C.St.C., 1985, Comparison of marine sabkha (subaerial) and salina (subaqueous) evaporites: modern and ancient: *American Association of Petroleum Geologists Bulletin*, v. 69, p. 1013-1023.

Warren, J.K., Havholm, K.G., Rosen, M.R., and Parsley, M.J., 1990, Evolution of gypsum karst in the Kirschberg Evaporite Member near Fredericksburg, Texas: *Journal of Sedimentary Petrology*, v. 60, p. 721-734.

AUTHIGENIC SILICA FABRICS ASSOCIATED WITH CAMBRO-ORDOVICIAN UNCONFORMITIES IN THE UPPER MIDWEST

George L. Smith¹, Robert H. Dott, Jr.², and Charles W. Byers²

ABSTRACT

Authigenic silica fabrics associated with the Cambro-Ordovician, mid-Lower Ordovician, and Lower-Middle Ordovician unconformities in the Upper Midwest occur to depths of 30 m below unconformities, but are most abundant within 0-5 m of unconformities. Reworked clasts of silicified material above these unconformities indicate that silicification occurred before and/or during unconformity development. Authigenic silica fabrics are most abundant within the outcrop area surrounding the Wisconsin Arch, and diminish in abundance to the west and east. These silica fabrics are important indicators of subaerial exposure because they are easily identified in well cuttings and have not been masked by pervasive, regional dolomitization.

INTRODUCTION

Silica translocation is a common phenomenon in subaerial weathering profiles. Within the central United States the association of authigenic silica with ancient subaerial unconformities was first recognized by Bain and Ulrich (1905), who described a variety of authigenic silica fabrics beneath the Lower-Middle Ordovician Sauk-Tippecanoe unconformity. In "Silicification of Erosion Surfaces" Leith (1925) summarized the association of authigenic silica with subaerial unconformities: (1) Authigenic silica is most abundant immediately beneath the unconformity surface, but (2) fingers of silicified material commonly extend deep beneath unconformities along fractures and paleokarst. (3) A discontinuous layer of reworked silicified material typically occurs above the unconformity. (4) Limestone is more commonly silicified than other rock types.

The term "silcrete" was introduced by Lamplugh (1902, 1907) to describe surficial deposits indurated by authigenic silica by infiltrating groundwater. Woolnough (1927) later introduced the related term "duricrust" to describe surficial crusts in Australia composed of authigenic silica and other diagenetic phases. Wopfner and Twidale (1967), Dury (1969), and Langford-Smith (1978) discuss related terminology. Silcreted and duricrusts are by definition crusts on the upper surface or within the upper horizons of soils. Similar genetic terminology does not exist for authigenic silica types formed 5-30 m beneath unconformities, even in cases where silicification oc-

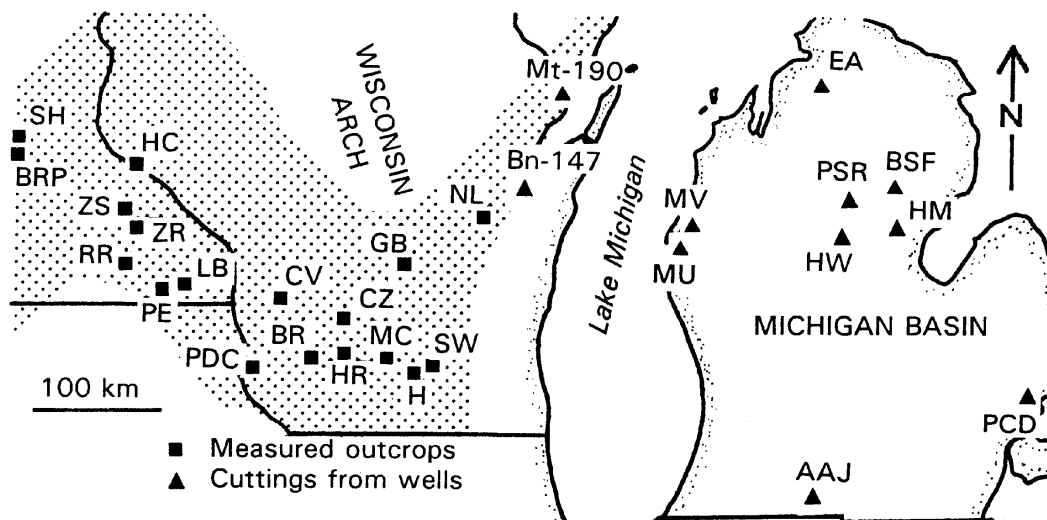
curred during intervals of subaerial exposure (for example, Leith, 1925).

Authigenic silica fabrics within the Lower Ordovician dolostone of the Mississippi Valley region have long been recognized as markedly different from the familiar nodular chert of many younger carbonate rock successions. Whereas the latter faithfully replace primary carbonate grains with dense, finely crystalline, fairly homogeneous quartz, Lower Ordovician "chert" tends to be very vuggy (with drusy quartz linings), botryoidal, and heterogeneous. Their genesis has been a long-standing mystery for which this paper presents a new hypothetical solution through silcrete formation.

This paper documents the distribution of silica cements and replacement fabrics within Cambro-Ordovician strata of the Upper Midwest (figs. 1 and 2) and demonstrates the association of authigenic silica cements and replacement fabrics with regional subaerial unconformities. By analogy with Cenozoic examples (for example, Alley, 1977; Ambrose and Flint, 1981; Hutton and others, 1972, 1978; Khalaf, 1988; Langford-Smith, 1978; Meyer and Pena dos Reis, 1985; Smale, 1973; Summerfield, 1983a, 1983b; Thiry and Millot, 1987; Thiry and others, 1988; Watts, 1978), this paper proposes that many of the Cambro-Ordovician chert occurrences are the remnants of patchily-distributed, regionally-extensive ancient authigenic silica fabrics formed at the surface and at depths extending 5-30 m beneath subaerial unconformities.

¹Department of Geology, Lawrence University, Appleton, Wisconsin 54912-0599; currently at Department of Earth Sciences, SUNY College at Brockport, Brockport, New York 14420-2936

²Department of Geology and Geophysics, University of Wisconsin-Madison, Madison, Wisconsin 53706



Key to Locations

Outcrops

- BR Blue River, Wisc.
- BRP Bryant Rock Products, Shakopee, Minn.
- CV Coon Valley, Wisc.
- CZ Cazenovia, Wisc.
- GB Glovers Bluff, Wisc.
- H Homburg Quarry, Madison, Wisc.
- HC Hager City, Wisc.
- HR "House on the Rock" Quarry, Wisc.
- LB Lanesboro, Minn.

- MC Millers Curve, Cross Plains, Wisc.
- NL New London, Wisc.
- PDC Prairie du Chien, Wisc.
- PE east of Preston, Minn.
- RR Root River, Minn.
- SH Shakopee, Minn.
- SW Shorewood Hills, Wisc.
- ZR Zumbro River, south of Zumbro, Minn.
- ZS south of Zumbrota, Minn.

Oil and Gas Wells

- AAJ ARCO-ARCO/Johnson 1-3, Branch Co., Mich.
- BSF Brazos-St. Foster 1, Ogemaw Co., Mich.
- EA Energy Acquisition-NML&O, Charlevoix Co., Mich.
- HM Hunt-Martin 1-15, Gladwin Co., Mich.
- HW Hunt-Winterfield A-1, Clare Co., Mich.
- MU Miller-USA 1-26, Mason Co., Mich.
- MV Miller-Victory 2-26, Mason Co., Mich.
- PCD Patrick-Cusumano/Divito 1-22, Macomb Co., Mich.
- PSR Petrostar-St. Roscommon 1-30, Roscommon Co., Mich.

Water Wells

- Bn-147, Brown Co., Wisc.
- Mt-190, Marinette Co., Wisc.

Figure 1. Location map of study area. Stippled pattern identifies the outcrop area of the Jordan, Oneota, Shakopee, and St. Peter Formations. Squares indicate the locations of measured outcrop sections. Triangles indicate the locations of wells from which cuttings were examined.

CONDITIONS OF AUTHIGENIC SILICIFICATION

In general, the prerequisites for near-surface silicification appear to include prolonged subaerial exposure, relatively slow rates of tectonic uplift and erosion, and temperate to tropical climate (for example, Hutton and others, 1972, 1978; Twidale and Hutton, 1986). Based on field and laboratory evidence for the slow rates of silica crystallization (for example, Siever, 1962; Ernst and Calvert, 1969; Maliva and Siever, 1988) long-term stability of the sediment sur-

face may be the single most important factor limiting authigenic silicification in otherwise appropriate settings (for example, Hutton and others, 1978). Petrographic textures indicate that silica precipitates as solid amorphous silica (opal-A), opal-CT, chalcedony, or quartz (for example, Maliva and Siever, 1988, 1989).

Deposits of authigenic silica from a localized geographic area may display a broad range of characteristics related to variations in topography and bedrock composition, and patterns of colluvial transport. Authigenic silica from the Kalahari Basin of southern

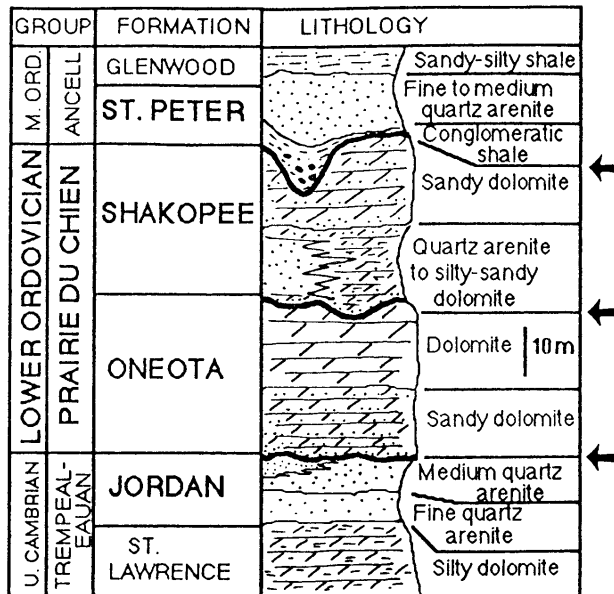


Figure 2. Generalized stratigraphic column for the Jordan, Oneota, Shakopee, and St. Peter Formations in southwestern Wisconsin. Arrows indicate the positions of major, sequence-bounding unconformities overlying silicified intervals.

PREVIOUS WORK

Following early work by Ulrich (1924) and Leith (1925), the study of authigenic silica fabrics in the Upper Midwest experienced several decades of neglect. Silica fabrics were first identified as silcrete by Dury and Knox (1971), Habermann and Dury (1974), and Habermann (1978), all of whom attributed the formation of authigenic silica crusts and weathering profiles to deep weathering under humid, tropical conditions during the Mesozoic to mid-Miocene, an interval of subaerial exposure and cratonic stability. Some of these features identified by Dury and Knox (1971) and Habermann (1978) instead may have formed during subaerial exposure associated with development of Cambro-Ordovician unconformities (for example, Smith, 1991, 1992).

METHODS AND GEOLOGIC SETTING

Authigenic silica fabrics were examined in uppermost Cambrian to Middle Ordovician strata within a region encompassing portions of Iowa, Michigan, Minnesota, and Wisconsin (fig. 1). Lithostratigraphic units studied include the uppermost Upper Cambrian Jordan Formation, the Lower Ordovician Oneota and Shakopee Formations (Prairie du Chien Group), and the Middle Ordovician St. Peter Formation (fig. 2). These Cambro-Ordovician strata were primarily deposited in tropical epeiric seas during four relative highstands of sea level that flooded most of the central North American craton (Smith and others, 1993, 1996). Development of the Cambro-Ordovician, mid-Lower Ordovician, and Lower-Middle Ordovician (Sauk-Tippecanoe) unconformities occurred during intervening lowstands of sea level (fig. 2). Measured sections and samples were obtained from 18 outcrops, 2 water wells, and 9 oil and gas wells (fig. 1). Approximately 350 thin sections were examined petrographically.

AUTHIGENIC SILICA IN OUTCROP

Nodular chert

Most nodular chert observed in outcrop is in the form of compact 1- to 10-cm diameter nodules concentrated along individual horizons. Viewed in thin

Africa and of valley floors of the Beda Valley region of south-central Australia consists mainly of surficial crusts developed in semi-arid to arid settings on a variety of continental deposits, including fluvio-lacustrine and playa sediments, and calcretes (Hutton and others, 1972, 1978; Smale, 1973; Summerfield, 1983a, 1983b). In contrast, authigenic silica deposits from topographic highs in south-central Australia (Hutton and others, 1972, 1978) and from the relatively humid coastal setting of south Africa (Smale, 1973; Summerfield, 1983a, 1983b) commonly display relatively well-developed weathering profiles up to 10-20 m thick.

Authigenic silica deposits of the Paris Basin described by Thiry and Millot (1987) and Thiry and others (1988) are petrographically similar but not as thick (2-3 m, as opposed to 10-20 m) as weathering-profile deposits of South Africa (Summerfield, 1983a). Unlike authigenic silica deposits formed in the relatively stable geologic setting of South Africa, authigenic silica deposits of the Paris Basin developed through repeated silica dissolution, transport, and reprecipitation within progressively falling water tables associated with Pliocene-recent fluvial downcutting (Thiry and others, 1988; Thiry and Millot, 1987).

Silica in Paris Basin groundwater is typically present at low concentrations (12 mg/l), with Paris Basin silica deposits precipitating from neutral (pH = 7.2-7.4) groundwater (Thiry and others, 1988). In contrast, authigenic silica deposits formed in arid and semi-arid regions precipitate both in evaporative pedogenic settings, and at deeper levels from dilute groundwater (Thiry and Milnes, 1991).

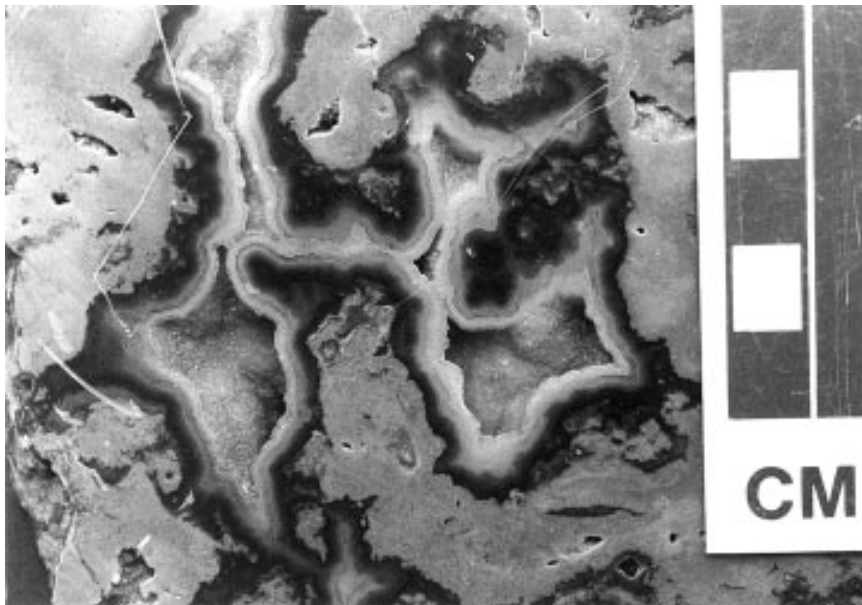


Figure 3. *Polished slab from the upper Oneota Formation near Hager City (HC), Wisconsin. Multiple bands of isopachous length-fast chalcedony and megaquartz are visible. The darker of these cements are distinctively colored purple, black, and reddish brown. Reddish-orange iron oxides and hydroxides superficially coat silica cements and fractures within the host dolomite.*

section, nodular chert from the Cambro-Ordovician section is uniformly microcrystalline and preserves micron-scale textures in exceptional detail. These chert nodules probably formed by the replacement of carbonate sediment by opal-CT, which later recrystallized to quartz, and/or by the direct precipitation of quartz as generally described by Maliva and Siever (1988, 1989).

Chalcedony-quartz aggregates

Unlike finely-microcrystalline nodular chert, most of the authigenic silica observed in Cambro-Ordovician rock of the upper Midwest consists of chalcedony and quartz aggregates displaying complex paragenetic relationships. Most chalcedony-quartz aggregates are irregular centimeter- to meter-scale masses of chalcedony and quartz containing open vugs lined with drusy quartz crystals (fig. 3). Drusy quartz crystals commonly line vugs within adjacent, relatively unaltered nearby dolomite. Chalcedony-quartz aggregates are commonly stained shades of yellow, red, purple, brown, and black by iron oxides and hydroxides. Paragenetic sequences are highly variable between outcrops.

Chert associated with hydrothermal minerals

Non-economic occurrences of Mississippi Valley-type mineral assemblages, mainly marcasite and pyrite, are present throughout the study area in rock of Cambrian to Silurian age (for example, Jenkins, 1968; Heyl and West, 1982; Kutz and Spry, 1989). Mineralizing fluids

precipitated chert in addition to a variety of sulfides and carbonates (for example, Jenkins, 1968; McLimans, 1977), but little of the authigenic silica within Cambro-Ordovician strata is associated with Mississippi Valley-type mineral assemblages.

PETROGRAPHIC CHARACTERISTICS OF AUTHIGENIC SILICA

Microquartz (< 0.02 mm)

Replacement microquartz is abundant in Proterozoic-Paleozoic silcrete, where it may represent recrystallization of opal-CT and/or direct precipitation as quartz (for example, Rubin and Friedman, 1981; Ross and Chiarenzelli, 1985; Mustard and Donaldson, 1990). Microquartz (< 0.02 mm crystalline quartz, for example, Folk and Pittman, 1971) is the most abundant authigenic silica type observed in our study. Microquartz occurs as both a replacement phase and as a cement within carbonate rock with high primary permeability and porosity (for example, stromatolitic boundstone, oolitic grainstone, and paleokarst breccia). In thin section microquartz consists of melange of equant to elongate, anhedral to subhedral crystal aggregates containing abundant microdolomite inclusions and ghosts of peloids, ooids, and anhydrite (fig. 4). As a replacement phase, microquartz is typically associated with length-slow, spherulitic chalcedony. As a cement, microquartz forms isopachous pore-linings of isopachous, elongate, subhedral crystals that grade from microquartz into larger, euhedral megaquartz with well-defined

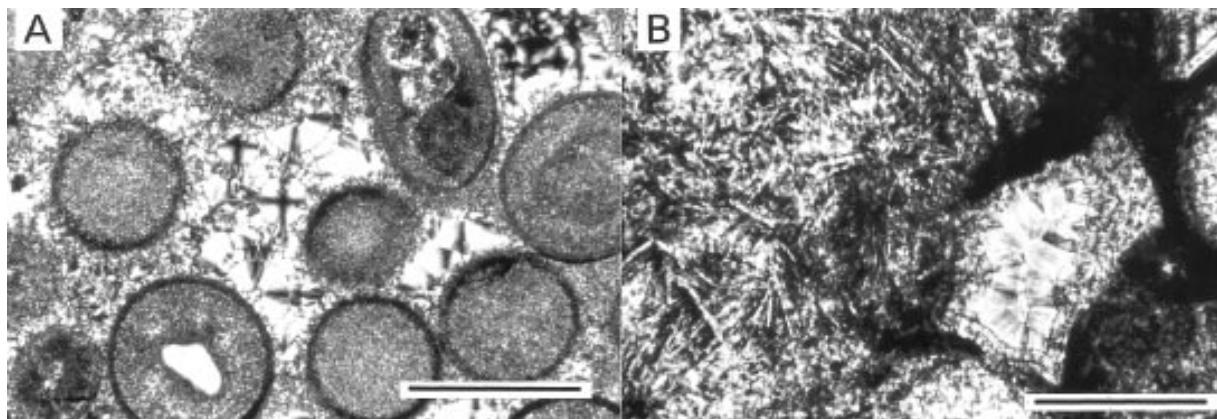


Figure 4. *Microquartz. A) Silicified oolitic grainstone from middle Oneota Formation at Hager City (HC), Wisconsin. Microquartz replaces ooids and occurs as an early pore-lining cement. Remaining porosity is filled by botryoids of length-fast chalcedony. Crossed nicols. Scale bar: 1 mm. B) Silicified anhydrite from basal Oneota Formation at Cazenovia (CZ), Wisconsin. Anhydrite ghosts are present within the lefthand portion of the photomicrograph. The vuggy pore within the righthand portion of the photomicrograph is filled primarily by isopachous, length-fast chalcedony cement. Crossed nicols. Scale bar: 0.5 mm.*

growth bands (fig. 5).

Megaquartz (> 0.02 mm)

Megaquartz (> 0.02 mm, for example, Folk and Pittman, 1971) forms distinctive drusy pore linings of euhedral, equant to slightly-elongate crystals up to 2 mm in length (for example, figs. 3 and 5). Colors range from clear to light orange, red, or purple. Megaquartz is less common as a replacive phase and occurs rarely as equant to elongate, subhedral to euhedral crystals containing needle-like anhydrite inclusions (fig. 6). Replacement of anhydrite by megaquartz is well-documented and is typical of evaporite silicifica-

tion in shallow-burial diagenetic settings (for example, Milliken, 1979; Friedman and Shukla, 1980).

Syntaxial quartz overgrowths

Within the outcrop area, syntaxial quartz overgrowths are restricted to quartz arenite, sandy grainstone, and the quartz cores of moldic ooids (for example, Austin, 1974; Habermann, 1978). Subhedral to euhedral quartz overgrowths are readily visible in hand sample as tiny, reflective facets on freshly-exposed grain contacts. Simultaneous crystallization of quartz overgrowths and microquartz-megaquartz cements occurred where quartz overgrowths and microquartz-

megaquartz overgrowths on carbonate grains meet at pore throats. Quartz overgrowths have been documented in a variety of Cenozoic silcretes (for example, Ambrose and Flint, 1981; Thiry and Millot, 1987; Khalaf, 1988; Thiry and oth-

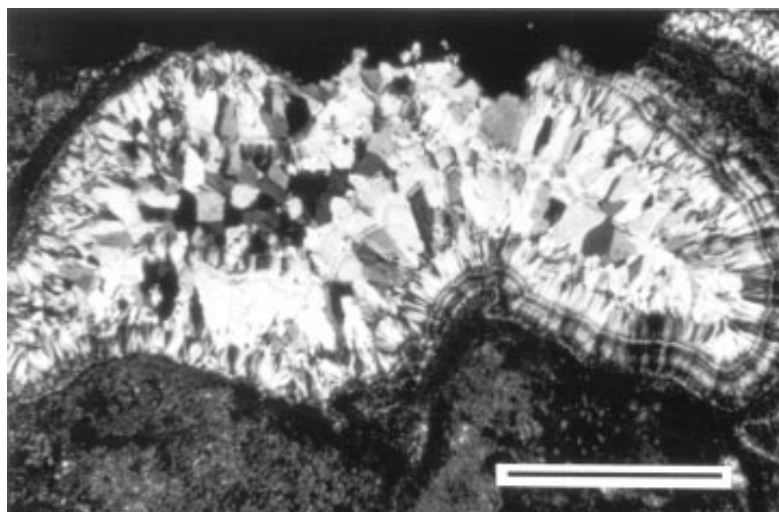


Figure 5. *Multiple generations of silica cements in the basal Shakopee Formation at the HR location: length-fast isopachous chalcedony, microquartz “palisade”, and megaquartz (final cement phase). Crossed nicols. Scale bar: 1.5 mm.*

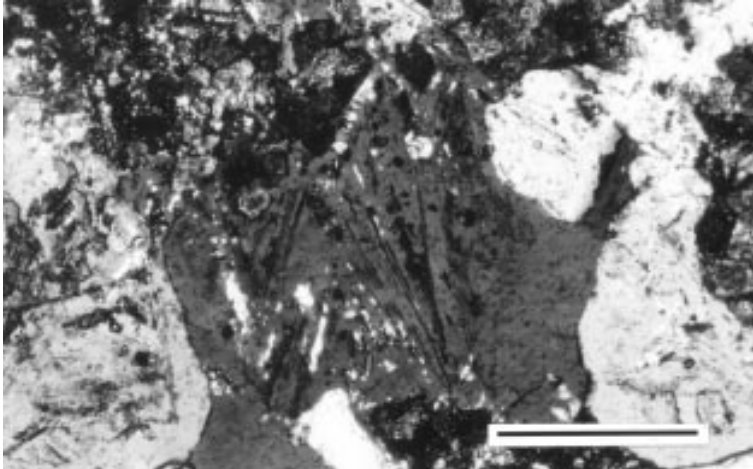
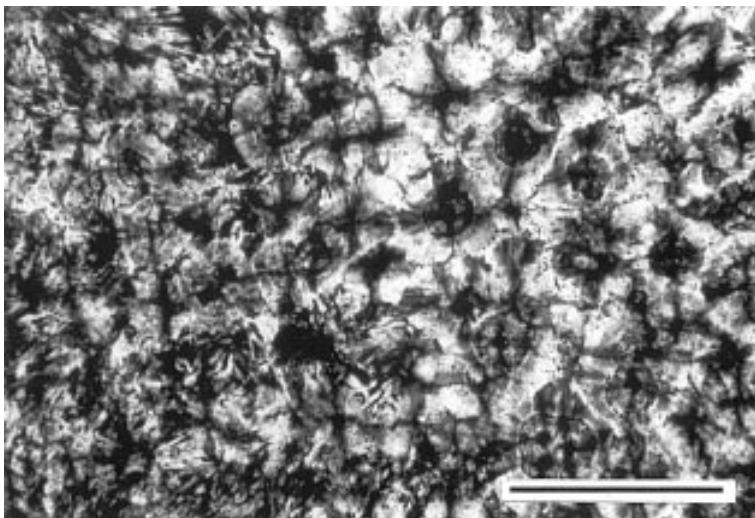


Figure 6. *Megaquartz replacing anhydrite. Silicified anhydrite nodule from basal Shakopee Formation east of Coon Valley (CV), Wisconsin. Silicification has preserved anhydrite texture. Bright needle-shaped patches within megaquartz crystal are anhydrite inclusions. Crossed nicols. Scale bar: 0.1 mm.*

ers, 1988), but are not by themselves necessarily indicative of near-surface weathering conditions.

Length-slow spherulitic chalcedony

Length-slow spherulitic chalcedony consists of irregular spherical masses of clear to brown, radiating-fibrous, length-slow chalcedony (for example, Noble and Van Stempvoort, 1989), displaying undulose extinction and pseudo-uniaxial crosses (fig. 7). Length-slow spherulitic chalcedony occurs as isolated spherules and coalesced masses within all of the studied silicified carbonate rocks. Length-slow spherulitic chalcedony is commonly associated with microquartz, but chalcedony is generally less abundant than microquartz. Length-slow chalcedony commonly replaces evaporite and carbonate (for example, Folk and Pittman, 1971; Jacka, 1974), but is not considered diagnostic of evaporite replacement.



Length-fast chalcedony

Length-fast chalcedony is locally abundant as a cement phase within silicified oolitic grainstone and other

rock containing abundant pores. In hand-sample, length-fast chalcedony is isopachous, gray to milky-white in color, and contains millimeter-scale bands. In thin section, length-fast chalcedony is concentrically-banded, inclusion-rich, and yellow-brown in color. Botryoids of length-fast chalcedony commonly coalesce and are overgrown by isopachous length-fast chalcedony, although other sequences occur (figs. 3 and 8). Chalcedony cements are typically overgrown by microquartz and megaquartz cements (for example, fig. 3), a feature sometimes associated with evaporite silicification (for example, Milliken, 1979; Khalaf, 1988; Murray, 1990). Length-fast chalcedony cements growing directly on quartz grains are extremely rare (Austin, 1974).

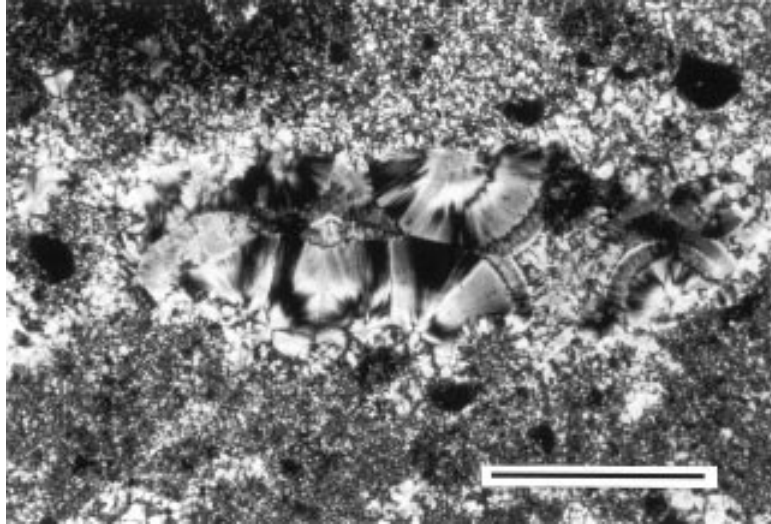
STRATIGRAPHIC DISTRIBUTION OF AUTHIGENIC SILICA

Silica beneath unconformities

Authigenic silica fabrics are patchily distributed below unconformities. Stratigraphic intervals vary greatly in degree of silicification (for example, figs. 9 and 10). In general, beds with high primary and/or secondary porosity have been preferentially silicified,

Figure 7. *Length-slow spherulitic chalcedony replacing anhydrite (left) and dolomite (right) in basal Oneota Formation at Cazenovia (CZ), Wisconsin. Note needle-shaped ghosts of anhydrite crystals within lefthand side of photomicrograph. Crossed nicols. Scale bar: 0.5 mm.*

Figure 8. Length-fast chalcedony from the lower Oneota Formation at Blue River (BR), Wisconsin. A) Botryoids of length-fast chalcedony cement within vuggy pore in silicified peloidal(?) packstone. Crossed nicols. Scale bar: 1 mm.



as noted by Leith (1925). The largest siliceous masses were observed in a roadcut and quarry east of Prairie du Chien, Wisconsin (figs. 9 and 10), where a 3-m thick stromatolitic layer located 3 to 6 m below the mid-Lower Ordovician unconformity has been altered to a massive cherty rock with abundant decimeter-scale vugs lined with chalcedony and quartz. Within the study area, large chalcedony- and quartz-lined vugs are unique to the Prairie du Chien Group.

Another distinctive silicified rock type occurs within a series of Oneota Formation outcrops within

the upper Mississippi River valley (from HC to PDC, fig. 1). This rock type consists of partially-silicified 10- to 20-cm thick beds of 2-cm diameter vertical vugs, secondarily lined with chalcedony and drusy quartz cements (fig. 11). These tubular vugs are the molds of vertically-stacked stromatolites. Similar “piping” textures have been observed within silcrete profiles by Smale (1973) and Watts (1978), although stromatolites are not implicated in these Cenozoic examples.

Anhydrite beds and nodules were preferentially silicified, producing silicified anhydrite nodules and stratiform breccia. Brecciation suggests that volume loss by dissolution and compaction accompanied silicification. In contrast, individual silicified anhydrite nodules do not appear compacted, indicating anhydrite replacement after at least partial lithification.

At several locations (for example, PE, LB, PDC, and CZ, fig. 1), the upper 2-20 cm of the unit beneath the unconformity is pervasively silicified, forming an erosion-resistant cap (for example, fig. 12A). It is not clear whether the silicified layer represents a surface crust or exhumed beds originally silicified some dis-

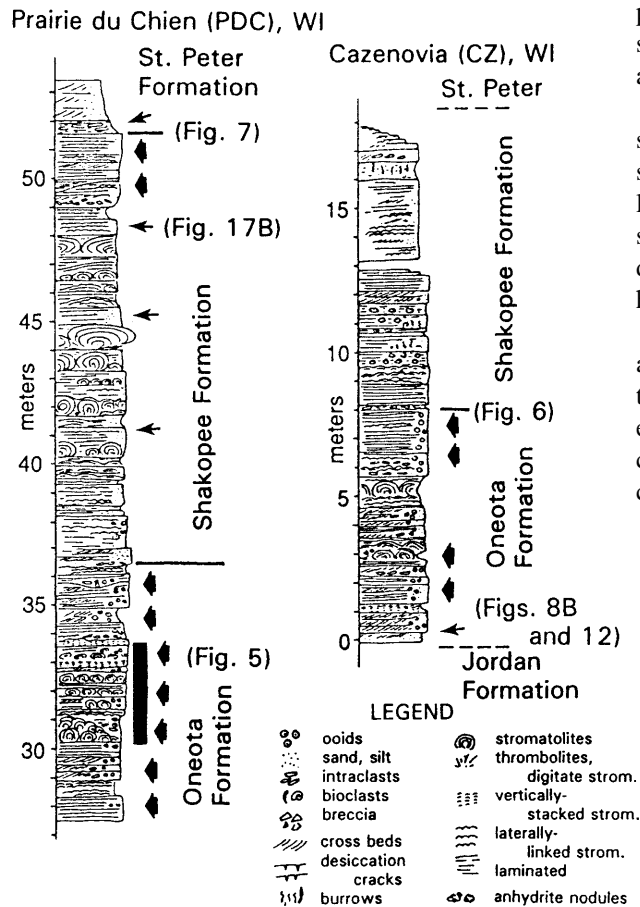


Figure 9. Measured sections at the Prairie du Chien (PDC) and Cazenovia (CZ), Wisconsin, showing the stratigraphic distribution of diagenetic silica at these two localities. Broad arrows indicate zones of intense silicification. Thin arrows indicate the positions of reworked silcrete lithoclasts. Heavy bar indicates 3 m-thick zone of massive silicification within the upper Oneota Formation at the PDC section.



Figure 10. Roadcut exposure of the upper Oneota Formation at Prairie du Chien (PDC), Wisconsin. Open arrows indicate the positions of the Oneota-Shakopee contact (upper arrow) and a 1.5 m-tall staff (lower arrow). Black arrows indicate the position of the upper end of a massive 3 m-thick zone of chert.



Figure 11. Outcrop view of silicified tubular vugs, the molds of vertically-stacked stromatolites, from the upper Oneota Formation near Hager City (HC), Wisconsin.

tance below the ground surface.

Reworked silicified material

Reworked clasts form patchy, discontinuous breccia and conglomerate. Where silicified material is exposed along an unconformity surface, reworked clasts are abundant above the unconformity (fig. 12B). Reworked sand-sized grains occur up to 10-15 m above unconformities (for example, figs. 9 and 10). Silicified material also occurs within paleokarst, indicating that at least some silicification preceded paleokarst development.

GEOGRAPHIC DISTRIBUTION OF AUTHIGENIC SILICA

In the area of the axis of the Wisconsin Arch (for example, fig. 1., localities MC, SW, CZ, GB, and NL) the Cambro-Ordovician unconformity consists of an irregular surface locally overlain by conglomerates containing silicified clasts (Smith and others, 1993, 1996). Silicified oolitic-grainstone, quartz arenite, and anhydrite nodules underlie the Cambro-Ordovician unconformity surface, which is in turn overlain by reworked clasts (for example, fig. 13). The mid-Lower Ordovician, Oneota-Shakopee unconformity is an eroded paleokarst surface associated with abundant authigenic silica fabrics and reworked clasts (Smith and others, 1993, 1996). Both *in situ* and reworked silicified material are patchily distributed throughout the entire outcrop area and have been identified as far east as western Michigan (for example, fig. 1, locality MU).

The Lower-Middle Ordovician unconformity is another paleokarst surface developed during prolonged subaerial exposure. Both *in situ* and reworked silicified material are patchily distributed throughout the entire outcrop area. Despite recent work by Nadon and Smith (1992) documenting subaerial exposure of the Lower-Middle Ordovician unconformity across the Michigan Basin, silcrete appears restricted to the western margin of the Michigan Basin in eastern Wisconsin (for example, fig. 1, localities Bn-147, Mt-190, and NL). In the outcrop area, post-Early Ordovician dissolution and fluvial erosion produced 60-m-deep sinkholes and valleys in Lower Ordovician carbonate strata (Mai and Dott, 1985). This deep erosion potentially exposed the entire 60 m thickness of Lower Ordovician strata to surficial weathering processes, possibly resulting in

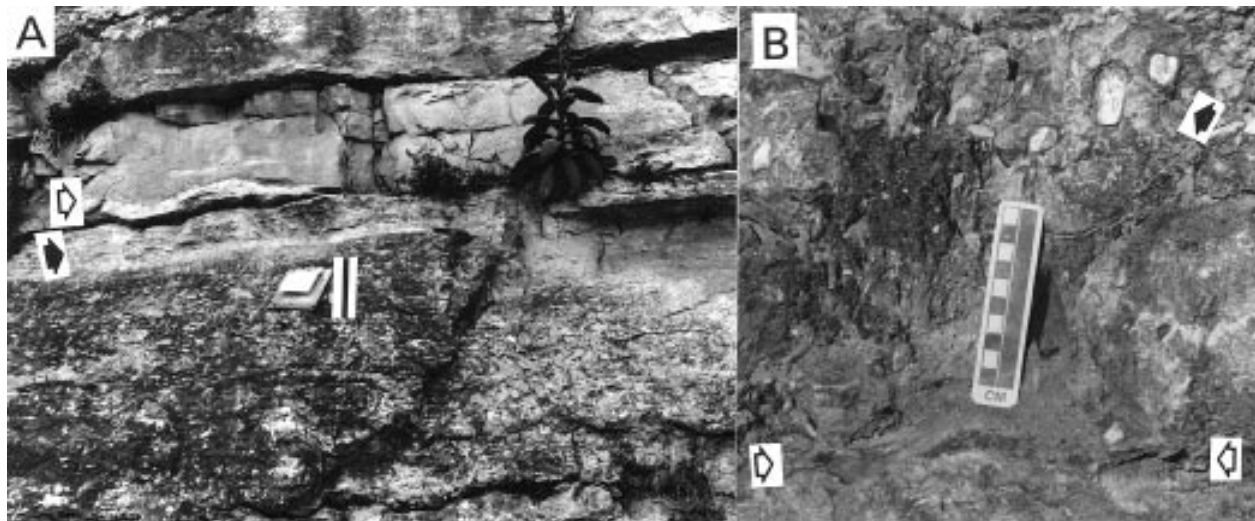


Figure 12. A) Silicification beneath the Oneota-Shakopee contact east of Preston (PE), Minnesota. Open arrow indicates the position of the contact. Black arrow indicates a 30 cm-thick zone of massive cherty silicification beneath contact. Reworked silcrete lithiclasts (not visible in this photograph) suggest partial erosion of silcrete cap prior to Shakopee deposition. Scale bar: 30 cm. B) Close-up of Oneota-Shakopee contact at Lanesboro (LB), Minnesota. Open arrows indicate the contact. Black arrow indicates chert-pebble conglomerate (reworked silcrete lithiclasts) above contact.

superimposed authigenic silica fabrics of different ages.

PALEOCLIMATIC INTERPRETATIONS

The most convincing paleoclimatic interpretations based on authigenic silica fabrics are supported by independent criteria, such as the presence of climate-sensitive minerals (for example, Habermann, 1978; Ross and Chiarenzelli, 1985; Khalaf, 1988; Mustard and Donaldson, 1990), fossil evidence (for example, Alley, 1977; Ambrose and Flint, 1981), and records of recent climate (for example, Thiry and others, 1988). Problems of interpretation commonly arise when interpreting fossil Cenozoic silcretes formed in a different climatic regime than the existing one (for example, Hutton and others, 1978).

Cambro-Ordovician strata of the Upper Midwest contain diagenetic features suggestive of both semiarid and humid climates. The mid-Lower and Lower-Middle Ordovician unconformities are associated with extensive paleokarst (Smith, 1989; Smith and others, 1993, 1996) and the

Lower-Middle Ordovician unconformity appears to contain some fluvial channels (Mai and Dott, 1985), both of which imply relatively humid conditions. In contrast, nodular and bedded primary anhydrite (now moldic or silicified) within the Prairie du Chien Group suggests relatively arid conditions. The disparate evidence for both arid and humid climatic conditions sug-

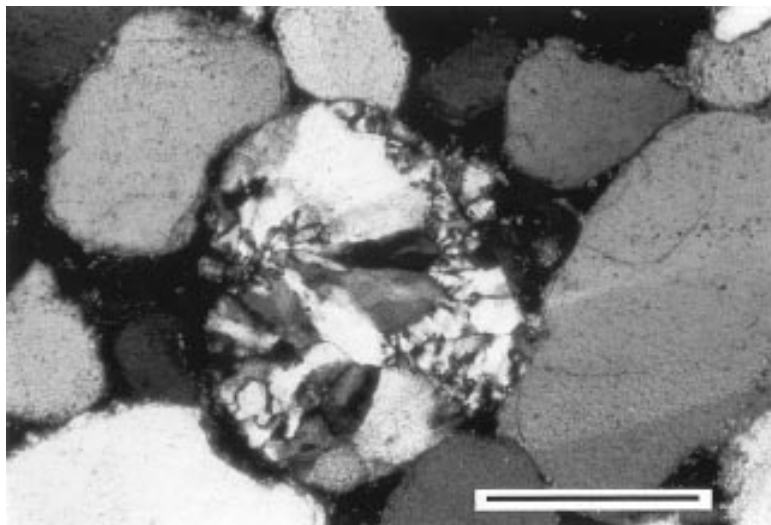


Figure 13. Reworked silcrete clast containing truncated microquartz and megaquartz cements from the upper Shakopee Formation at Prairie du Chien (PDC), Wisconsin. Crossed nicols. Scale bar: 0.5 m.

gests that a simple paleoclimate model based on authigenic silica fabrics would be inaccurate, but the climatic conditions inferred for Cenozoic silcretes are no less ambiguous (see Summerfield, 1983b; Twidale and Hutton, 1986).

CONCLUSIONS

Authigenic silica fabrics associated with the Cambro-Ordovician, mid-Lower Ordovician, and Lower-Middle Ordovician unconformities in the Upper Midwest show striking macroscopic and petrographic similarities to Cenozoic silcretes and are thus also interpreted as having formed during subaerial exposure. *In situ* silica is patchily distributed up to 30 m beneath unconformities, but is most abundant within 5 m of unconformities. Reworked clasts of silicified material are present above unconformities. Silica fabrics are best developed in exposures near the Wisconsin Arch axis. Authigenic silica fabrics are valuable indicators of subaerial exposure in carbonate rocks of the Upper Midwest because they are easily identified in well cuttings and are not masked by regional dolomitization.

ACKNOWLEDGMENTS

This research was partially supported by grants from the American Association of Petroleum Geologists, ARCO Oil and Gas Company, the Gas Research Institute, Sigma Xi—The Scientific Research Society, and the University of Wisconsin-Madison Graduate School. W.B. Harrison, III, and D.A. Barnes of Western Michigan University provided access to cores and cuttings from the Michigan Basin. K. McSweeney of the Department of Soil Science at the University of Wisconsin-Madison provided valuable insight and advice in the field and in discussions. C.R. Twidale and M.J. McFarlane introduced Dott to silcretes in Australia in 1992, including the Beda Valley examples.

REFERENCES

- Alley, N.F., 1977, Age and origin of laterite and silcrete duricrusts and their relationship to episodic tectonism in the mid-north of South Australia: *Journal of the Geological Society of Australia*, v. 24, p. 107-116.
- Ambrose, G.J., and Flint, R.B., 1981, A regressive Miocene lake system and silicified strandlines in northern South Australia—Implications for regional stratigraphy and silcrete genesis: *Journal of the Geological Society of Australia*, v. 28, p. 81-94.
- Austin, G.S., 1974, Multiple overgrowths on detrital quartz sand grains in the Shakopee Formation (Lower Ordovician) of Minnesota: *Journal of Sedimentary Petrology*, v. 4, p. 358-362.
- Bain, H.F., and Ulrich, E.O., 1905, Copper deposits of Missouri: U.S. Geological Survey Bulletin 267, 50 p.
- Dury, G.H., 1969, Rational descriptive classification of duricrusts: *Earth Science Journal*, v. 3, p. 77-86.
- Dury, G.H., and Knox, J.C., 1971, Duricrusts and deep-weathering profiles in southwest Wisconsin: *Science*, v. 174, p. 291-292.
- Ernst, W.G., and Calvert, S.E., 1969, An experimental study of the recrystallization of porcellanite and its bearing on the origin of some bedded cherts: *American Journal of Science*, v. 267-A, p. 114-133.
- Folk, R.L., and Pittman, J.S., 1971, Length-slow chalcedony, a new testament for vanished evaporites: *Journal of Sedimentary Petrology*, v. 41, p. 1045-1058.
- Friedman, G.M., and Shukla, V., 1980, Significance of authigenic quartz euhedra after sulfates—Example from the Lockport Formation (Middle Silurian) of New York: *Journal of Sedimentary Petrology*, v. 50, p. 1299-1304.
- Habermann, G.M., 1978, Mineralogic and textural variations of the duricrust in southwestern Wisconsin: unpublished Ph.D. dissertation, University of Wisconsin-Madison, 153 p.
- Haberman, G.M., and Dury, G.H., 1974, Deep weathering and duricrusting in the Driftless Area, in Knox, J.C., and Mickelson, D.M., eds., Late Quaternary Environments of Wisconsin: Wisconsin Geological and Natural History Survey, p. 118-124.
- Hall, W.E., and Friedman, I., 1963, Composition of fluid inclusions, Cave-in-Rock fluorite district, Illinois, and Upper Mississippi Valley zinc-lead district: *Economic Geology*, v. 38, p. 886-911.

- Heyl, A.V., and West, W.S., 1982, Outlying mineral occurrences related to Upper Mississippi Valley mineral district, Wisconsin, Iowa, Illinois, and Minnesota: *Economic Geology*, v. 77, p. 1803-1817.
- Hutton, J.T., Twidale, C.R., and Milnes, A.R., 1978, Characteristics and origin of some Australian silcretes, in Langford-Smith, T., ed., *Silcrete in Australia*: University of New England, Armidale, New South Wales, p. 19-39.
- Hutton, J.T., Twidale, C.R., Milnes, A.R., and Rosser, H., 1972, Composition and genesis of silcretes and silcrete skins from the Beda Valley, southern Arcoona Plateau, South Australia: *Journal of the Geological Society of Australia*, v. 19, p. 31-39.
- Jacka, A.D., 1974, Replacement of fossils by length-slow chalcedony and associated dolomitization: *Journal of Sedimentary Petrology*, v. 44, p. 421-427.
- Jenkins, R.A., 1968, Epigenetic sulfide mineralization in the Paleozoic rocks of eastern and southern Wisconsin: unpublished M.S. thesis, University of Wisconsin-Madison, 46 p.
- Khalaf, F.I., 1988, Petrography and diagenesis of silcrete from Kuwait, Arabian Gulf: *Journal of Sedimentary Petrology*, v. 58, p. 1014-1022.
- Kutz, K.B., and Spry, P.G., 1989, The genetic relationship between Upper Mississippi Valley district lead-zinc mineralization and minor base metal mineralization in Iowa, Wisconsin, and Illinois: *Economic Geology*, v. 84, p. 2139-2154.
- Lamplugh, G.W., 1902, "Calcrete" [letters]: *Geological Magazine*, v. 9, p. 575.
- Lamplugh, G.W., 1907, The geology of the Zambesi Basin around the Batoka Gorge (Rhodesia): *Quarterly Journal of the Geological Society of London*, v. 63, p. 162-216.
- Langford-Smith, T., 1978, A select review of silcrete research in Australia, in Langford-Smith, T., ed., *Silcrete in Australia*: University of New England, Armidale, New south Wales, p. 1-12.
- Leith, C.K., 1925, Silicification of erosion surfaces: *Economic Geology*, v. 20, p. 513-523.
- McLimans, R.K., 1977, Geological fluid inclusion and stable isotope studies of the Upper Mississippi Valley zinc-lead district, southwest Wisconsin: unpublished Ph.D. dissertation, Pennsylvania State University, State College, 175 p.
- Mai, H., and Dott, R.H., Jr., 1985, A subsurface study of the St. Peter Sandstone in southern and eastern Wisconsin: Wisconsin Geological and Natural History Survey Information Circular 47, 26 p.
- Maliva, R.G., and Siever, R., 1988, Pre-Cenozoic nodular cherts: evidence for opal-CT precursors and direct quartz replacement: *American Journal of Science*, v. 288, p. 798-809.
- Maliva, R.G., and Siever, R., 1989, Nodular chert formation in carbonate rocks: *Journal of Geology*, v. 97, p. 421-433.
- Meyer, R., and Pena dos Reis, R.B., 1985, Paleosols and alunite silcretes in continental Cenozoic of western Portugal: *Journal of Sedimentary Petrology*, v. 55, p. 76-85.
- Milliken, K.L., 1979, The silicified evaporite syndrome—Two aspects of silicification history of former evaporite nodules from southern Kentucky and northern Tennessee: *Journal of Sedimentary Petrology*, v. 49, p. 245-256.
- Murray, R.C., 1990, Diagenetic silica stratification in a paleosilcrete, north Texas: *Journal of Sedimentary Petrology*, v. 60, p. 717-720.
- Mustard, P.S., and Donaldson, J.A., 1990, Paleokarst breccias, calcretes, silcretes, and fault talus breccias at the base of upper Proterozoic "Windermere" strata, northern Canadian Cordillera: *Journal of Sedimentary Petrology*, v. 60, p. 525-539.
- Nadon, G.C., and Smith, G.L., 1992, Identification of subaerial unconformities in the subsurface—an example from the Lower-Middle Ordovician of the central Michigan Basin, in Candelaria, M.P., and Reed, C.L., eds., *Paleokarst, Karst-Related Diagenesis, and Reservoir Development: Examples from Ordovician-Devonian Age Strata of West Texas and the Mid-Continent: Permian Basin Section-SEPM 1992 Field Trip Guidebook*, Publication 92-33, p. 153-164.

Noble, J.P.A., and van Stempvoort, D.R., 1989, Early burial quartz authigenesis in Silurian platform carbonates, New Brunswick, Canada: *Journal of Sedimentary Petrology*, v. 59, p. 65-76.

PROPOSED REFERENCE SECTIONS AND CORRELATION OF UPPER SILURIAN AND DEVONIAN STRATA, EASTERN WISCONSIN

Charles W. Rovey II¹

ABSTRACT

Three new rock cores are designated as reference sections for the Upper Silurian Waubakee and the Devonian Lake Church and Thiensville Formations. They were taken near each respective type section in Ozaukee County, each of which is now virtually obscured. Based on the cores, correlation to strata in Milwaukee County is now more certain. The type Waubakee, and strata assigned with some uncertainty to the Waubakee in Milwaukee County, have virtually identical stratigraphic sequences, namely an upward gradational change over several meters from the fossiliferous open-marine Racine Formation to a barren, laminated, tidal flat deposit. Therefore, the two deposits appear to be properly correlated.

The Lake Church Formation is absent in Milwaukee County where the Waubakee Formation is directly overlain by the Thiensville Formation. Strata assigned to the basal Thiensville in Milwaukee County contain lithologies generally dissimilar to previous descriptions of the type Thiensville, but the new cores are proof that the same lithologic sequence is also present at the Thiensville type section.

In Ozaukee County member subdivisions previously established within the Lake Church Formation were poorly defined and are unrecognizable within the new reference section core, taken less than a kilometer from the type section. Therefore, the member subdivisions are abandoned.

INTRODUCTION

The western-most Upper Silurian and Devonian strata of the Michigan basin are present along a narrow band parallel to the Lake Michigan Shoreline in Milwaukee and Ozaukee Counties, Wisconsin (figs. 1, 2). However, these strata are largely covered with glacial drift, and the few existing quarry and natural exposures are not sufficient for detailed stratigraphic analysis. Recently, the Milwaukee Metropolitan Sewerage District (MMSD) constructed over 50 km of deep tunnels to store and convey overflows from combined sewers. For their geotechnical data base over 100 rock cores were taken within or through the Silurian/Devonian strata.

Data from the cores are sufficient to interpret depositional environments and confirm general stratigraphic relationships for the Upper Silurian and Devonian formations in Milwaukee County (Mikulic and Kluessendorf, 1988; Kluessendorf and others, 1988), but additional questions were raised concerning correlation to their type areas in Ozaukee County (fig. 1). Specifically, the MMSD cores contain strata assigned to the Thiensville Formation (MMSD, 1981; fig. 2)

which were not previously described at the type section or in any other exposure. They do, however, contain limited strata with a lithology and fauna similar to a distinctive part of the upper (type) Lake Church Formation. The general Lake Church lithology, however, is absent in the cores, raising the possibility that a complex facies relationship exists between the two formations.

The final question pertains to strata assigned to the Waubakee Formation. Although the strata are lithologically similar to the type-Waubakee, they pinch out in northern Milwaukee County (fig. 3). Hence, the two rock bodies are not continuous, raising the question of whether they are truly correlative or not.

These questions could not be addressed with existing data. Not only are the type sections of all three formations largely or totally obscured, but a complete published description, including upper and lower contacts, did not exist for any specific location, including the type sections. Therefore, cores were taken through the Upper Silurian/Devonian as close as possible to each type section to address these questions and serve as permanent reference sections.

¹Geoscience Department, Southwest Missouri State University, 901 S. National Ave., Springfield, Missouri 65804

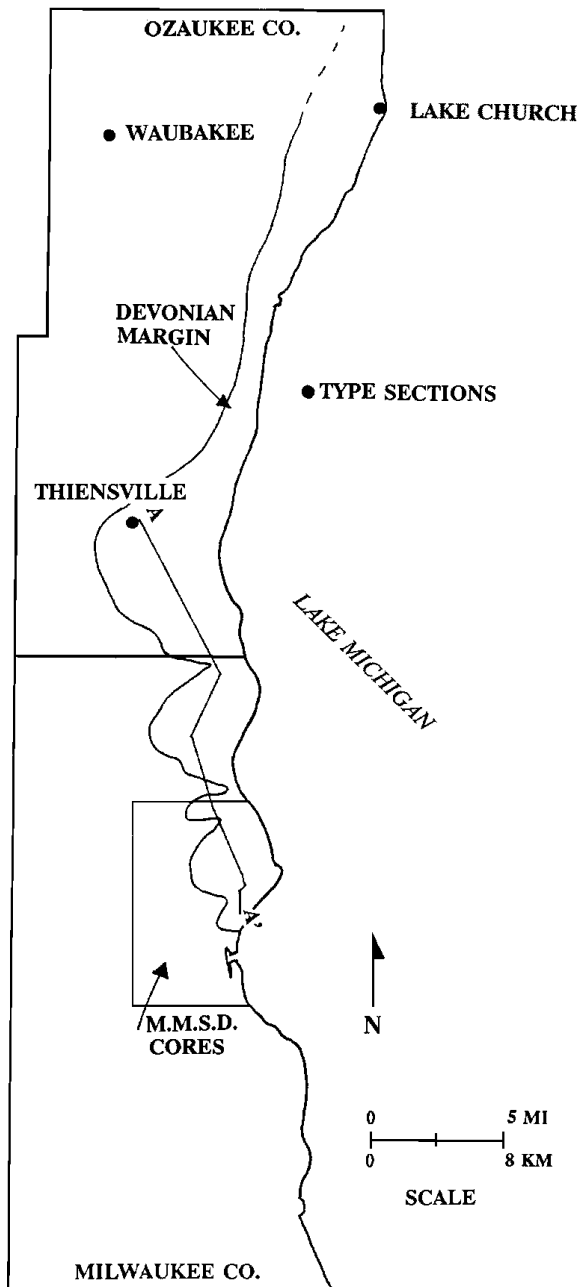


Figure 1. Location map, southeastern Wisconsin. Devonian margin taken from Rovey (1990).

HISTORY AND TYPE SECTION DESCRIPTIONS

Waubakee Formation

The Lake Church and Thiensville Formations were once included within the Waubakee Formation. Chamberlin (1883) first described a laminated dolomite in

Milwaukee County between (today's) Racine and Milwaukee Formations. He described the lower part (today's Waubakee) as thin-bedded, hard, brittle, light gray and laminated. Elsewhere in Milwaukee County he described a variably-bedded, brown, porous, laminated dolomite (Thiensville) directly below the Milwaukee Formation, but he considered the different beds parts of the same unit.

Chamberlin (1877, 1883) also described two small quarries on opposite banks of the Milwaukee River approximately 1.5 km west of the Village of Waubeka and correlated those rocks to the exposures in Milwaukee County based on lithologic similarity. Alden (1906) later introduced the name Waubakee for the entire sequence, designating the northern quarry at Waubeka as the type section. Today, no trace of the north quarry remains, but the nearby south quarry still exposes 2 m of rock.

The sequence was subdivided into the current formations by Raasch (1935). He restricted the term Waubakee to the lower gray dolomite by placing the upper brown beds into the Thiensville Formation. He

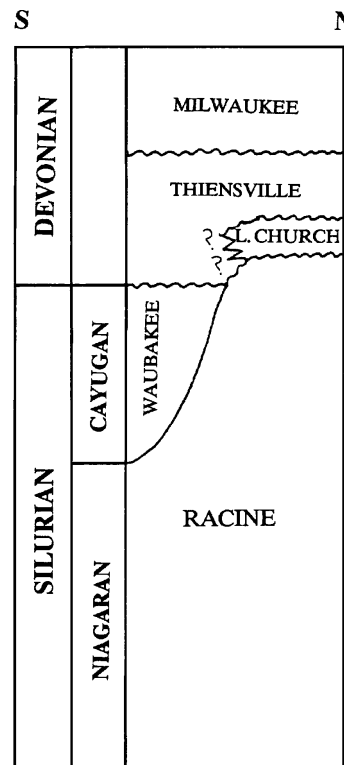


Figure 2. Upper Silurian and Devonian stratigraphy, southeastern Wisconsin. Lithostratigraphic names are at the formation level.

also designated fossiliferous strata between the Thiensville and Waubakee as the Lake Church Formation.

Lake Church Formation

Currently there are only two known exposures of the Lake Church Formation; both are in quarries now mostly flooded. Several meters of the upper type section are exposed in Harrington Beach State Park. The second exposure is the upper meter of an abandoned quarry approximately 240 m west of the Thiensville type section (fig. 1). Raasch (1935) stated that the Lake Church disappears south of the Milwaukee/Ozaukee County line, but the reasons for the disappearance are not clear.

Belgium Member

Raasch (1935) subdivided the Lake Church into two members and described the lower Belgium Member as being present only in the extreme north, presumably meaning the extreme north of Ozaukee County. By inference a basal conglomerate above the Silurian/Devonian contact is included in the Belgium Member, but his wording is ambiguous; it could also mean the strata immediately above and exclusive of the conglomerate.

He described the Belgium Member as thin-bedded "chocolate brown" dolomite. The brachiopod *Chonetes* dominates the fauna, with common bivalves and other brachiopods. He did not describe an upper contact.

Ozaukee Member

Raasch (1935) described the Ozaukee Member of the Lake Church Formation as thick-bedded, brown to dark gray, pyrite-rich dolomite. The fauna is more limited than the Belgium Member, but locally includes coral, bivalves, high-spined gastropods, and crinoids. Specific genus and species names were not given, however. He placed the upper Ozaukee contact at an erosional unconformity and conglomerate at the base of the overlying Thiensville Formation. However, the contact was not exposed at the type section, nor were any specific locations described.

Thiensville Formation

Raasch (1935) designated a road cut along Highway 57 in Thiensville as the Thiensville type section. The cut remained partially exposed until 1989 when it was covered with fill. Currently there are only two addi-

tional known exposures of the Thiensville. Several meters of the upper Thiensville are exposed along the Milwaukee River in Estabrook Park at Shorewood, and less than 1 m of (apparently) basal Thiensville is periodically exposed along the Lake Michigan shoreline approximately 2 km south of Port Washington.

Raasch (1935) characterized the Thiensville as variably-bedded with a succession of lithologies. Beds of brown, bituminous, porous, laminated dolomite alternate with lighter-colored, less-porous beds. He found only a limited fauna, and that from beds described as being near the bottom of the formation. A fossiliferous bed was formerly exposed along the base of the roadcut, but there is an approximate 6-m gap in exposure between the base of the cut and the top of the adjacent quarry where the Lake Church Formation is present. Therefore, it is difficult to judge whether or not the fossiliferous beds are actually at the base of the formation, since the lower contact was never exposed, nor reported from any other locality.

Based on the discussion above, the stratigraphic units in question are vaguely defined and characterized, and the type section designations do not meet the modern requirements of the North American Stratigraphic Code (North American Commission on Stratigraphic Nomenclature, 1983). There is an obvious need to re-visit the type sections and establish permanent reference sections to characterize each formation.

MILWAUKEE METROPOLITAN SEWER-AGE DISTRICT CORES

Waubakee Formation

Strata assigned to the Waubakee Formation in the MMSD cores are approximately 25 m thick and are hard, brittle, well-laminated dolomite mudstone with a distinct petroliferous odor when broken. Laminae range from less than 1 mm to approximately 1 cm in thickness and alternate between dark and light gray. They are parallel to sub-parallel, sometimes wavy, and sometimes discontinuous. Rarely, the laminae are crenulated with a minute fenestrate porosity, and mud-cracks and gypsum pseudomorphs are present at multiple horizons. The lower contact generally is gradational over 1.5 to 3 m with the Racine Formation, but Racine reefs, where present, may protrude into or through the Waubakee (fig. 3).

The upper Waubakee contact is sharp and erosional, as proven by reworked Waubakee clasts in the basal Thiensville. The upper 1 m interval directly beneath the basal Thiensville contact is typically discolored to a very dark gray. Locally, however, a weathering profile originating in the overlying

Thiensville extends into the upper Waubakee, obscuring the contact.

In Ozaukee County, the Waubakee has never been found outside the type area. Even where the younger Lake Church Formation is preserved, the Racine Formation, not Waubakee, is present directly beneath the Lake Church (Mikulic, 1979). Based on figure 3, the Waubakee in Milwaukee County abuts a thickened wedge of Racine Formation and, therefore, was probably never continuous with the type Waubakee. Whether the two were deposited contemporaneously, however, remains unanswered.

Thiensville Formation

In Milwaukee County, strata assigned to the Thiensville Formation are divisible into three informal subunits (fig. 4).

Lower unit

The lower unit is 6 to 7.5 m thick. Core recovery was poor within this interval because it is soft and highly weathered. The dominant lithology is a semi-consolidated dolomitic mud containing irregularly-shaped nodules and clasts of chalky dolomite. In some cores the entire interval appears relatively uniform, but in others two to three specific horizons of more intense weathering are detectable. Where the beds are relatively unweathered, they appear to be brown, granular, laminated dolomite.

This lithology was not previously reported within the Thiensville Formation. It was included because of the similarity with the upper Thiensville and the obvious lithologic contrast and erosional unconformity between it and the underlying Waubakee.

Middle unit

The middle unit is approximately 3 m thick. The lowermost lithology is brown, fine-grained, granular, friable, parallel-laminated dolomite. At the top of this interval a distinct marker bed 1 m or less thick is delineated by abundant bivalves, gastropods and silt-size quartz grains. This bed grades upward into a dark brown, highly-organic dolomite containing zones of interlaced carbonaceous laminae and thin (1 to 3 cm) interbeds of nearly black, extremely carbonaceous material.

The lithology of the middle unit also was not specifically described for the Thiensville, but may correlate to the base of the type section exposure, based on the common occurrence of fossiliferous beds, which elsewhere are extremely rare in the Thiensville. Alternatively, Mikulic and Kluessendorf (1988) and Kluessendorf and others (1988) noted the resemblance between these beds and the upper fossiliferous beds at the Lake Church type section, raising the possibility that the lower "Thiensville," as mapped in Milwaukee County, actually correlates in some manner to the Lake Church Formation. Unfortunately, specific

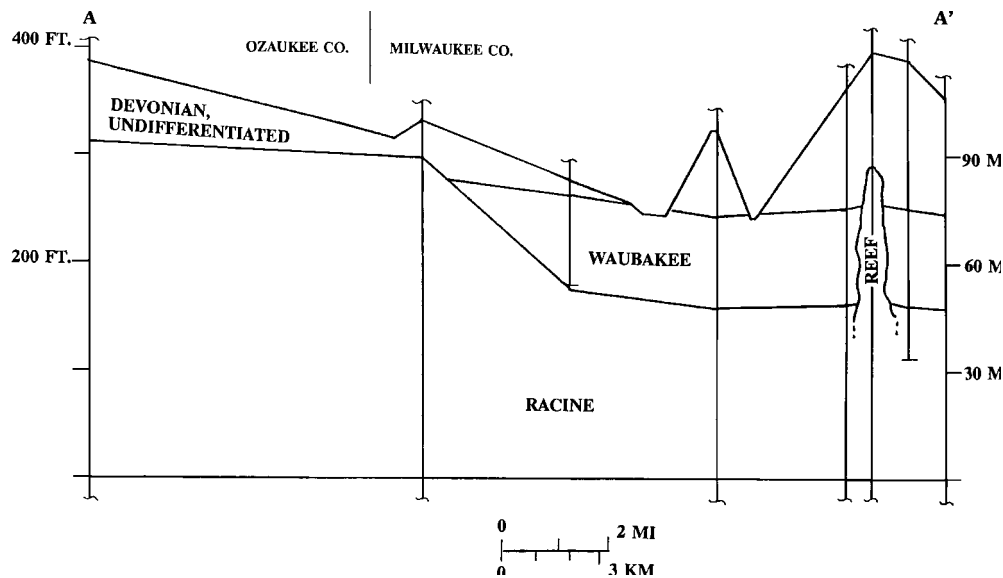


Figure 3. Geologic cross section A-A'. Modified from Rovey (1990). Line A-A' is shown on figure 1.

paleontologic data relevant to the problem are still lacking.

Upper unit

Only the upper Thiensville definitely corresponds to previous descriptions in Ozaukee County. It is generally 9 to 11 m thick and is strikingly rhythmic, consisting of brown, porous, laminated beds alternating with gray, dense, unlaminated beds. The gray beds are locally vuggy and commonly brecciated. The transition between the two lithologies is frequently an erosive, scoured contact, particularly at the top of brown intervals, and the bottom few centimeters of overlying gray beds may contain reworked clasts from the brown beds below.

Rhythmic bedding is less developed in the lowest 3 m, marking a transition to increasing dominance of weathering effects which increasingly obscure the original lithology.

The upper Thiensville contact was observed *in situ* in a dropshaft being blasted into an MMSD tunnel (see Rovey, 1990). It is marked by iron sulfide mineralization along an undulatory surface with approximately 15 cm of local relief. Large clasts (up to 0.5 m in diameter) of Thiensville are reworked into the base of the overlying Milwaukee Formation.

NEW CORES

Relevant parts of three new rock cores are described below. All are now stored at the Wisconsin Geological and Natural History Survey (WGNHS) core repository. The first core, UWM-WB is assigned the WGNHS identification number CJ-294-OZ-521-X. It was taken approximately 1000 m southwest of the Waubakee type section at the small quarry on the south bank of the Milwaukee River, approximately 1.5 km west of the Village of Waubeka (SW 1/4, NW 1/4, SE 1/4, S. 29, T 12N, R 21E, Fredonia 7.5 Minute Quadrangle). It is designated as a supplementary reference section for the Waubakee Formation.

The second core, UWM-LC (identification number CJ-295-OZ-522-X) was taken in the parking lot of the boat ramp at the dead end intersection of Ozaukee County Highway D with Lake Michigan (NW 1/4, NE 1/4, NW 1/4, S. 19, T 12N, R 23E, Port Washington East 7.5 Minute Quadrangle). This location is approximately 640 m north of Quarry Lake in Harrington Beach State Park, the Lake Church type section. The core is designated as part of the composite Lake Church primary reference section.

The third core, UWM-FF (identification number CJ-296-OZ-523-X) was taken in the truck turn-around

area northwest of the loading docks at the Federal Foods plant, Thiensville, Wisconsin (NW 1/4, NE 1/4, SE 1/4, S. 10, T 9N, R 21E, Cedarburg 7.5 Minute Quadrangle). This location is approximately 300 m east of the Thiensville type section. The core is designated as a primary reference section for the Thiensville, and part of the composite reference section for the Lake Church.

Waubakee Formation

Because the Waubakee in Milwaukee County is not continuous to the type area, it may be impossible to prove beyond doubt that the two occurrences are strictly correlative. However, if most diagnostic features are common to both sites, confidence in the traditional correlation is increased. The core at Waubeka was, therefore, taken to determine whether the type Waubakee is similar in stratigraphic sequence with underlying strata, whether it is lithologically similar over its entire thickness and whether the bottom con-

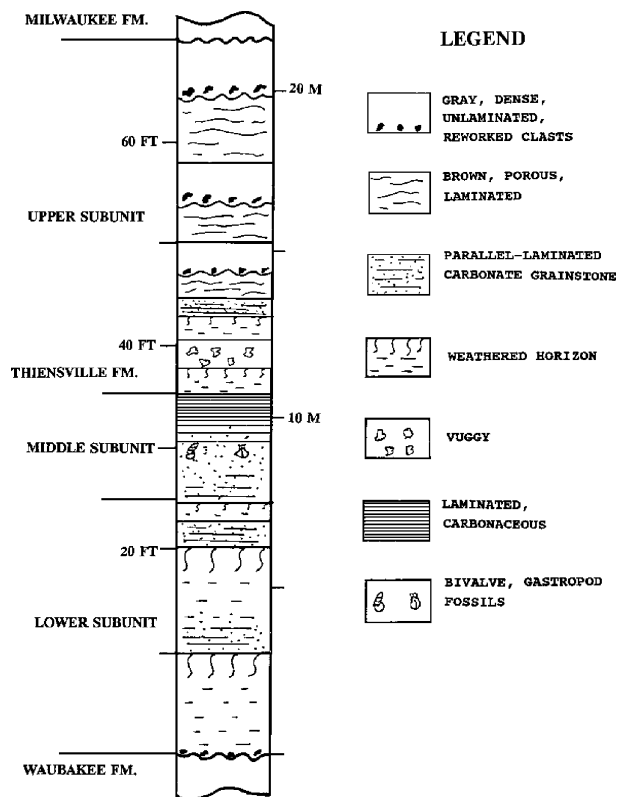


Figure 4. Generalized stratigraphic sequence with the Thiensville Formation, Milwaukee County. All lithologies are dolomite.

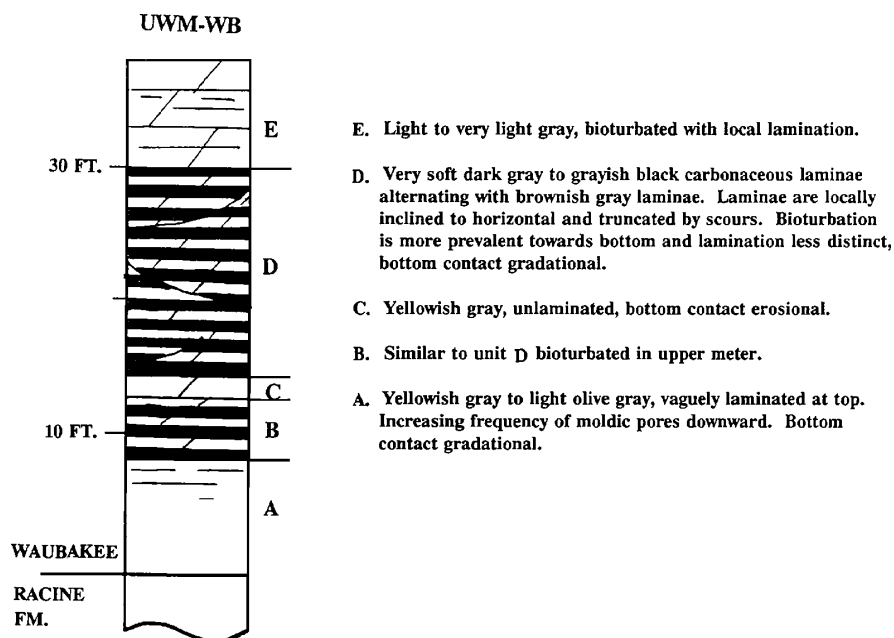


Figure 5. Graphic log and description of Waubakee reference section, core UWM-WB. All lithologies are dolomite.

tact is also gradational.

Figure 5 is a graphic log and description of relevant portions of core UWM-WB. The upper beds, still exposed in the adjacent quarry, can be confidently correlated to the former type exposure, based on both Chamberlin's (1877, 1883) and Alden's (1906) descriptions. The core, however, begins at the quarry floor, and consists of lithologies not specifically described at the type section. Therefore, it is not designated as a primary reference section for the Waubakee Formation, but as a secondary or supplementary reference section to fulfill criteria stated in the stratigraphic code (North American Committee on Stratigraphic Nomenclature, 1983, p. 853): "To illustrate the diversity or heterogeneity of a defined unit or some critical feature not evident or exposed in the stratotype."

The upper 1.5 m (exposed in the quarry) is virtually identical lithologically with the Waubakee in Milwaukee County, so the description is not repeated. The underlying strata (recovered from the core), however, vary significantly. As in Milwaukee County the contact between the upper Racine and the lower Waubakee is gradational over 2.5 m from massive fossiliferous to laminated barren dolomite. However, at Waubeka the lamination in the lower beds is distinct from that in Milwaukee County. Instead of hard, brittle, gray and dark gray laminae, the lithology is

very dark and organic-rich, with alternating soft, carbonaceous and brownish-gray laminae. At Waubeka numerous laminae are also inclined to the horizontal and truncated by scour surfaces.

Although neither Chamberlin (1877, 1883) nor Alden (1906) described the carbonaceous beds at the actual type section, Chamberlin (1883, p.197) included them within the same unit and described them from nearby exposures as: "a softer dark dolomite, colored by carbonaceous matter, sometimes disposed in frequent black, or dark brown laminae, which give to the rock an appearance quite peculiar." His description leaves little doubt that these lower beds are properly considered part of the type Waubakee Formation.

The similar stratigraphic sequences in the two locations is evidence supporting use of the term "Waubakee" for strata in Milwaukee County. At Waubeka the fossiliferous upper Racine Formation grades over approximately 2.5 m into the Waubakee, similar to the transition in Milwaukee County. Although carbonaceous laminae are not present in the MMSD cores, the predominance of lamination at both sites is evidence that the gradational contact marks a major episode of increased restriction, from open marine to tidal-flat conditions. Because such a drastic restriction is only known at one stratigraphic position in the Upper Silurian of the Michigan basin (Niagaran

- 1D: Brownish gray dolomite, fossiliferous near top, with scattered moldic porosity. Base contains undulating laminae
- 1C: Light to dark gray dolomite with local argillaceous laminae and interbeds of dark, carbonaceous laminated shale.
- 1B: Breccia, dark gray dolomite clasts encased in light gray dolomite matrix.
- 1A: Breccia, with gradual change from above to matrix of dark green shale.
- 2C: Dark gray dolomite, scattered chert, moldic porosity and corals in upper meter.
- 2B: Dark gray dolomite alternating with seams of dark irregularly-laminated shale.
- 2A: Argillaceous, nodular dolomite overlying breccia.

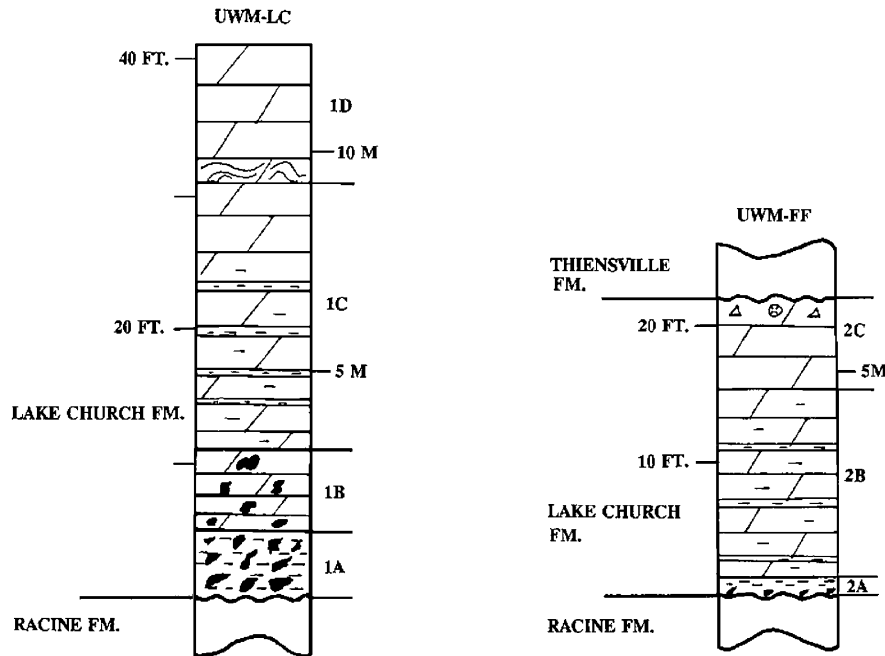


Figure 6. Graphic log and description of composite Lake Church reference section, cores UWM-LC and UWM-FF. All lithologies are dolomite.

to Cayugan transition, fig. 2), the two deposits appear generally synchronous, although paleontologic evidence is lacking.

Lake Church Formation

Figure 6 is a graphic log and description of relevant portions of cores UWM-LC and UWM-FF. Both cores are designated as a composite (primary) reference section for the Lake Church Formation, to include both upper and lower contacts.

In UWM-LC the most striking feature is the breccia in the lowest 4 m of the Devonian. The beds correspond to the basal conglomerate described by Raasch (1935), but, as mentioned, his description was unclear as to whether they should be included in the Belgium Member. The strata above the conglomerate are generally dark gray argillaceous dolomite mudstone containing pyrite and a limited fauna. They match

Raasch's description for the Ozaukee Member and have none of the characteristics of the Belgium Member. Therefore, the member subdivisions cannot be recognized in the reference section.

Besides the problem of member recognition, there is currently a conflict in nomenclature as well. The lowest member of the Quaternary-age Kewaunee Formation was recently designated as the Ozaukee Member (Mickelson and others, 1984) in the same geographic area and locally may directly overlie the Devonian-age Ozaukee Member. Although the latter usage conflicts with the priority of the original, it has become entrenched and far more widespread. Considering that the Devonian members are vaguely defined, and that the distinction between members cannot be recognized less than one kilometer from the type section, the best solution is to abandon member subdivisions within the Lake Church Formation.

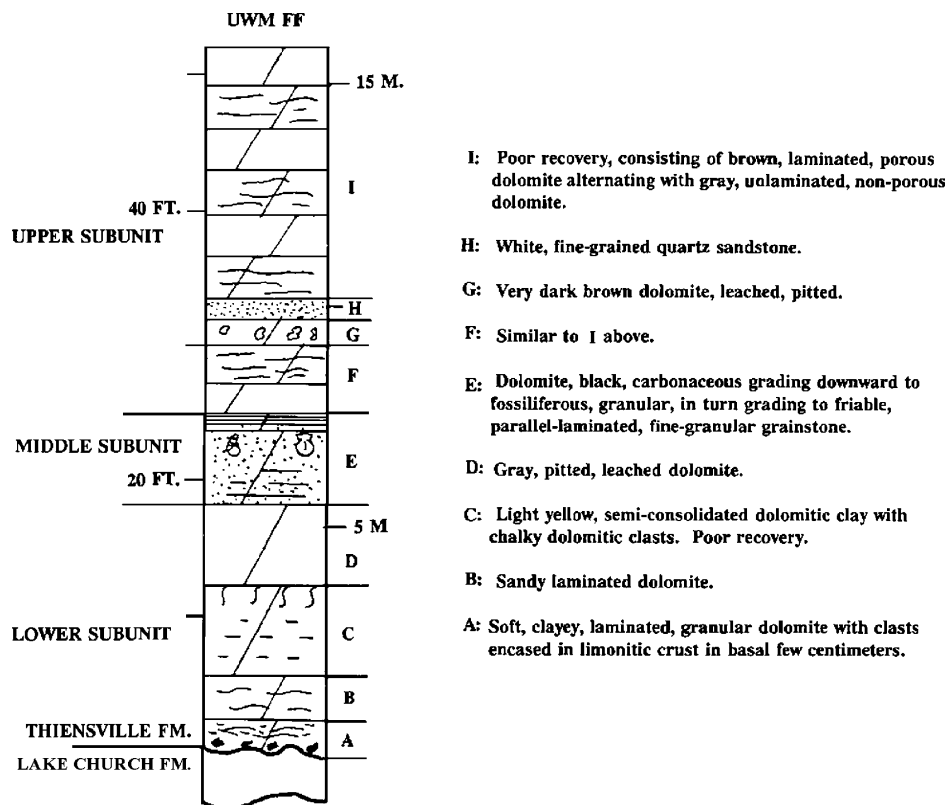


Figure 7. Graphic log and description of Thiensville reference section, core UWM-FF.

Thiensville Formation

Figure 7 is a graphic log and description of relevant portions from core UWM-FF, designated as a primary reference section for the Thiensville Formation, and part of the composite Lake Church reference section. Although core recovery was poor, enough detail is present to divide the Thiensville into three main units, correlative to the three subunits in Milwaukee County.

The lowest Thiensville is a highly-weathered, poorly-consolidated, clay-rich interval overlying a conglomeritic erosional base. The middle division has a brown, finely-laminated, fine-granular lithology grading upward through a highly fossiliferous intermediate into a dark brown to black carbonaceous bed. The upper Thiensville is dominantly a coarse-grained, brown, porous, laminated lithology alternating with a denser, unlaminated, gray lithology. The upper Thiensville contact unfortunately is not present.

The lower subunit is problematic, because its elevation is below road level, but above the top of the adjacent quarry which exposes Lake Church strata. Therefore, it was not exposed along the roadcut and not originally defined as part of either the Thiensville

or the Lake Church. The lithology, however, is clearly similar to the overlying Thiensville and contrasts strongly with the underlying Lake Church. The unconformable contact at the base of the subunit also marks an abrupt break in sedimentation and change in sediment character. Therefore, these beds are now designated as part of the Thiensville.

The organic-rich bed in the middle unit is greatly reduced in thickness from the MMSD cores and probably was not exposed during Raasch's visits, but the underlying fossiliferous bed apparently is the bottom fossiliferous zone; its elevation in the core is the same as the base of the cut. The upper subunit corresponds to the general type section description by Raasch (1935).

Is the question of Thiensville - Lake Church equivalency settled? The answer can only be given conditionally. It is now clear that the middle and lower Thiensville subunits from the MMSD cores are present at the Thiensville type section *and* that they are properly part of the type Thiensville. However, this does not preclude the possibility of a facies relationship between the type Thiensville and Lake Church, unless the upper fossiliferous beds at the

Lake Church type section correlate exactly with the (somewhat fossiliferous) Lake Church beds beneath the type Thiensville. Future research should address this issue of correlation between the two type sites.

SUMMARY AND CONCLUSIONS

The Upper Silurian Waubakee and Devonian Lake Church and Thiensville Formations were vaguely defined and characterized at their respective type areas in Ozaukee County. Lack of information on lithologic variation, internal subdivision and bounding contacts, caused uncertainty regarding correlation to their possibly - equivalent units in Milwaukee County. Data from new rock cores near the type sections are defined as reference sections for each respective formation, and clarify much of the previous uncertainty, generally confirming previous correlations.

Although the type Waubakee includes 9 m of highly carbonaceous basal strata not present in Milwaukee County, a similar stratigraphic sequence in both cases is evidence supporting correlation. Both deposits grade upward over several meters from the fossiliferous Racine Formation into a barren, laminated, deposit. The transition, therefore, marks an upward change from open, normal marine to shallow, restricted, tidal flat sedimentation. Because such a drastic restriction is known only at the Niagaran/Cayugan transition for Michigan basin strata, the two deposits appear generally correlative.

The Lake Church Formation is not present in Milwaukee County. Reasons for its disappearance are not yet clear, however. Formal member subdivisions within the Lake Church are unrecognizable in the new reference section, and are, therefore, abandoned.

Three informal lithologic subdivisions within the Thiensville Formation are present at both the type area and in Milwaukee County. Research on these subdivisions should continue to determine if their elevation to formal member status is warranted. Because of their common occurrence, fossiliferous strata near the middle of the Thiensville in Milwaukee County are properly assigned to the Thiensville Formation in spite of lithologic and faunal similarity with portions of the type Lake Church. However, the possibility of a facies relationship between the fossiliferous beds, also present at the type section, and the type Lake Church cannot be ruled out without further research.

ACKNOWLEDGMENTS

This research was funded by the University of Wisconsin Sea Grant College Program, National Oceanic

and Atmospheric Administration, U.S. Department of Commerce, and from the State of Wisconsin Federal Grant NA 90AA-D-SG469, project R/NI-14.

REFERENCES

- Alden, W.C., 1906, Description of the Milwaukee quadrangle, Wisconsin: U.S. Geological Survey Atlas, Milwaukee Folio 140, 12 p.
- [Chamberlin, T.C., ed., 1877], Geology of Wisconsin, Survey of 1873-1877, Volume II: [Wisconsin] Commissioners of Public Printing, 768 p.
- [Chamberlin, T.C., ed., 1883], Geology of Wisconsin, Survey of 1873-1877, Volume I: [Wisconsin] Commissions of Public Printing, 725 p.
- Kluessendorf, J.L., Mikulic, D.G., and Carman, M.R., 1988, Distribution and depositional environments of the westernmost Devonian rocks in the Michigan basin, in McMillan, N.J., Embry, A.F., and Glass, D.J., eds., Devonian of the World: Canadian Society of Petroleum Geologists Memoir 14, v. 1, p. 251-263.
- Mickelson, D.M., Clayton, Lee, Baker, R.W., Mode, W.N., and Schneider, A.F., 1984, Pleistocene stratigraphic units of Wisconsin: Wisconsin Geological and Natural History Survey Miscellaneous Paper 84-1.
- Mikulic, D.G., 1979, The paleoecology of Silurian trilobites with a section on the Silurian stratigraphy of southeastern Wisconsin: unpublished Ph.D. dissertation, Oregon State University, 864 p.
- Mikulic, D.G., and Kluessendorf, J.L., 1988, Subsurface stratigraphic relationships of the upper Silurian and Devonian rocks of Milwaukee County, Wisconsin: *Geoscience Wisconsin*, v. 12, p. 1-23.
- Milwaukee Metropolitan Sewerage District [MMSD], 1981, Inline storage facilities plan: draft / [prepared for the Milwaukee Metropolitan Sewerage District by the] Program Management Office, Milwaukee Water Pollution Abatement Program ... [and others]: Milwaukee, Wis.: [The District, 1981]
- North American Commission on Stratigraphic Nomenclature, 1983. North American Stratigraphic Code: *American Association of Petroleum Geologists Bulletin.*, v. 67, p. 841-875.
- Raasch, G.O., 1935, Devonian of Wisconsin: Kansas Geological Society, 9th Ninth Annual Field Conference, p. 261-267.

Rovey, C.W., 1990, Stratigraphy and sedimentology of Silurian and Devonian carbonates, eastern Wisconsin, with implications for ground-water discharge into Lake Michigan: unpublished Ph.D. dissertation, University of Wisconsin-Milwaukee, 427 p.

GRAVITY SIGNATURE OF THE WAUKESHA FAULT, SOUTHEASTERN WISCONSIN

*Keith A. Sverdrup¹, William F. Kean¹, Sharon Herb^{1,2}, Susan A. Brukardt¹,
and Ronald J. Friedel¹*

ABSTRACT

Gravity data were collected at approximately 1.6 km spacing over the Waukesha Fault in parts of Washington, Ozaukee, Waukesha, and Milwaukee Counties. The gravity signature of the fault trends northeast with gravity values to the northwest, on the upthrown side, approximately 10 mgal higher than on the downthrown side. Gravity models that closely approximate the observed gravity were constructed. The smallest residuals are obtained from models of the fault that have a gentle dip of about 10° to 20° to the southeast with a maximum offset across the fault of about 600 m.

INTRODUCTION

Although the presence of the Waukesha Fault in southeastern Wisconsin has been recognized for some time (Foley and others, 1953; Thwaites, 1957) the location, linear extent, and subsurface geometry of the fault have, until recently, been poorly constrained. The ambiguity related to the fault geometry is the result of previous reliance on predominantly shallow well data and only one significant surface exposure at the Waukesha Stone and Lime Quarry in the city of Waukesha. The fault strikes N 40° E at the quarry and appears to be a high angle normal fault downthrown to the southeast. The near-surface displacement on the fault has been estimated at between 10 (Mikulic and Mikulic, 1977) and 30 m (Foley and others, 1953). The displacement at depth is thought to be as great as 450 m (Thwaites, 1957). The first detailed geophysical work over the fault was a gravity survey covering Waukesha County conducted by Brukardt (1983). Preliminary interpretation of the data yielded a model of the fault that was consistent with the above mentioned characteristics. The survey also suggested that the gravity signature from the fault remained strong at the northeastern corner of the county, indicating that the fault continues toward Lake Michigan. Additional gravity data were collected by Sharon Herb in 1985 in parts of Washington, Ozaukee, and Milwaukee Counties to map the continuation of the fault northeast of Waukesha County. This paper presents the results of an interpretation of the combined gravity data sets of Brukardt and Herb.

DESCRIPTION OF THE SURVEY

The data were collected at approximately 1.6 km spacing at road intersections and benchmarks where elevations were given on US Geological Survey topographic maps. The survey area is outlined in figure 1.

A contour map of the data is shown in figure 2 and a 3-dimensional representation in figures 3a and b. The gravity signature of the fault is characterized by a northeast-trending zone roughly five km wide of tightly spaced contours that separate a region to the northwest with gravity values approximately 10 mgal greater than the region on the southeastern side of the

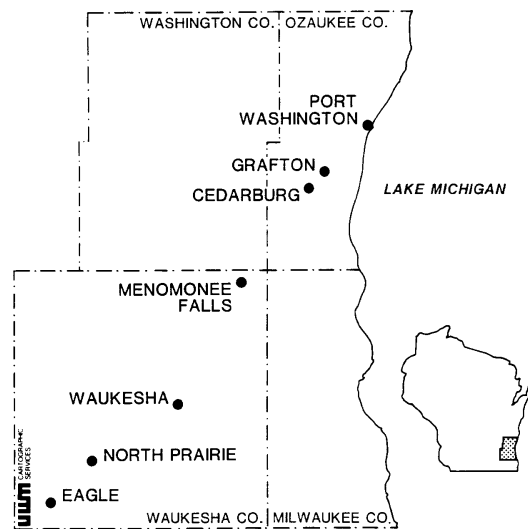


Figure 1. Four county area of the gravity survey

¹Department of Geological & Geophysical Sciences, University of Wisconsin-Milwaukee, Milwaukee, Wisconsin 53012

²Deceased

fault. This is particularly evident in figures 3a and b where the perspective of the views are N 50° W, which is perpendicular to the gravity trend, and S 40° W, which is along the trend. When examined in greater detail, this zone of tightly spaced contours can be seen to change strike and is apparently offset in one location. At the southwestern end, the gravity signature trends roughly N 19° E for 10 km from a point 3 km south of Eagle, Wisconsin on the Waukesha-Walworth County line to the town of North Prairie. At North Prairie it turns to N 47° E and continues for about 13 km to a point due west of Waukesha where it is offset in a right-lateral sense 3 km to the western edge of the city of Waukesha. The location of this offset is evident in figure 3a where there is a pronounced break in the linear gravity high that appears as a valley in the Bouguer gravity surface. From that point it extends 23 km at N 38° E through Menomonee Falls to the Washington-Waukesha

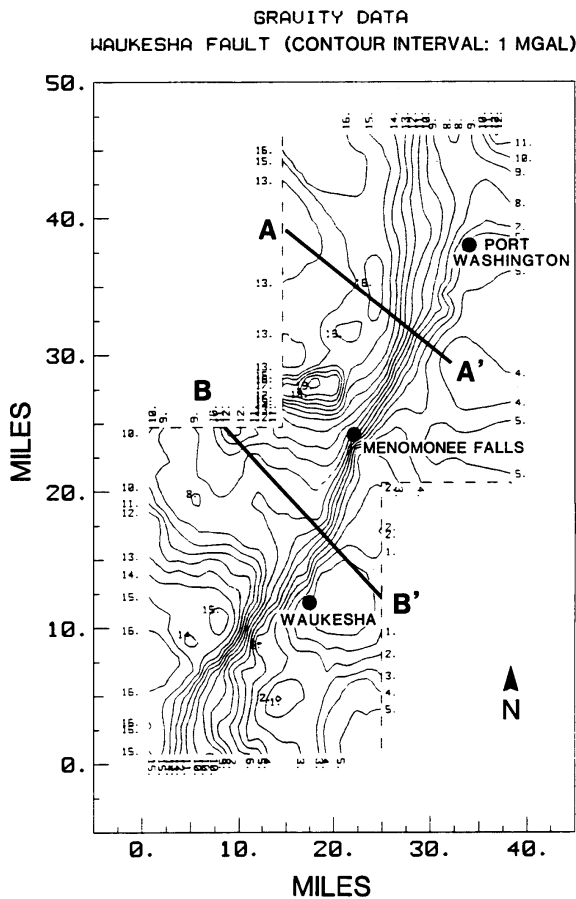


Figure 2. Contour plot of the gravity data. Contour interval is one mgal. Locations of the two modelled profiles are indicated.

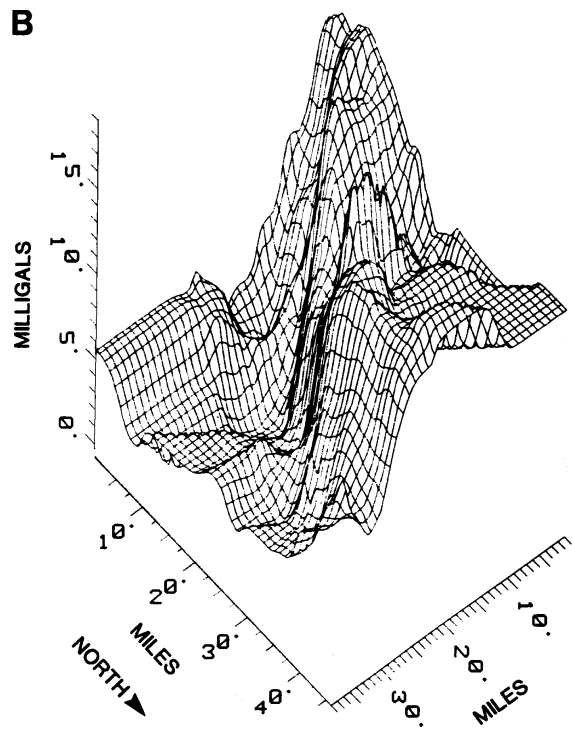
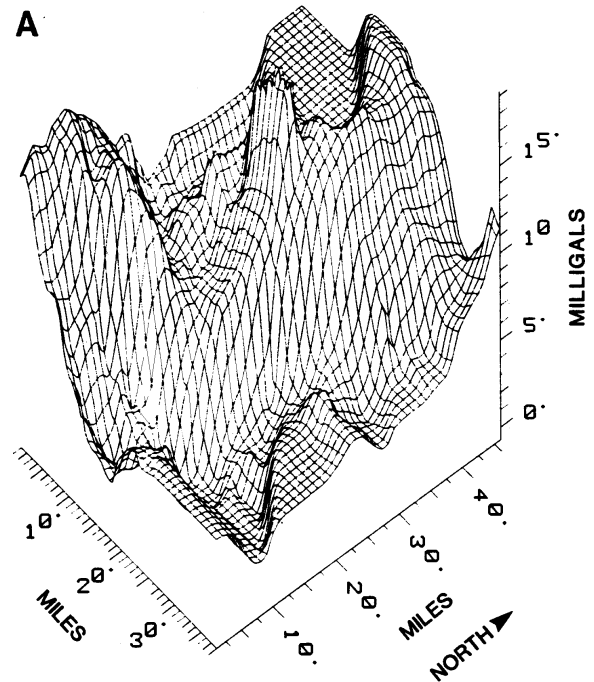


Figure 3. 3-dimensional plot of the gravity signature of the Waukesha Fault viewed from the southeast in a direction N 50° W (3a) and from the northeast in a direction S 40° W (3b).

county line roughly 2.5 km west of the Ozaukee County line. It then continues for 6 km with a strike of N 27° E until, about 5 km southwest of Cedarburg, it changes strike to N 36° E and extends through Cedarburg and Grafton 22 km to Port Washington. The offset in the fault west of Waukesha was interpreted by Brukardt (1983) to be due to a second fault striking N 60° W.

MODEL GEOLOGY

Bedrock in southeastern Wisconsin dips gently to the east from the Wisconsin Dome into the Michigan Basin. The area was differentially eroded before Pleistocene deposition so that the contact between bedrock and glacial deposits is irregular (Distelhorst, 1967; Brukardt, 1983).

The basement Precambrian consists of granite, slate, and quartzite which dip to the east. The Precambrian is overlain by Cambrian and Ordovician sandstone. These are in turn overlain by Ordovician and Silurian shale and dolomite (Thwaites, 1940; Dutton and Bradley, 1970). The surficial materials are glacial deposits that vary in thickness from essentially zero to several hundred meters.

The general stratigraphy down to the Precambrian is from Moretti (1970) and the Wisconsin Utility Project report on the Haven nuclear power plant site (Wisconsin Electric Power Company, and others, 1979a). The depth of Lake Michigan and the depth to bedrock beneath the lake are from Wold and others (1981). The gross characteristics of the thickness of the unconsolidated material were obtained from Distelhorst (1967), Skinner and Borman (1973), Gruetzmacher (1974), Brukardt (1983), and well logs obtained from the Wisconsin Geological and Natural History Survey.

The general distribution of the Precambrian quartzite and granite is based on work by Thwaites (1940) and Dutton and Bradley (1970). Well data to the northwest of the fault is sufficient to fix the depth to the Precambrian in a regional manner. However, no known wells extend to the Precambrian on the southeastern side of the fault. In addition, Thwaites (1940) states that the Precambrian surface is more than 800 meters below sea level on the southeast side.

Gabbro was included in the models because of the presence of mapped gravity and magnetic highs in the Lake Michigan Basin that come onshore in Ozaukee County and are attributed to mafic rock at depth (Wisconsin Electric Power Company, and others, 1979b). In addition, models without the gabbro present required 2000 meters or more of displacement

Table 1. *Densities used for model calculations.*

Density (g/cm ³)	Rock
1.00	Lake Michigan
1.80	Unconsolidated Sediment
2.60	Sandstone (Ordovician - Cambrian)
2.63	Quartzite (Precambrian)
2.67	Dolomite and Shale (Silurian - Ordovician)
2.69	Granite (Precambrian)
2.74	Crustal Rock at Depth
3.00	Gabbro

on the fault to produce the observed amplitude of the gravity signature, which is far in excess of any previous estimates.

DISCUSSION

Two profiles across the fault were chosen for modeling. The locations of the profiles, labelled A-A' and B-B', are shown in figure 2. The observed gravity along the profiles is given in figure 4.

The rock types and associated densities used in the modelling are given in table 1. In the modelling process we found it necessary to slightly alter some of the densities depending on the nature of the model in order to obtain reasonable residuals. A Talwani computer program was used in the calculations (Talwani and Ewing, 1959). The models used in the program were extended on either side of the ends of the profiles for a distance roughly equal to the lengths of the profiles to eliminate edge effects.

Our initial models were of steeply dipping faults because the Waukesha Fault has been generally accepted as being nearly vertical. Model 1 along profile B-B' is an example of these and is illustrated in figure 5. This model incorporates a fault having a dip of 80 degrees to the southeast. The vertical offset of the Silurian and Ordovician dolomite and shale is 30 m. The underlying Ordovician and Cambrian sandstone are offset by 30 m at the top and 400 m at the bottom. This results in a significant thickening of the sandstone east of the fault. The gabbro in this model appears as two distinct intrusive bodies rather than a single mass offset by the fault. The residual gravity values for this model are plotted in figure 9. The magnitudes of the station residuals are generally less than 0.2 mgal with the exception of stations 19 and 22 on either side of the fault and station 34 at the eastern end of the profile. The RMS error for this model is a relatively large 0.128 mgal.

Although the data are adequately modelled at

stations several km away from the fault, the residual gravity curve has a characteristic shape in the immediate vicinity of the fault that suggests the dip is too steep. The expected residual gravity curve produced by a model with a fault dipping at an angle greater than the actual fault being studied is shown in figure 6. The characteristic signature of a growing negative

residual approaching the fault that reverses and passes through zero across the fault and then grows to a maximum positive residual on the other side is quite clear. As a result, we elected to try models that included shallow dipping faults despite the long-standing belief that the Waukesha Fault is a high angle fault.

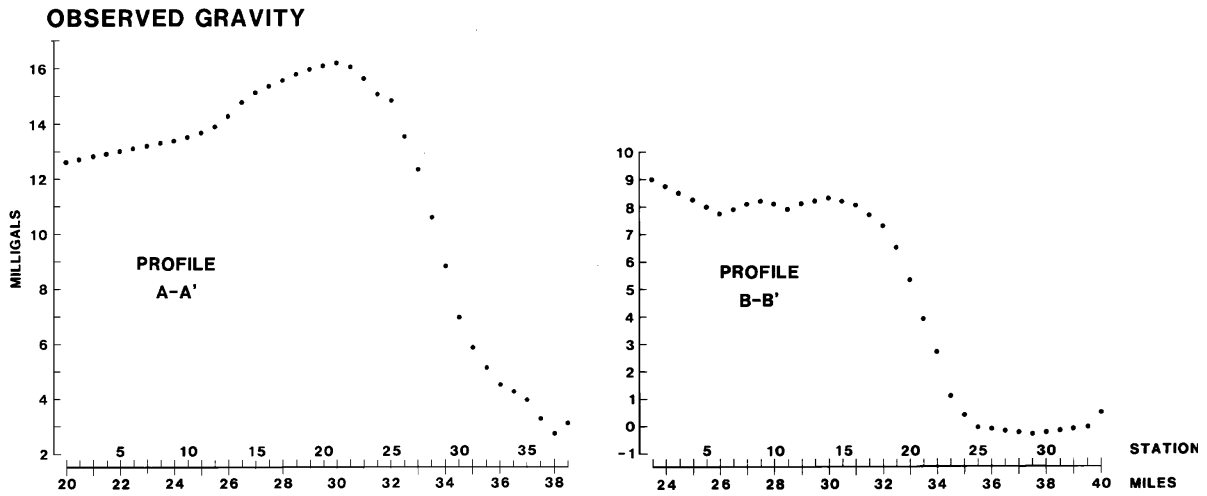


Figure 4. Observed gravity along profiles A-A' and B-B' (fig. 2).

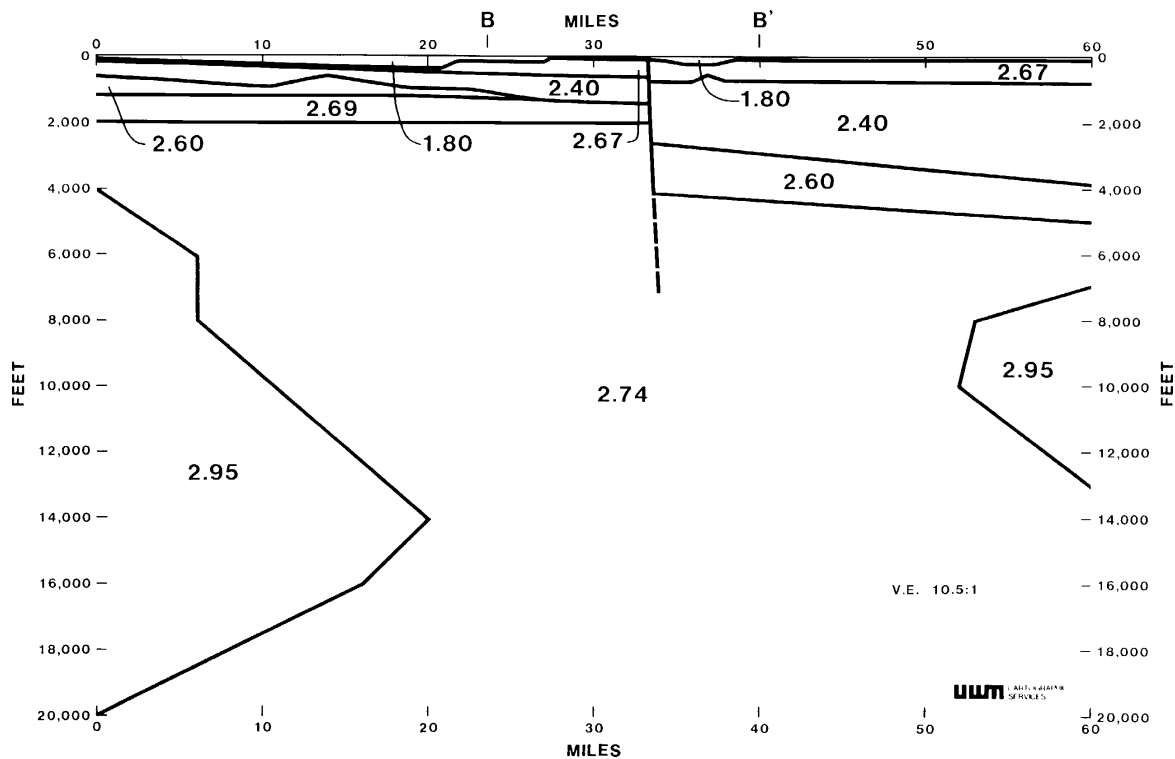


Figure 5. Geological model 1 along profile B-B'. Dip of the fault is approximately 80°.

Two models with shallow dipping faults were constructed. Model 2 is also along profile B-B' and model 3 is along profile A-A' (fig. 2). Models 2 and 3 are illustrated in figures 7 and 8 respectively. In both models the residual gravity values at all stations are within our expected measurement accuracy and the RMS error for each profile is 0.03 mgal, which is well below our measurement accuracy (fig. 9). The dip of the fault in models 2 and 3 is roughly 9 and 20

degrees respectively. While this is substantially lower than expected, it is not contradicted by any available well data. The observation that the fault is nearly vertical at its exposure in the Waukesha Stone and Lime Quarry suggests that it may be a listric fault steeply dipping near the surface for a relatively short distance and then rapidly decreasing in dip with increasing depth. If this is the case, the overall geometry of the fault remains constrained by the gravity data to have a relatively shallow dip to first order.

The offset of the fault in the Silurian rock in these two models is 30 m. The offset of the sandstone unit increases from 30 m to about 500 m from top to bottom similar to model 1. The other large difference in these two models is that the gabbro has been modelled as a single intrusive mass that is offset by the fault. The maximum offset is seen at the base of the gabbro where it reaches roughly 600 m.

The results of this study show that the Waukesha Fault extends through Waukesha and Ozaukee Counties to Lake Michigan. Models of two profiles across the fault indicate that it may be a high angle normal fault as previously expected but can also be modelled accurately as

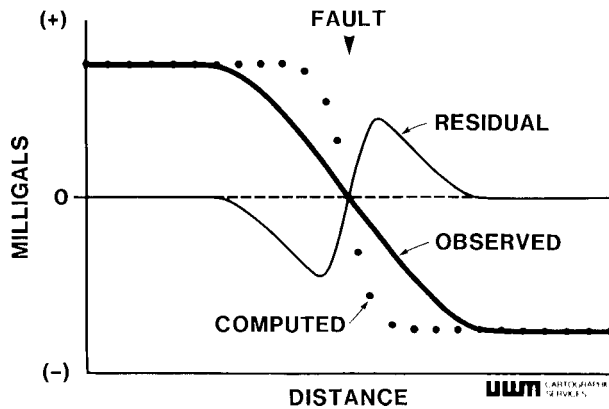


Figure 6. Plot of the observed, model and residual gravity where the model fault is steeper than the actual fault.

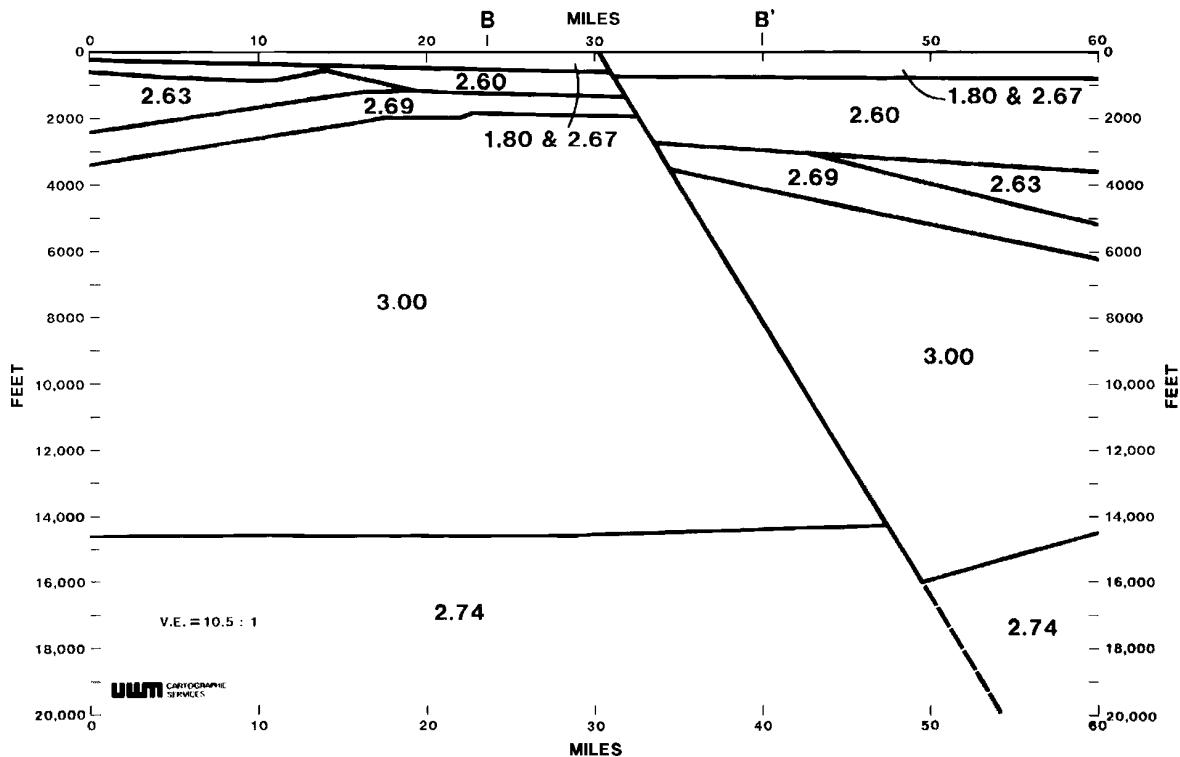


Figure 7. Geological model 2 along profile B-B'. Dip of the fault is approximately 9°.

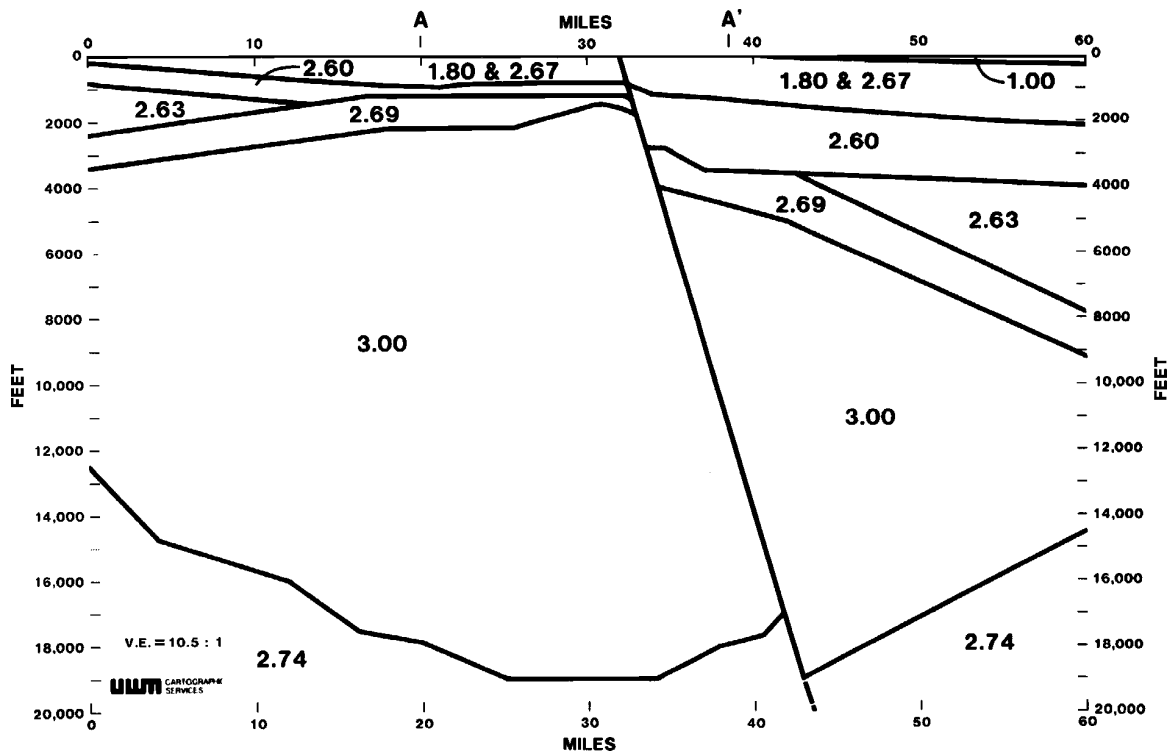


Figure 8. Geological model 3 along profile A-A'. Dip of the fault is approximately 20°.

a listric fault with a shallow dip at depth ranging between roughly 10 and 20 degrees to the southeast. We believe that further work on the fault is needed before this ambiguity can be eliminated.

REFERENCES

- Brukardt, S.A., 1983, Gravity survey of Waukesha County, Wisconsin: unpublished M.S. thesis, University of Wisconsin-Milwaukee, 131 p.
- Distelhorst, C., 1967, Bedrock formations of Milwaukee County: unpublished M.S. Thesis, University of Wisconsin-Milwaukee, 130 p.
- Dutton, C.E., and Bradley, R.E., 1970, Lithologic, geophysical, and mineral commodity maps of Precambrian rocks in Wisconsin, U.S. Geological Survey Miscellaneous Geologic Investigations Map I-631.
- Ervin, C.P., 1983, Wisconsin gravity base station network: Wisconsin Geological and Natural History Survey Miscellaneous Paper 83-1, 43 p.
- Foley, F.C., Walton, W.C., and Drescher, W.J., 1953, Ground water conditions in the Milwaukee-Waukesha area, Wisconsin: U.S. Geological Survey Water Supply Paper 1229, p. 23 p.
- Gruetzmacher, J., 1974, Surficial geology of southern Washington County, Wisconsin: unpublished M.S. thesis, University of Wisconsin-Milwaukee, 52 p.
- Mikulic, D.G., and Mikulic, J.L., 1977, History of geologic work in the Silurian and Devonian of southeastern Wisconsin: Guidebook for the 41st Annual Tri-State Field Conference, p. A1-A5.
- Moretti, G., 1971, Reference section for Paleozoic rocks in eastern Wisconsin: Van Driest No. 1, Sheboygan County: unpublished M.S. thesis, University of Wisconsin-Milwaukee, 138 p.
- Skinner, E.L., and Borman, R.G., 1973, Water Resources of Wisconsin-Lake Michigan Basin: U.S. Geological Survey Hydrologic Investigations Atlas HA-432.
- Talwani, M., and Ewing, M., 1959, Rapid computation of gravitational attraction of three dimensional bodies of arbitrary shape: *Geophysics*, v. 25, p. 203-225.

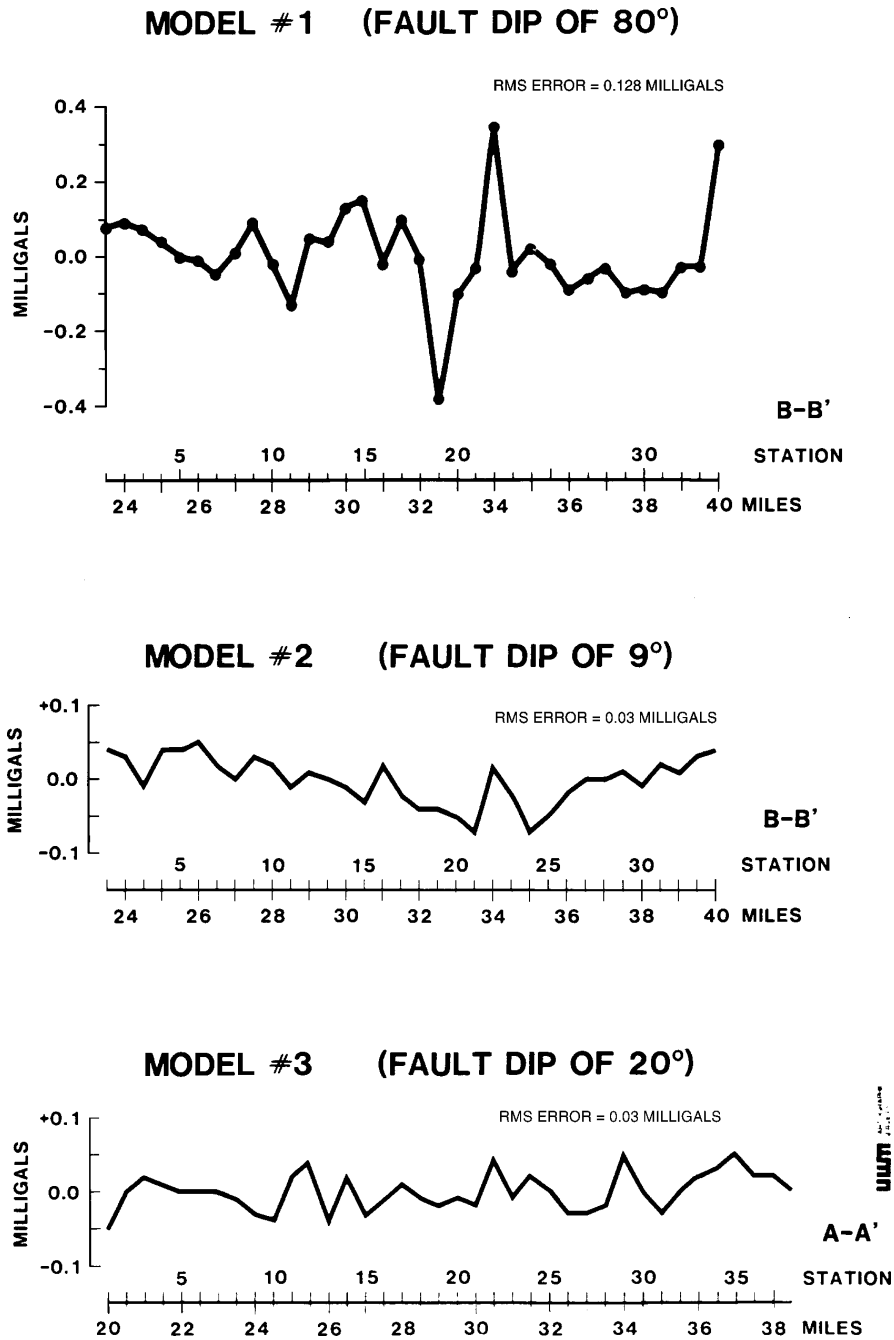


Figure 9. Plots of the residual gravity produced by the models.

Thwaites, F.T., 1940, Buried pre-Cambrian of Wisconsin: *Wisconsin Academy of Sciences, Arts, and Letters Transactions*, v. 32, p. 233-242.

Thwaites, F.T., 1957, Buried Precambrian of Wisconsin: Wisconsin Geological and Natural History Survey map, scale 1:2,500,000.

Wisconsin Electric Power Company, Wisconsin Power & Light Company, Wisconsin Public Service Corporation, and Madison Gas & Electric Company, 1979a, Haven Nuclear Plant Units 1 and 2: Site Addendum Preliminary Safety Analysis Report, Volume 2: section 2.5 Geology and Seismology, p. 46-52.

Wisconsin Electric Power Company, Wisconsin Power & Light Company, Wisconsin Public Service Corporation, and Madison Gas & Electric Company, 1979b, Haven Nuclear Plant Units 1 and 2: Site Addendum Preliminary Safety Analysis Report, Volume 3: appendix 2T, Regional Basement Geology of Lake Michigan, Norbert O'Hara, p. 2-21.

Wold, R.J., Paull, R.A., Wolosin, C.A., and Friedel, R.J., 1981, Geology of central Lake Michigan: *AAPG Bulletin*, vol. 65, p.1621-1632.

RADON EMANATION FROM SOIL OF KENOSHA, RACINE AND WAUKESHA COUNTIES, SOUTHEASTERN WISCONSIN

Nancy S. Kochis^{1,2} and Steven W. Leavitt^{1,3}

ABSTRACT

The radon (²²²Rn) emanation from soil of Kenosha, Racine and Waukesha Counties was measured and related to the soil chemistry, inherent radioactivity and grain-size distribution. Our twelve study sites were in soil of the Horicon, New Berlin and Oak Creek Formations, lake plain sediment and where bedrock is close to the surface. Canisters containing activated charcoal were placed into holes bored into the soil. The hole openings were covered, and field radon emanations were collected for a period of over 50 hours.

Radon emanation concentration at all sites other than the shallow bedrock site was above 4 pCi/l; at three locations radon concentration exceeded 100 pCi/l. Sites where subsoil had high clay or silt plus clay content tended to have lower radon emanation concentration. Soil permeability may also influence whether relatively high inherent soil radioactivity results in high radon emanation concentration.

We found no significant relationship between radon emanation concentration and pebble lithology, atmospheric pressure, or uranium (²³⁸U) concentration determined by airborne gamma ray and magnetic surveys. Water-soluble phosphate concentration of surface soil were low; therefore, the natural radon concentration was probably not augmented by uranium-bearing phosphate fertilizer additions.

In an ancillary study, we found that radon emanation concentration was highest at the ground surface and decreased to nearly zero at a depth of 6.9 m. The higher radon concentration at the surface may be due to more conduits for soil gas movement present in the weathered zone than at depth.

INTRODUCTION

Radon (²²²Rn) is a chemically inert gas produced from the decay of radium (²²⁶Ra), and has a half-life of 3.8 days. Its decay produces a sequence of 4 short-lived progeny followed by lead (²¹⁰Pb) whose half-life is 19.4 years. The short-lived progeny attach to dust and aerosols and lodge in the lung tissue when inhaled. The decay of polonium (²¹⁸Po and ²¹⁴Po) gives off alpha particles which are the main source of radiation hazard when they decay in the lungs (Robkin, 1987).

Airborne radon concentration is usually expressed in picocuries per liter, pCi/l, a measure of the number of radioactive disintegrations per minute in a liter of air. The pCi/l measurements can be converted to S.I. units (Bq/m³) by multiplying by 37.18.

The ultimate source of radon is uranium in rock and soil. Typical uranium concentration in soil and rock is a few ppm (Bodansky, 1987). The crustal mean concentration of uranium is about 3 ppm;

granite and shale average about 5 and 3.5 ppm uranium, respectively; phosphate rock contains 50-100 ppm uranium (NCRP, 1976; Krauskopf, 1979). As radon atoms are liberated from geologic materials they become part of the soil gas. Soil gas can be drawn into basements of buildings via cracks in walls and floors in response to air pressure differences.

Soil gas movement depends on rock/soil permeability (Tanner, 1986). There is greater soil gas movement, and therefore a potential for high radon emanation rates when soil water content is low (Nevissi and Bodansky, 1987). Radon solubility in water ranges from 51.0 cm³ of radon gas (at 0°C, 1 atmosphere) per 100 cm³ of water at 0°C to 13.0 cm³ radon per 100 cm³ of water at 60°C (Chemical Rubber Company, 1988).

Our study was conducted following a survey of indoor airborne radon in Wisconsin homes (Wisconsin Department of Health and Social Services, 1987). According to the survey, an estimated 44.3% of

¹Department of Geology, University of Wisconsin-Parkside, Kenosha, Wisconsin 53141-2000

²Currently at Wisconsin Department of Commerce, 101 West Pleasant Street Suite 205, Milwaukee, Wisconsin 53212

³Currently at Laboratory of Tree-Ring Research, University of Arizona, Tucson, Arizona 85721

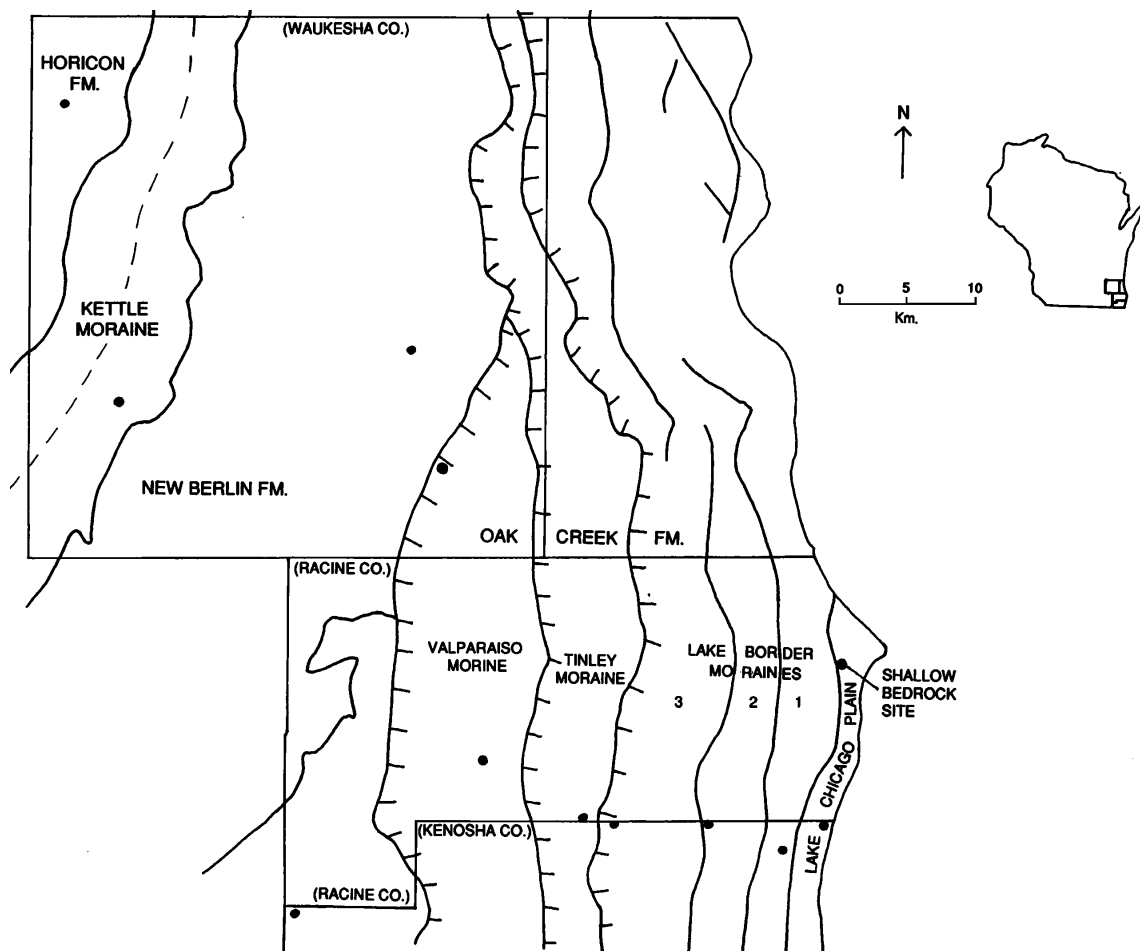


Figure 1. Map of sites in the study area in southeastern Wisconsin. Geology after Schneider (1983).

homes in an area of southeastern Wisconsin (including Kenosha, Racine and Waukesha Counties) have indoor radon concentration greater than 4 pCi/l, the Environmental Protection Agency's recommended limit for indoor air. The purpose of our research was to measure the radon emanation from soil and relate it to soil chemistry, inherent radioactivity and grain-size distribution. Our ancillary study was conducted to determine if the weathered zone of an unconsolidated formation contains higher radon emanation concentration than the unweathered zone.

METHODS

Ten of our twelve sites were located in the moraines of the Oak Creek, Horicon and New Berlin Formations (fig. 1). The moraines vary in thickness from 0 to 125 m and overlie Silurian dolostone bedrock (Schneider, 1983). The glacial material is weathered

to a depth of 3 to 4 m. Two more sites were near Lake Michigan in lake plain sediment and where dolostone bedrock is close to the surface. At the shallow bedrock site, the surficial deposit is lacustrine clay. As we were concerned that radon from uranium-bearing phosphate fertilizer additions could augment the natural radon concentration, wooded sites with medium to large trees were selected to ensure the site had not been recently farmed, and therefore not fertilized.

Twenty-cm-diameter holes were dug with a power auger to depths of 27 to 79 cm; most holes were 33 to 42 cm deep (table 1). The holes extended to the upper part of the B soil horizon. Soil samples were collected from the surface and from the bottom of each hole (herein referred to as "surface soil" and "subsoil"). To determine variability of the radon concentration over short distances, two adjacent holes, 4 to 7 m apart, were installed at each of the 8 sites in Racine and Kenosha Counties.

Ten-cm-diameter canisters containing activated charcoal with diffusion barrier in desiccant were used to measure the radon concentration. Prior to being placed in the hole, filter paper was taped over the top of each canister to keep soil out. The canisters were placed on small wooden boards which were inserted into the side of each hole. This allowed for air circulation around the canister and for drainage of any water that might enter the hole. The canisters were 15 - 37 cm below the ground surface (table 1). A plastic sheet, a wooden board, and soil were placed over the hole so that equilibrium between the soils and air in the hole would be established. The canisters were exposed to soil gas for over 50 hours, retrieved, sealed and taken to the Wisconsin Department of Health and Social Services, Section of Radiation Protection in Madison where the radon concentration was determined using gamma ray spectroscopy. Average atmospheric pressure during the time each can was exposed was determined using hourly weather records from the National

Weather Service Forecast Office in Milwaukee (table1).

The water-soluble phosphate content of surface soil at each site was determined by the Truog and Meyer method (Chapman and Pratt, 1961) and the ascorbic acid reduction method was used to determine phosphate concentration in each extract. Particle-size distribution of the subsoil was determined using screens (pebble- and sand-size fractions) and settling tubes (silt- and clay-size fractions). The particle-size divisions were: >2 mm = pebbles; 2 mm to 0.063 mm = sand; 0.063 mm to 0.004 mm = silt; and <0.004 mm = clay. The lithology of the pebbles and constituents of the sand were determined by microscopic examination.

The inherent radioactivity of subsoil from 6 holes was determined using the method described in Edgington and Lucas (1970). In summary, 160 g soil samples were analyzed for counting periods of 21 to 70 hours using a sodium iodide crystal to detect

Table 1. Hole and canister depth, duration of canister exposure, and average atmospheric pressure for each site.

Site	Canister number	Hole depth cm	Canister depth cm	Canister open		Canister closed		Exposure hr	Pressure mb
				Date	Time	Date	Time		
HORICON FORMATION									
Waukesha Co.	061	56	28	11/5/88	11:41 AM	11/7/88	2:22 PM	50.68	969.4
NEW BERLIN FORMATION									
Kettle Moraine, Waukesha Co.	130	36	18	"	10:55 AM	"	1:32 PM	50.62	969.3
Ground Moraine, Waukesha Co.	149	38	23	"	10:09 AM	"	12:56 PM	50.78	968.9
Pitted Outwash, Kenosha Co.	147	41	20	11/4/88	5:14 PM	"	12:37 PM	67.38	967.3
	131	79	23	"	5:10 PM	"	12:31 PM	67.35	967.3
OAK CREEK FORMATION									
Valparaiso Moraine									
Racine Co.	095	27	15	"	4:15 PM	"	11:45 AM	67.50	967.3
	089	29	17	"	4:22 PM	"	11:49 AM	67.45	967.3
Waukesha Co.	157	33	20	11/5/88	9:33 AM	"	12:21 PM	50.80	968.6
Tinley Moraine, Racine Co.	104	36	20	11/4/88	3:40 PM	"	11:13 AM	67.55	966.7
	055	27	15	"	3:44 PM	"	11:19 AM	67.58	966.7
Lake Border Moraines, Kenosha Co.									
3	009	64	37	"	3:09 PM	"	11:00 AM	67.85	967.0
	046	42	30	"	3:17 PM	"	10:53 AM	67.60	967.0
2	150	33	22	"	2:43 PM	"	10:30 AM	67.78	967.0
	033	36	20	"	2:48 PM	"	10:35 AM	67.78	967.0
1	004	33	23	"	2:13 PM	"	10:07 AM	67.90	966.7
	036	41	28	"	2:20 PM	"	10:00 AM	67.67	966.7
LAKE PLAIN SEDIMENTS,									
Racine Co.	052	71	38	"	1:54 PM	"	9:45 AM	67.85	966.7
	080	41	30	"	1:45 PM	"	9:37 AM	67.87	966.7
SHALLOW BEDROCK SITE,									
Racine Co.	038	53	34	"	1:00 PM	"	9:00 AM	68.00	966.5
	032	58	33	"	1:05 PM	"	9:06 AM	68.02	966.5

gamma ray emissions, and identify their nuclide source based on their energy.

We compared the radon emanation concentration measured in our study to airborne gamma ray and magnetic surveys of southeastern Wisconsin (Geometrics, 1981, and High Life Helicopters, Inc./QEB, Inc., 1981). The gamma ray and magnetic surveys measured bismuth (^{214}Bi) concentration in the upper 46 cm of the ground and converted the measurements to equivalent ^{238}U . The ^{238}U distribution was determined from "pseudocontour maps." County boundaries and our study sites were located using latitude and longitude.

To determine whether radon emanation concentration changes with depth, an ancillary study was conducted. The study site was an 8-month old, approximately 9 m deep excavation in the Oak Creek Formation, lake border moraine 1 in Racine County. Steel drive-points were hammered 40 cm deep into undisturbed surface soil, the top of the unweathered till and to depths of 2.3, 4.6 and 6.9 m (vertical distance) below the top. The drive-points were open at the top and had a few small holes along the bottom 3 cm. A portable electric pump drew the standing air in the pipe and an equal volume of soil gas through a gas filter and into EDA Instruments, Inc. (Toronto, Canada) scintillation cells. Pumping time was 5 sec. Two samples were collected from the undisturbed surface soil and from depths of 2.3 and 6.9 m; one sample was collected from a depth of 4.6 m. The gas samples equilibrated for 2-3 hours before being placed into Radon Detector RDA-200 devices, manufactured by EDA Instruments, Inc. The scintillation cells have a ZnS phosphor coating which emits ultraviolet light when hit by alpha particles originating from radon and its decay products. The light flashes, detected by the RDA-200 photo-multiplier tube, are converted to electrical impulses and the accumulation of impulses is digitally displayed. We used a counting period of 30 minutes. The concentration of radon was calculated using an algorithm provided by the RDA operations manual.

RESULTS AND DISCUSSION

Radon emanation concentration was from 3.08 to 188.15 pCi/l (table 2). The highest concentration was in the Tinley Moraine, the lowest were at the shallow bedrock site.

To determine whether radon emanation concentration varies over short distances, we examined the results from the eight sites where two adjacent holes were installed. At two sites (Tinley and Valparaiso

Moraine in Racine County) the experiment set-up remained intact and no canisters were contaminated with soil or diluted with surface air. Adjacent holes differed by 12 and 21% in the Tinley and Valparaiso sites, respectively. Based on these results, it appears that there are only small variations in radon concentration over short distances.

However, at six other sites where two adjacent holes were installed, air dilution and/or soil contamination occurred at one of the two holes. The surface cover collapsed inward at four of the six sites (lake plain sediments, lake border moraines 1, 2 and 3 of the Oak Creek Formation). The radon emanation concentration at these sites varied 73 to 78% between the two adjacent holes. In each pair, the lower radon emanation concentration corresponds to the hole with the collapsed cover; the lower value may be a result of surface air diluting the radon emanations.

The board holding the canister became slanted or fell at two sites (New Berlin Formation pitted outwash and shallow bedrock site) and as a result, soil got into the canisters. In both cases, the radon concentration of the contaminated canister was higher than the uncontaminated ones.

Thus, out of 20 canisters, the radon emanation concentration from six canisters is not considered valid. Only radon concentration from the 14 canisters which remained uncontaminated and in place is considered accurate and have been included in the tables.

Sand was the dominant constituent of the subsoil at seven sites, the highest amount was 97.1% at the New Berlin Formation pitted outwash site (table 2, figure 1). Silt was dominant at four sites. At all but one site (lake plain sediments), silt was either the highest or second highest percentage component. Clay was the major constituent at one site (Valparaiso Moraine in Waukesha County).

Based on information from Tanner (1986), we expected high radon concentration where the soil is coarse and well-drained, and therefore permeable to soil gas containing radon. However, in our study, the relationship between the sand content of the subsoil and radon emanation concentration is inconsistent. For example, at the Horicon Formation site, subsoil contains 71.4% sand and radon concentration is 50.40 pCi/l. However, at the Valparaiso Moraine in Racine County where subsoil contains about the same amount of sand (70.6%), radon emanation concentration is much lower (13.77 and 16.69 pCi/l). We noted that the highest radon emanation concentration in our study (167.44 and 188.15 pCi/l at the Tinley Moraine) were at locations where silt is the dominant constituent of the subsoil.

At locations where subsoil had high clay content, radon emanation concentration tended to be low. The three lake border moraines illustrate this relationship. As clay content increases from lake border moraine 3 to 1, radon emanation concentration decreases. At the shallow bedrock site, where the surficial deposits are lacustrine clays, the radon emanation concentration was the lowest of all 12 sites, 3.08 pCi/l. At this site, the soil was saturated when we did our field work. Therefore, the qualitative inverse relationship between clay content and radon emanation concentration may relate to the fact that clay, particularly if wet, inhibits radon movement (Tanner, 1986).

The two sites in the Valparaiso Moraine are about 25 km apart (fig. 1), yet radon emanation concentration at the two sites (three holes) is similar (13.77 and 16.69 pCi/l in Racine County, 11.43 pCi/l in Waukesha County). This is surprising considering that there were differences in grain-size distribution between the two sites. In Racine County the Valparaiso Moraine subsoil contains 70.6% sand, however, in Waukesha

County it is silty and clayey (89.9% silt plus clay).

To determine how radon emanation concentration, inherent soil radioactivity, and subsoil permeability are related, we looked at the data for the six sites where inherent soil radioactivity was measured (table 3). Inherent soil radioactivity measurements are expressed as counts per 1000 seconds of radium and bismuth (^{226}Ra , ^{214}Bi). The $^{226}\text{Ra}/^{214}\text{Bi}$ ratios are very similar for the six sites tested (table 3). The constancy of the ratios may be a basis for inferring that radon production is proportional to the ^{226}Ra and/or ^{214}Bi counts. If we assume radon production is approximately proportional to either its parent nuclide, ^{226}Ra , or one of its daughter nuclides, ^{214}Bi , then (of the six sites tested) the highest radon production is at the Valparaiso moraine in Waukesha County, and the lowest is at the Horicon Formation site.

At the Valparaiso Moraine in Waukesha County, inherent soil radioactivity is relatively high and radon emanation concentration is relatively low. The subsoil at this site contains 89.9% silt and clay. The low per-

Table 2. Radon concentration, water-soluble phosphate concentration and subsoil grain-size distribution for each site.

Site	Canister number	Radon pCi/l	Water-soluble phosphate ppm	Subsoil grain-size			
				>sand (%)	sand (%)	silt (%)	clay (%)
HORICON FORMATION, Waukesha Co.	061	50.40 ± .76	—	3.6	71.4	17.1	7.9
NEW BERLIN FORMATION							
Kettle Moraine, Waukesha Co.	130	123.61 ± 1.11	—	6.9	56.4	24.1	12.6
Ground Moraine, Waukesha Co.	149	47.78 ± .76	2.65	5.8	39.8	38.5	15.9
Pitted Outwash, Kenosha Co.	147	17.48 ± .58	0.25	.1	97.1	2.4	.4
	131	41.80 ± .92**					
OAK CREEK FORMATION							
Valparaiso Moraine							
Racine Co.	095	13.77 ± .54	0.25	.1	70.6	24.5	4.8
	089	16.69 ± .55					
Waukesha Co.	157	11.43 ± .46	1.25	1.4	8.7	41.2	48.7
Tinley Moraine, Racine Co.	104	188.15 ± 1.51	0.25	.9	28.6	55.1	15.4
	055	167.44 ± 1.34					
Lake Border Moraines, Kenosha Co.							
3	009	54.98 ± .88	2.0	1.9	42.7	39.8	15.6
	046	14.53 ± .62*					
2	150	35.03 ± .70	0.50	.2	35.5	45.0	19.3
	033	8.01 ± .48*					
1	004	25.54 ± .66	4.50	2.2	32.9	40.0	24.9
	036	16.53 ± .58*					
LAKE PLAIN SEDIMENTS, Racine Co.	052	116.09 ± 1.16	2.85	5.6	87.2	4.1	3.1
	080	24.67 ± 3.58*					
SHALLOW BEDROCK SITE, Racine Co.	038	3.08 ± .45	0.75	.6	19.2	53.6	26.6
	032	3.26 ± .47**					

*Hole cover collapsed

**Soil in canister

Table 3. *Inherent soil radioactivity, radon concentration and grain-size distribution for six sites. Background counting lasted 91.8 hr.*

Site	Count time hours	²²⁶ Ra* Counts per 1000 sec minus background	²¹⁴ Bi**	²²⁶ Ra/ ²¹⁴ Bi	Radon pCi/l	Grain-size distribution	
						>sand+ sand (%)	Combined silt+ clay (%)
HORICON FORMATION, Waukesha Co.	69.5	2.62	5.28	0.50	50.40 ± .76	75.0	25.0
NEW BERLIN FORMATION Kettle Moraine, Waukesha Co.	26.5	4.35	10.34	0.42	123.61 ± 1.11	63.3	36.7
OAK CREEK FORMATION Valparaiso Moraine Racine, Co.	50.4	3.17	7.73	0.41	13.77 ± .54 16.69 ± .55	70.7	29.3
Waukesha Co.	27.1	10.90	26.36	0.41	11.43 ± .46	10.1	89.9
Lake Border Moraine, Kenosha Co. 2	24.5	10.33	19.86	0.52	35.03 ± .70	35.7	64.3
1	20.6	8.81	20.29	0.43	25.54 ± .66	35.1	64.9

*180-192 Mev channel

**604-616 Mev channel

meability soil may have restricted the movement of soil gas containing radon, resulting in a relatively low radon emanation concentration. A different relationship occurs at the Kettle Moraine and Horicon Formation sites, where inherent soil radioactivity is relatively low but radon emanation concentration is relatively high. There, the subsoil is more permeable with 75.0% and 63.3% pebble- and sand-size particles. The radon emanation concentration we measured may originate from sediment or bedrock deeper than the hole we installed. The high soil permeability may cause radon gas movement from depth to the surface.

For some of the six sites, the data were inconsistent. For example, we noted that the inherent soil radioactivity and subsoil grain-size distribution of the Valparaiso Moraine Racine County and Horicon Formation sites are about the same. Yet the radon emanation concentration is more than three times higher at the Horicon Formation site than at the Valparaiso Moraine Racine County site.

Based on our comparison of radon emanation concentration, inherent soil radioactivity, and subsoil permeability data for the six sites where inherent soil radioactivity was measured, we believe there is a relationship between the three factors. However, the relationship could be obscured at some locations by factors not included in this study.

Water-soluble phosphate content of the surface soil was generally low, less than 5 ppm (table 2). A few ppm of water-soluble phosphate are considered background concentration in soil (Chapman and Pratt, 1961). Therefore, it is unlikely that the land has been heavily fertilized with rock phosphate. Phosphate is probably not a significant source of radon in our study

unless there are high amounts of insoluble phosphate compounds present.

The dominant pebble (>2 mm) lithologies in the subsoil were quartz, granite/gneiss and carbonate (table 4). The sand was >90% quartz at all sites. Cobbles encountered during hole construction were mostly carbonate. Because granite and shale are more likely to contain higher concentration of uranium than other rock (Krauskopf, 1979), we expected higher radon emanation concentration at sites where they are the dominant pebble lithology. We used Pearson correlation coefficients to determine if there is a statistical relationship between radon concentration and lithology, and found that there were no significant linear correlations between radon concentration and percent of each lithology.

Average atmospheric pressure while the canisters were exposed only varied 2.98 mb among the 14 valid data points. Atmospheric pressure can influence soil gas movement. Therefore, Pearson correlation coefficients were used to determine if there is a relationship between average atmospheric pressure and radon concentration. The r^2 value is virtually zero ($r^2 = 2.4 \times 10^{-7}$); therefore there is no relationship.

Figure 2 is a map of ²³⁸U concentration as determined by airborne gamma ray and magnetic survey. Statistical uranium anomalies, marked on the map with short dashes, can result from a number of situations, such as the true concentration of uraniumiferous minerals, differential soil and vegetation cover, and others (Geometrics, 1981). However, the pattern of uranium anomalies in southeastern Wisconsin could also be related to urban and industrial development. Pearson correlation coefficients were used to deter-

Table 4. Subsoil pebble lithology distribution for each site. The value "n" is the number of pebbles examined.

Site	n	Pebble lithology (%)				
		Quartz	Granite/gneiss	Mafic	Carbonate	Shale
HORICON FORMATION, Waukesha Co.	40	60	28	—	10	2
NEW BERLIN FORMATION						
Kettle Moraine, Waukesha Co.	16	38	31	—	31	—
Ground Moraine, Waukesha Co.	61	13	44	23	20	—
Pitted Outwash, Kenosha Co.	1	—	—	—	100	—
OAK CREEK FORMATION						
Valparaiso Moraine						
Racine Co.	10	10	70	—	10	10
Waukesha Co.	3	33	67	—	—	—
Tinley Moraine, Racine Co.	21	29	14	—	57	—
Lake Border Moraines, Kenosha Co.						
3	30	3	17	3	77	—
2	3	—	—	—	100	—
1	16	44	37	—	19	—
LAKE PLAIN SEDIMENTS, Racine Co.	23	4	18	—	78	—
SHALLOW BEDROCK SITE, Racine Co.	12	—	—	8	84	8

mine if there was a relationship between the radon emanation concentration at our sites and the ^{238}U concentration. The r^2 value is 0.002; therefore there is no relationship. We noted that the higher uranium concentration roughly match the boundaries of the Oak Creek Formation. The inherent soil radioactivity measurements generally correspond to the airborne-measured uranium concentration when they are compared qualitatively.

In our ancillary study we looked at changes in radon emanation concentration with depth in Oak Creek Formation till. The radon emanation concentration was highest in the surface soil (39.3 pCi/l) (a second value of 0.7 was discounted as air contamination). At the top of unweathered till, the radon emanation concentration was 17.2 pCi/l, and radon concentration progressively decreased with depth. At a depth of 2.3 m, radon emanation concentration was 13.2 and 5.0 pCi/l; at a depth of 4.6 m, 0.7 pCi/l; and at a depth of 6.9 m, 0.2 and 0 pCi/l. The higher radon emanation concentration at the surface than at a depth may be due to openings in the weathered surface zone. Soil gas containing radon is likely to flow more freely there than in the relatively dense, unweathered till.

CONCLUSIONS

Radon emanation concentration at the locations we studied appears to be primarily related to subsoil permeability. Based on our work, we believe that high silt and clay content in the subsoil restricts soil gas (containing radon) movement. Even locations with high inherent soil radioactivity may not have high radon

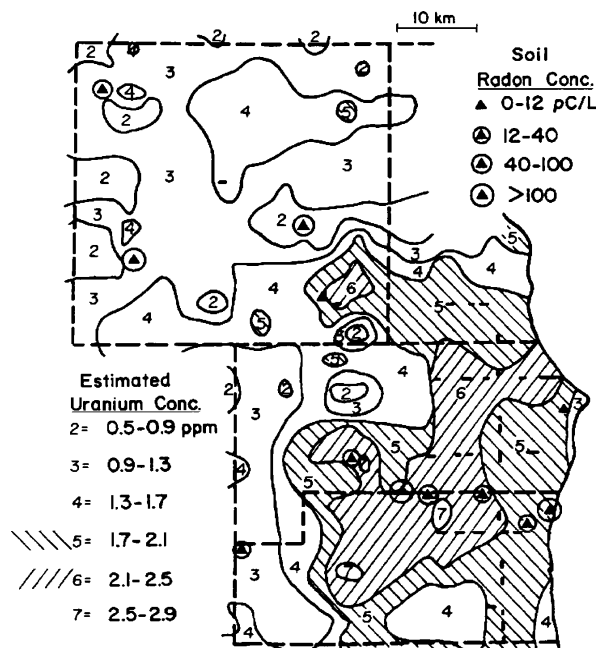


Figure 2. Airborne-measured uranium (^{238}U) concentration in the upper 46 cm of the ground (Geometrics, 1981; High Life Helicopters, Inc./QEB, Inc., 1981), and radon concentration at each site for Kenosha, Racine, and Waukesha Counties.

emanation concentration due to low soil permeability. Likewise, subsoil with high sand content would permit radon to move from depth to the surface; this could result in relatively high radon emanation con-

centration even where inherent soil radioactivity is relatively low. At some of our sites the relationship between radon emanation concentration and soil permeability is more apparent than at others. We recognize that many factors influence radon emanation concentration and that it may be not possible to isolate the relationship between radon emanation concentration and any one, or combination of, factors.

We found no significant relationship between the radon emanation concentration and subsoil pebble lithology, atmospheric pressure when the canister was exposed, and ^{238}U concentration of the soil as determined by airborne gamma ray and magnetic survey. In our ancillary study we found that radon emanation concentration decrease with depth. This may be a result of more pathways for soil gas movement in the weathered surface zone than in unweathered till at depth.

ACKNOWLEDGMENTS

We thank the Wisconsin Department of Health and Social Services, Section of Radiation Protection, for the use of the charcoal canisters and for doing the radon analysis. David Edgington of the Center for Great Lakes Studies measured the inherent soil radioactivity. Austin Long of The Laboratory of Isotope Geochemistry, University of Arizona, loaned us the RDA-200 and scintillation cells. Steve Orlovsky assisted with the field work and did the grain-size analysis.

REFERENCES

- Bodansky, D., 1987, Overview of the indoor radon problem: *in* Bodansky, D., Robkin, M.A., and Stadler, D.R., eds., *Indoor Radon and Its Hazards*: Seattle, WA, University of Washington Press, p. 3-16.
- Chapman, H.D., and Pratt, P.F., 1961, *Methods of Analysis for Soils, Plants and Waters*: Riverside, CA, University of California, 309 p.
- Chemical Rubber Company, 1988, *CRC Handbook of Chemistry and Physics*: Cleveland, OH, CRC Press.
- Edgington, D.N., and Lucas Jr., H.F., 1970, A system for the neutron activation analysis of trace elements in samples of biological and environmental interest: *Journal of Radioanalytical Chemistry*, v. 5, p. 233-250.
- Geometrics, 1981, Aerial gamma ray and magnetic survey, Racine and Grand Rapids Quadrangles Michigan, Wisconsin and Illinois: DOE Open-File Report GJBX-237(81), 161 p.
- High Life Helicopters, Inc./QEB, Inc., 1981, Airborne gamma-ray spectrometer and magnetometer survey, Rockford Quadrangle, Aurora Quadrangle (IL.), Madison, Quadrangle (WI.): DOE Open-File Report GJBX-181 (81), 353 p.
- Krauskopf, K.B., 1979, *Introduction to Geochemistry*: New York, McGraw-Hill, 617 p.
- NCRP, 1976, Environmental radiation measurements: Bethesda, MD, National Council on Radiation Protection and Measurements Report No. 50, 246 p.
- Nevisi, A.E., and Bodansky, D., 1987, Radon sources and levels in the outside environment, *in* Bodansky, D., Robkin, M.A., and Stadler, D.R., eds., *Indoor Radon and Its Hazards*: Seattle, WA, University of Washington Press, p. 30-41.
- Robkin, M.A., 1987, Terminology for describing radon concentrations and exposures: *in* Bodansky, D., Robkin, M. A., and Stadler, D. R., eds., *Indoor Radon and Its Hazards*: Seattle, WA, University of Washington Press, p. 17-29.
- Schneider, A.F., 1983, Wisconsinan stratigraphy and glacial sequence in southeastern Wisconsin: Wisconsin Geological and Natural History Survey, *Geoscience Wisconsin*, v. 7, p. 59-85.
- Tanner, A.B., 1986, Indoor radon and its sources in the ground: U.S. Geological Survey Open-File Report 86-222, 5 p.
- Wisconsin Department of Health and Social Services, Section of Radiation Protection, 1987, Determination of airborne radon ^{222}Rn concentrations in Wisconsin homes: Report of EPA/Wisconsin Department of Health Survey of December 1986, 19p.